AVERAGED EQUATIONS FOR ELECTRICAL POTENTIAL AND ION TRANSPORT IN BRAIN TISSUE

by

CHRISTOPHER DERRICK MAH

A THESIS SUBMITTED IN PARTIAL FULFILMENT OF
THE REQUIREMENTS FOR THE DEGREE OF

DOCTOR OF PHILOSOPHY

in

THE FACULTY OF GRADUATE STUDIES

Department of Mathematics

Institute of Applied Mathematics

We accept this thesis as conforming

to the required standard

THE UNIVERSITY OF BRITISH COLUMBIA

August 1989

67

In presenting this thesis in partial fulfilment of the requirements for an advanced degree at the University of British Columbia, I agree that the Library shall make it freely available for reference and study. I further agree that permission for extensive copying of this thesis for scholarly purposes may be granted by the head of my department or by his or her representatives. It is understood that copying or publication of this thesis for financial gain shall not be allowed without my written permission.

Department of   MATHEMATICS

The University of British Columbia
Vancouver, Canada

Date   SEPTEMBER 28th 1989

ABSTRACT

The accurate modelling of bulk passive properties of neural tissue is essential to the modelling of macroscopic phenomena in the brain such as spreading depression and epilepsy. Properties which characterise the passive and active flows of ions or electric current through tissue are referred to as transport properties. Such properties associated with passive flows include bulk conductivity, bulk diffusion coefficient, and those associated with electrically mediated ionic flux which is called 'spatial buffer flux'. While models for such transport properties of cortical tissue have been published, each of these models contained different assumptions about the structure of the tissue. Recent data on potassium transport through neural tissue are important for the construction of a unified model (i.e., based on a consistent set of assumptions) because they provide measurements of the amount of bulk electric current passing through cell membranes.

In this thesis the Nernst-Planck equation is used as the governing equation for ion transport and electric potential, with specification of the jump conditions at the cell membrane. An asymptotic expansion and averaging procedure is described which reduces the computation of bulk properties to a calculation for a single cell. The idea of transport numbers (a proportionality constant between ion transport and electric field vectors) in electrolytes is introduced and it is shown that this idea applies to bulk tissue. Estimates of the coefficients in the averaged equations are computed numerically for different geometries and a range of microscopic parameter values including cell size, membrane conductance, intracellular conductivity, extracellular space fractional volume. An important finding is that theoretical transcellular current, i.e., the bulk current flow through disconnected cells, is significant and relatively

insensitive to several of these parameters, in particular cell size and membrane conductance.

The role of electrotonic parameters (the parameters involving electrical constants) in the tissue model is discussed and a formal analogy between transcellular current and electrostatic polarization is introduced as an aid to physical understanding of the transport properties of arrays of disconnected (physically separated) cells. Asymptotic analyses of the electrotonic parameters are performed in order to supplement the numerical solutions with qualitative results, and it is shown how to incorporate asymptotic assumptions about these parameters into an asymptotic model.

The properties of steady solutions to the averaged equations are discussed and it is shown that some coefficients of the equations cannot be estimated in a steady experiment. It is argued that the general model proposed here is simpler and more appropriate than cable theory for bulk tissue. For example, it is concluded that specialized transfer cells are unnecessary to explain transcellular flux and spatial buffering, that disconnected cells cannot be neglected, and that cells of differing sizes may contribute significantly to transcellular flux. Since transcellular flux is significant and insensitive to geometry and intracellular conductivity in our model, our results imply that spatial buffering occurs very generally.

This model is chosen to include most measurable quantities such as extracellular potential and extracellular K^+ concentration, and to be mathematically simple. Since it is shown that the bulk parameters of the model are relatively insensitive to many of the microscopic parameters of the tissue, the resulting governing equations should be applicable to many physiological

situations.

TABLE OF CONTENTS

List of Tables

List of Figures

ACKNOWLEDGEMENT

' When the mind wills to recall something, this volition causes the little [pineal] gland, by inclining successively to different sides, to impel the animal spirits toward different parts of the brain, until they come upon that part where the traces are left of the thing which it wishes to remember; for these traces are nothing else than the circumstance that the pores of the brain through which the spirits have already taken their course on presentation of the object, have thereby acquired a greater facility than the rest to be opened again the same way by the spirits which come to them; so that these spirits coming upon the pores enter therein more readily than into the others'.

R. Descartes (1664)

Passions of the Soul.

Part I, Article 42

' The concept of the brain cell microenvironment rests on a triadic relationship, as yet very incompletely defined, between neuron, glia, and the encompassing extracellular space. Glia remain the least categorized element and for this reason are sometimes included as constitutents of the microenvironment and sometimes not .... Ambiguity of definition is desirable in our present ignorance because too much rigor would stifle imaginative conception. The brain cell microenvironment does indeed resemble that of a social environment, such as a city, where both structure and space play constantly varying roles in the total ambience.'

C. Nicholson, (1980)

Dynamics of the brain cell microenvironment.

Neuroscience Research Program Bulletin, Vol.18, no. 2, p185.

' The postulate that the transfer cells form a syncytium is not strictly necessary. Independent transfer cells with processes that overlap with their neighbours by distances much greater than their electrical space constants would behave in essentially the same way. '

A. Gardner-Medwin (1983 b)

Analysis of potassium dynamics in mammalian brain tissue.

Journal of Physiology, Vol.335, p397.

I. GENERAL INTRODUCTION

1.0. OBJECTIVES

Studies of the brain from a variety of points of view, e.g., experimental, theoretical, microscopic, macroscopic, vertebrate, invertebrate, functional, structural, chemical, electrical, etc. have enormously increased our understanding of many different brain phenomena.† Current research on <u>excitable</u> cells seeks to understand the sub-microscopic processes controlling the permeation (passage) of <u>ions</u> through the membrane which imbue the membrane with so called <u>active properties</u>. The behavior of single ion conducting channels is being studied in experimental electrophysiology, molecular biology, and by theoretical means. From a more general point of view these studies are valuable for at least the following reasons. Firstly, the study of the brain ultimately may illuminate the nature of thought and behavior, as Descartes realized (see page xi). Secondly, the medical treatment of pathological conditions such as <u>epilepsy</u> requires a basic scientific understanding of brain function.

Since the operation of the brain depends upon physical and chemical mechanisms, the physics and chemistry of the nervous system are relevant to thought and behavior, to medicine, and to the principles of brain function. The present work is intended to advance the understanding of the physics of brain function.

---

† For a general introduction to neurophysiology, the reader is referred to a reference such as Kandel & Schwartz, (1983). While it is not possible to provide a detailed introduction to neurophysiology here, many terms which may not be familiar to every reader will be defined. Despite Nicholson's remark (see page iii), which referred to nomenclature rather than mathematical definitions, definitions are essential to construction of models. Biological terms which are standard, but which may not be familiar to mathematicians such as <u>anion</u>, <u>membrane</u>, etc. are underlined and defined in the glossary which appears at the end of this introductory Chapter.

1

In this thesis a mathematical model of electrical potential and ionic concentrations in mammalian nervous tissue is derived, as much as possible, from first principles. The resulting equations are analysed, solved numerically, and the physiological implications of the analysis are discussed. Our ultimate aim is to produce a single model for the macroscopic electrical and ionic properties of neural tissue, so that results on tissue conductivity, ion transport, cell swelling and electrical potential can be correctly incorporated within the same model. Here, we derive and solve (approximately) an equation for the membrane potentials of a collection of electrically discontinuous potassium permeable cells of differing physical and electrotonic lengths, subjected to an electric field, and spatially varying potassium concentration.

Many of the interesting aspects of brain function, the most important example of which is behavior, occur at a macroscopic scale, involving the joint activity of many cells. Understanding the physical processes underlying membrane potential changes in individual cells is generally recognized to be inadequate, in itself, to account for learning, memory, and the computing capabilities of the brain (Kandel & Schwartz, 1983, p11,23; Lashley,1950). For this reason it is desirable to study the properties of large numbers of cells in bulk.

The cells which are thought to be important in most present theories of brain function are <u>neurons</u> (Kandel & Schwartz, 1983; Hebb, 1955,1958). While the active properties of neurons are seen as the primary mediators of brain function, many significant manifestations of active properties such as neuronal firing rates are sensitive to the <u>resting transmembrane potential</u>. The resting transmembrane potential is determined to a great extent by the prevailing electrical potential gradients within the tissue and the extracellular concentration

of potassium. Thus, an essential preliminary to the study of active properties in bulk tissue is an understanding of the factors affecting the electrical potential gradients and extracellular potassium concentration.

The present work is a theoretical study of these factors. The work will be directly relevant to several types of experiment; namely those which involve electrical brain stimulation, measure ionic concentrations in tissue, measure effective bulk physical properties of tissue, such as impedance or diffusion coefficient, or involve electrically mediated potassium transport (which is discussed in detail below). From an understanding of the factors influencing these parameters, (indirect) inferences may be drawn as to the electrical and ionic 'microenvironment' or ambient conditions experienced by neurons (Nicholson, 1980) in vivo and hence about processes of direct physiological interest. Along with the modelling of ion homeostasis, the determination of bulk current-voltage relations is an essential step in developing accurate continuum models of gross phenomena in the nervous system, such as spreading cortical depression (Tuckwell & Miura, 1978) and epilepsy (Prince, 1978).

The use of mathematical models in modelling microscopic properties is well established (Hodgkin & Huxley, 1952 d). In the present chapter the classical (microscopic) model of the neuron is described and we indicate how basic physics as embodied in the cable equation (described below) has influenced theory and experiment. The relatively new field of macroscopic neural modelling is briefly described, with its connections to neuroanatomy and the brain cell microenvironment. If successful, the theory of tissue properties presented here will play a role in macroscopic modelling analogous to the role of cable theory in discussions of the neuron.

The general mathematical problem is to determine the bulk average flow of an ion which flows according to the Nernst-Planck equations in an inhomogeneous medium containing periodically placed inclusions. Inside these inclusions the ionic concentrations and electrical conductivity are different from the surrounding medium, and the inclusions are surrounded by barriers (membranes) across which jump conditions are satisfied, relating the sizes of the discontinuities in electrical potential and ionic concentrations to the flux across the barrier. The solution of this mathematical problem will be applicable to the flow through tissue of permeating ions.

Related abstract mathematical problems are discussed in Bensoussan et al., (1978). There, it is shown how to construct formal multiple scale solutions to these related problems and the convergence of these expansions is proved under various assumptions. The application of such techniques to determining the average properties of inhomogeneous media is called homogenization. The application of the technique to the Nernst-Planck equations, and to the type of inhomogeneous medium described here is new, however. Exposition of the details of this reduction, solution, and interpretation of the mathematical problem and its application to ionic homeostasis form the substance of this thesis.

There are some novel physical features in our derivation. The final averaged equations for the membrane potential are non-linear. Each biological cell generates current through the extracellular space because of variations in the ionic Nernst potentials along its length. When the flux lines of these (or other) current sources pass through the membranes of adjacent cells, ions must enter/leave the extracellular space, thus complicating the description of the ionic concentration profiles.

2.0. PHYSIOLOGY AND PHYSICS DEVELOP IN PARALLEL

It will clarify the objectives to state our view of the relationship between neurophysiological phenomena and mathematical models of them, and to briefly review the history of this relationship.

Rene Descartes (1545-1650) the French philosopher, was one of the first writers to formulate a neurophysiological model different from those of the Greeks. While his model was not mathematical, the model sketched in the introductory quotation (see page xi) is similar to modern neurophysiological models because of its dependence on physical mechanisms.

Later, physiological models became more detailed in order to accommodate the measurements of a more mature physics and improved instrumentation technology. Once techniques had been invented to measure electrical phenomena, theoretical electrical mechanisms replaced the hydraulic physiological mechanisms postulated by Descartes, and theories began to be tested.

In his memoir of 1791, Luigi Galvani described the response of a frog nerve-muscle preparation to electrical stimulation from a sparking machine, atmospheric electricity, and a bi-metallic arc. The galvanometer was invented by Ampere and Babinet (1822); and the 'action current' of muscle and nerve† was discovered by du Bois-Reymond in the 1840's (e.g., du Bois-Reymond (1848,1849)).

Theoretical developments in physics also influenced the development of neurophysiology. Maxwell's Treatise on Electricity and Magnetism appeared in 1873, and the Nernst-Planck equations for diffusion of charged particles in an electric field were formulated about 1890. The availability of these equations was

---

† In modern terminology, the 'action potential' or 'nerve impulse'.

a factor in the development of several theories of ionically mediated bioelectric phenomena by Nernst (1899), Cremer (1906,1909), and Bernstein (1912) in the early part of this century.

The roles of ions and of electricity in physiology are inseparable. The dissociation of electrolytes in water into charged species called 'ions' was demonstrated by Arrhenius in 1883. Theories of bioelectric phenomena prevalant since the late nineteenth century depend on the potassium ion, (K^+), and other ions such as sodium, (Na^+), and chloride, (Cl^-) (Biedermann, 1895; Ostwald, 1890; Donnan, 1911). The apparently disparate topics of tissue electrical properties and ion transport are intimately intertwined from the physiological point of view.

In the post-World War II period, Hodgkin and Huxley (1952 a-d) used a mathematical model to describe the action potential as a regenerative change in ionic permeability of nerve cell membrane and this model is accepted today in most essential features. Their theoretical work was confirmed by detailed measurements using the (then) new technique of the voltage clamp, and clever experimental protocols.

Thus, since the eighteenth century, mathematical theory in physiology has advanced in tandem with physical theory and measurement techniques.

Recently, the invention of ion-selective micro-electrodes has made possible the in vivo recording of variations in extracellular ionic concentrations within nervous tissue (Zeuthen, 1981). To complement this development, a more detailed and rigorous mathematical theory of ion transport in inhomogeneous media would be valuable.

Following Aris (1978) a mathematical model may be defined as: 'any

[mathematically] complete and consistent set of mathematical equations which is thought to correspond to some other entity, its prototype.' By enforcing mathematical consistency among the relations of the model it is possible to summarize empirical relations economically, discover sources of inconsistency, and to formulate new testable hypotheses. A mathematical model applicable to neurophysiology will serve these purposes for neurophysiologists. Therefore, an applicable model must be tractable, and logical completeness does not entirely determine its value. However, it is necessary to accommodate relevant physical measurements which are presently possible.

3.0. NEURONS AND GLIA

Biological cells consist of <u>cytoplasm</u> and cell <u>organelles</u> surrounded by a lipid membrane.†

Anatomists of the eighteenth century believed that the brain was glandular and considered nerves to be ducts which conveyed the secretions of the brain to the periphery. The foundations of modern neuroanatomy were laid by Santiago Ramon y Cajal and Camillo Golgi in the nineteenth century (Cajal, 1892; Golgi, 1906) who (with others) developed the histological techniques such as the silver impregnation method (which allowed the visualization of an individual nerve cell in a tissue slice containing many cells) and the conceptual foundation which led to the modern view of the neuron as the primary active element in brain function.

Neurons are excitable cells, and they are able to transmit information

---

† The topics of these sections are technical, but treated in standard modern textbooks (e.g., Kandel & Schwartz, 1983; Jack <u>et</u> <u>al.</u>, 1975). Material to be used here will be given in self-contained form, but with relatively little commentary.

down the long process of the neuron, called the axon, by means of propagating action potentials.

The central nervous system of humans consists of some 10^{11} neurons of which 10^{10} are in the cerebral cortex. Neurons are surrounded by satellite cells, glia in the brain, and other morphologically distinct cells in the peripheral nervous system. Central glia are classified by morphology and location into astrocytes, oligodendrocytes, microglia, and ependymal cells and outnumber central neurons by about nine to one. The functions of glia have not been completely elucidated and have been the subject of increased speculation and experiment (Varon & Somjen, 1979; Walz & Hertz, 1983). Glia contribute a third to a half of the total intracellular volume, and are found in close association with both blood vessels and neurons. Because astrocytes typically possess many radiating processes they contribute a substantial fraction of the large membrane surface area separating the intracellular and extracellular spaces in brain tissue (Hertz, 1982). † Oligodendrocytes are physiologically important because they form the myelin which coats the axons of central neurons; however, data on the differences between the physical properties of astrocytes and oligodendrocytes are only recently becoming available (Hertz, 1982; Pevzner, 1982; Kettenman, et al., 1984 b), and data about other types of glia are sparse. The functions of glia other than astrocytes and oligodendrocytes have not been established. Because of this lack of data we will not differentiate between types of glia in this thesis.

Ions do not easily cross a lipid membrane; however, neural membrane contains pores which selectively permit the passage of certain ions such as K^+ and Na^+, and Cl^-. A pore which selectively passes potassium ions is called a

† The surface volume ratio in mammalian brain has been estimated at $5\mu^2$ per μ^3 of tissue (Horstmann & Meves, 1959).

potassium channel and a pore which selectively passes sodium ions is called a sodium channel. The abundance and properties of different membrane channels determine the permeability of the membrane to each ion. The states of these channels, and hence, the membrane permeabilities, may depend on the electrical potential difference across the membrane, as discussed in Section 5.0. In addition, the states of some membrane channels are governed by chemical factors released by neurons at synapses during synaptic transmission.

The passage of cations (positively charged ions) out of the cell, or anions (negatively charged ions) into the cell constitutes an outward electric current. For neurons and glia the intracellular potassium concentration, $[K^+]_i$, exceeds the extracellular potassium concentration, $[K^+]_o$, (where the subscripts i and o refer to intracellular and extracellular concentrations, respectively), and vice versa for $[Na^+]_i$ and $[Na^+]_o$. Because the concentrations of the ions inside and outside the cell are different, they tend to move across the membrane, carrying electrical charge with them. The resulting transmembrane electrical potential (inside potential minus outside potential) opposes the chemical gradient due to the concentration differences. A resting transmembrane electrical potential, V_r, is attained when the net transmembrane current remains zero.

If a membrane is permeable to only one ion, the transmembrane potential V_i associated with zero net transmembrane current is given by the Nernst equation:

$$(3.1) \qquad V_i = \frac{RT}{z_i F} \ln(C_i^o / C_i^j)$$

where

C_i^o is the extracellular concentration and C_i^i is the intracellular concentration of the ion and z_i is its ionic valence.†

When the membrane is permeable to several ions, the transmembrane potential is more difficult to calculate. In this case, the physics are approximately governed by the Nernst-Planck equations discussed in Chapter II, however, the internal parameters of the membrane and the correct physical model for the membrane are not certain (Plonsey, 1969; McGillivray & Hare, 1969). Such difficulties cannot be resolved by theoretical analyses alone. For this reason, we assume (Hodgkin & Huxley, 1952 a-d; Kandel & Schwartz, 1983) that the resting transmembrane potential satisfies the Goldman-Hodgkin-Katz equation (Goldman, 1943; Hodgkin & Katz, 1949):

$$(3.2) \qquad V_r = \frac{RT}{F} \ln\left(\frac{P_1[Na^+]_o + P_2[K^+]_o + P_3[Cl^-]_i}{P_1[Na^+]_i + P_2[K^+]_i + P_3[Cl^-]_o} \right)$$

where R is the gas constant (joule $K^{-1}mol^{-1}$), F is Faraday's constant, T is the absolute temperature, and the subscripted quantities P_i, $i = 1,2,3$ are the permeabilities of the membrane to Na^+, K^+, and Cl^-, respectively. This equation is empirically correct for the squid axon, (Hodgkin & Katz, 1949) which is the classical physiological model for nerve membrane, and may be derived heuristically from the Nernst-Planck equations assuming that the electric field within the membrane is constant and separate ionic fluxes are uncoupled. When the permeability to sodium, P_1, and to chloride, P_3, are zero, equation (3.2)

---

† Equations are numbered consecutively within Sections. Thus, the first equation of Section 3 of Chapter I is equation (I.3.1). Subsection numbers do not appear in equation numbers and the Chapter prefix is only used to refer to equations from other Chapters.

reduces to the Nernst equation (3.1) for potassium.. This assumption about the sodium and chloride permeabilities is supported by most reports on glial cells (Varon & Somjen, 1979), and (3.1) approximates the resting potential for neuronal membrane, presumably because P_2 is relatively large.

Although the net transmembrane current at rest is zero, the membrane may admit net fluxes of K^+, Na^+, and Cl^-. A steady concentration of these ions in the cytoplasm is maintained by the sodium-potassium pump; (Glynn & Karlish, 1975), a complicated assembly of protein subunits in the membrane which exchanges external K^+ ions for internal Na^+ at the expense of metabolic energy. Transport of ions which utilizes metabolic energy is called active transport, (Kandel & Schwartz, 1983). The distribution of anions between the cytoplasm and extracellular region may be determined by the distribution of cations. The net charge of the cell interior relative to the extracellular region is limited by the small capacitance of the membrane, so that the total electrical charges of intracellular anions and cations are equal. In the invertebrate nervous system, the distribution of ions in extracellular space is influenced by the presence of negative charges on molecules in the intercellular clefts. Because diffusion in the mammalian brain is unaffected by the charge of the diffusing ion, (Nicholson & Phillips, 1981) and in view of other evidence (Gardner-Medwin, 1983a) this effect is not considered here. The distribution of specific anions, especially Cl^- and HCO_3^-, may be modified by an anion transport system (Kimelberg & Bourke, 1982) in some cases. We will not model active transport of ions in this thesis, however. Unless otherwise stated it is simply assumed that the active transport flux is chosen to cancel the net transmembrane fluxes of K^+ and Na^+ over the entire cell at the resting potential.

It is assumed that neural membrane is of two types. First, glial membrane, which has a fixed permeability to K^+ (Pape & Katzman, 1972; Somjen & Trachtenberg, 1979) and exhibits a membrane potential given by (3.1), and second, neuronal membrane which has voltage- and time-dependent permeabilities to K^+, Na^+, and Cl^- with resting potential given by (3.2). The separate transmembrane ionic fluxes I_i are assumed to follow the equations:

$$(3.3) \qquad I_i = g_i(V - V_i)$$

where I_i is the outwardly directed flux of the ith ion, V is the transmembrane potential, V_i is the Nernst potential for the ith ion, and g_i is the ionic conductance of the membrane for the ith ion (mS). Each of I_i, g_i, V, and V_i is, in general, a function of space and time. For the case of glial membrane it is assumed that the g_i are fixed, and equal to zero for all ions except K^+. For neuronal membrane, the g_i will vary in a manner to be described.

These assumptions about neural membrane are simplifications of the real membrane properties of central neurons which are not completely known (Crill & Schwindt, 1986). For example, dendritic membrane has a significant permeability to the calcium ion Ca^{2+} at some membrane potentials (Kandel & Schwartz, 1983). This permeability is not expected to have a large influence on potassium concentrations, which are the focus of this work. Techniques which permit voltage clamp experiments on isolated microscopic patches of membrane have led to the recent discovery of many channels with varying properties, (e.g. Sonnhof, 1987) and the detailed characterisation of those already known (Aldrich et al., 1983).

The attempts to understand brain function have involved many different

types of experiment. The underlying purpose of such experiments is to understand physiological processes in vivo . However, for such understanding to be made precise in a mathematical model, it is necessary to obtain measurements of cell and tissue characteristics under controlled (or known) physical conditions, e.g., from in vitro experimentation.

4.0. BULK TISSUE PROPERTIES

4.1. Electrical Properties

The first systematic study of the effect of electrical brain stimulation was made by Fritsch & Hitzig in 1870, on the motor cortex of the dog. The first recording of electrical activity from the brain was reported by Richard Caton in 1875. The recent experimental literature on electrical currents in the brain is too vast to summarize here, though early references may be found in Brazier (1961). In this section we discuss the models which have been used to predict the passive electrical properties of cells and tissue.

The extensive use of electrophysiological methods as an investigative tool is an important reason to establish the bulk current-voltage relations of cerebral tissue. For example, the bulk current-voltage characteristics of cerebral tissue must be known in order to compute the distribution of current injected during stimulation experiments (Ranck, 1975), to compute the distribution of current sources in the cerebral cortex (Nicholson, 1973), or to interpret the impedance characteristics of neural tissue (Ranck, 1964).

When neurons are stimulated electrically with sufficiently small voltages, action potentials are not generated. Under these circumstances, the intracellular, extracellular, and transmembrane electric potentials are described by the classical

Maxwell governing equations for electricity in a conducting and/or dielectric medium. Neural signalling which depends on such phenomena is called electrotonic transmission. Electrotonic transmission in neurons or other cells depends on cell geometry, membrane properties, and electrical properties of the extracellular and intracellular media.

The use of the cable equation (described below) as a model for electrotonic transmission in the neuron is well-established (Jack et al., 1975). Generalizations of the cable equation have been discussed for branching structures, (Rall, 1959, 1969) bundles (Clark & Plonsey, 1970, a, b), and syncytia (Jack et al., 1975). The cable model and its generalizations are useful and are the motivation of much experimental work on the microscopic electrical properties of neural tissue (Pellionisz & Llinas, 1977; Johnston, 1980; Stafstrom et al., 1984; Turner & Schwartzkroin, 1984).

Because the nervous system is complex both microscopically and macroscopically, modelling of bulk tissue properties has not been attempted often (Ranck, 1964; Havstad, 1976). The lack of theory for the bulk electrical properties of tissue is particularly noticeable. For example, the first modern review of the distribution of stimulating electrical currents is due to J.B. Ranck (1975). General results on the bulk electrical properties of neural tissue (apart from ion transport) are useful in themselves (cf. Nicholson, 1973) because of their application to such experiments.

Cerebral tissue is an inhomogeneous medium of considerable complexity. In particular, conductivity varies with the direction and (more subtly) with the length scale on which it is being measured (Ranck & Bement, 1965; Nicholson & Phillips, 1981). This is because tissue elements which are sufficiently extended

relative to the distance between electrodes will alter impedance measurements in a complicated manner related to this distance.

Several treatments of the conductivity of cellular tissue have previously been published, (Ranck,1963; Nicholson, 1973; Nicholson & Freeman, 1975; Havstad, 1976; Eisenberg et al., 1979; Gardner-Medwin, 1983;). These treatments have modelled the effects described above in various ways. The two main assumptions used in electrophysiological models for the electrical potential in bulk tissue are the syncytial assumption (Jack et al., 1975) and the assumption of infinite membrane resistance (Nicholson, 1973). It is also possible to discuss effective bulk conductivity from an empirical point of view, so that no specific assumption about current through cells is made (Nicholson & Freeman, 1975). As discussed later in this chapter, however, current through cells is an important part of the present work.

In electrophysiology, the term syncytium refers to a collection of distinct biological cells whose intracellular regions are electrically continuous with each other, possibly due to gap junctions. The syncytial assumption is known to be valid for invertebrate glia (Varon & Somjen, 1979).

Equations describing the electrical potential in syncytial tissue were discussed by Jack et al., (1975), Eisenberg et al., (1979), Mathias et al., (1979), and Peskoff (1979). Syncytial tissues have been modelled by three-dimensional versions of cable theory assuming the extracellular and intracellular spaces are extensively interdigitated.

The existence of a glial syncytium in mammalian cortical tissue is still controversial. While intercell junctions have been observed (Varon & Somjen, 1979) and there is electrophysiological evidence of coupling between some glial

cells (Somjen, 1984; Schoffeniels et al., 1978), studies of bulk properties do not suggest that there is extensive coupling in mammalian tissue (Hounsgaard & Nicholson, 1983; Gardner-Medwin, 1983 a, b). In view of the complex nature of cerebral tissue, it is desirable to investigate the statement that isolated cells can behave like a syncytium and to investigate alternative models for bulk tissue.

The assumption of infinite membrane resistance implies that extracellularly generated currents cannot pass through neurons and glia, which therefore form opaque obstacles to current flow. The problem of determining the electrical potential in tissue under this assumption is formally equivalent to the problem of determining the steady concentration profile of a non-permeating ion in neural tissue. Both the electrical potential and steady concentration satisfy Laplace's equation in the extracellular space and no flux conditions at the cell membranes.

If the classical equations of electricity govern the extracellular potential and membrane resistance is infinite, then according to porous media theory, (Gray & Lee, 1977) the bulk electrical potential may be described by an equation in which the effective conductivity is a tensor $\vec{\sigma}$ (Nicholson, 1973) and the extracellular electrical potential ϕ satisfies

$$(4.1) \qquad \sum_{p=1}^{3} \sigma_p \frac{\partial^2 \phi}{\partial x_p^2} = i$$

where σ_p, $p=1,2,3$, are the constant components of $\vec{\sigma}$, i is a current source density, (possibly due to the currents generated by action potentials) and the potential ϕ is an average, defined in some appropriate way. Equation (4.1) is shown later to be valid under our more general assumptions when extracellular

ionic concentrations are constant, and the averaging procedure is specified precisely. The explicit dependencies of $\vec{\sigma}$ on geometry, the conductivities of the intracellular and extracellular media, and membrane resistance have not been calculated.

The assumption of infinite membrane resistance has been useful in the interpretation of field potentials (Nicholson & Freeman, 1975) because the fraction of extracellular current which passes through cells is small in many experimental paradigms. However, evaluation of the anisotropy of conductivity measurements in mammalian cortex (Gardner-Medwin, 1980) suggests that electric current passes through cells in sufficient quantity to appreciably influence the bulk resistance of neural tissue. Most importantly, because electrically mediated potassium transport occurs chiefly by means of current flow through cells, it would be inappropriate to employ the assumption of infinite membrane resistance in the computation of ion transport properties. For example, in Gardner-Medwin's current passing experiment, the small fraction of imposed current which passed through cells apparently accounted for a significant potassium flux.

The formulation of more general systematic physical models for tissue electrical potential might help to resolve difficulties in the interpretation of electrophysiological data in bulk tissue (cf. Somjen & Trachtenberg, 1979). For example, it is not known whether high or low membrane resistance of the cells (neurons or glia) might favor electrically mediated ion transport in tissue which is not syncytial.

4.2. Ion Transport Due to Diffusion and Spatial Buffering

In this thesis the term "transport" usually refers to the flux of some conserved quantity, such as net electric charge or an ionic species, in response to a gradient of intensity (e.g., potential, concentration) of that quantity (cf. Batchelor, 1974).

While electrophysiology dates from the mid-nineteenth century (du Bois-Reymond, 1848; Helmholtz, 1850,a,b) the concomitant measurement of ionic effects has become possible only recently. Experiments with squid axon to measure transmembrane ionic fluxes using radioactive tracers date from the 1950's (Hodgkin & Keynes, 1957), while useful ion selective microelectrodes became available only in the 1960's (Zeuthen, 1981; Nicholson, 1980). Thus, some of the electrophysiological literature does not explicitly treat ions and it is indeed possible to obtain theoretical predictions about electrical properties of tissue without including ionic effects.

Recently, it has become clear that within the mammalian central nervous system, physiological states such as spreading depression (Leão, 1944; Grafstein, 1956) and seizure activity (Moody et al., 1974; Fisher et al., 1976; Futamachi et al., 1979) can give rise to spatial variations in extracellular $[K^+]$. These spatial variations can vary in their characteristic spatial wavelengths from several mm to .5mm (approximately half the length of a Purkinje cell arborization). Thus, these variations have spatial wavelengths which are long compared to most cortical cells.

Potassium release occurs during nervous activity due to K^+ efflux from neurons during the repolarization phase of action potentials. Spatial gradients in depth presumably develop because K^+ release is primarily from the cell bodies

of neurons, which are concentrated in particular layers of the cortex (Futamachi et al., 1974; Moody et al., 1974; Sypert & Ward, 1974). Spatial gradients parallel to the surface of the cortex may occur because of an advancing wave of spreading depression, which is always accompanied by drastic changes in extracellular ion concentrations. The potassium released under the conditions described above is cleared from bulk tissue by several mechanisms, including active transport, diffusion, and spatial buffering.

The diffusion of ions in neural tissue is different from diffusion in a medium without cells because ions do not move freely across cell membranes. Solution of the diffusion equation for non-permeating ions is complicated by the tortuous geometry of the medium. In the physiological literature (Nicholson & Phillips, 1981) diffusion of non-permeating ions has been described by the equation:

$$(4.2) \qquad \frac{D}{\lambda^2} \nabla^2 \overline{C} \; + \; \frac{Q}{a} \; = \; \frac{\partial \overline{C}}{\partial t}$$

where D is the diffusion coefficient, a is the extracellular space volume fraction, Q is a source density and $\overline{C}$ is an averaged local extracellular concentration. The constant λ is a dimensionless geometrical factor called the tortuosity factor. Equation (4.2) is not the most general equation for diffusion in an inhomogeneous medium, because it has been assumed that diffusion is isotropic.

Assuming that the diffusion equation holds extracellularly for a non-permeating ion, the theory of porous media (Lehner, 1979; Gray & Lee, 1977) shows that equation (4.2) is a correct description of steady diffusion in a geometrically complicated medium, provided that the average is taken in an

appropriate way. The averaging procedure is precisely specified, and equation (4.2) can be derived using this procedure if there are no electrical forces and the ions are non-permeating. The explicit relation between λ and the geometry and parameters of the medium has not been determined in a physiological context. The constants a and λ have been determined empirically, however, for non-permeating ions in brain tissue (Nicholson & Phillips, 1981). The factor λ is approximately 1.5, and a about .2, in mammalian cerebellum and cerebral cortex.

Because potassium ions K^+ cross cell membranes under resting conditions, equation (4.2) is not appropriate for accurate computation of potassium spatial transport. The approach taken in this work will lead to the derivation of a more appropriate governing equation.

The gradients of $[K^+]_o$ described above give rise to electrical currents which cause an electrically mediated transfer of K^+ from regions of high $[K^+]_o$ to regions of low $[K^+]_o$, a transport mechanism called spatial buffering. Electrically mediated spatial transport of potassium was first described by Orkand et al., (1966) and is usually attributed to glial cells. In detail, the mechanism may be explained as follows. Glial and resting nerve membranes are predominantly permeable to K^+. Thus, extracellular $[K^+]$ is the primary factor determining the local transmembrane potential (cf. (3.1)). When the transmembrane potential varies along the length of an electrically continuous elongated cell, the longitudinal voltage gradient causes current flow through the cells and extracellular space.

A displacement of the membrane potential V toward zero is called a depolarization and a displacement of the membrane potential toward more negative potentials is called a hyperpolarization. Higher $[K^+]_o$ corresponds to

depolarized transmembrane potentials, and lower $[K^+]_0$ to hyperpolarized transmembrane potentials relative to the resting value. When a single cell is exposed to a spatial gradient of $[K^+]_0$ the local Nernst potentials (3.1) become different at different points of the cell. Since a return path for the current exists via the intracellular and extracellular media, a closed current loop is formed which passes inward through the cell membrane at one point, goes through the intracellular space, passes outward through the membrane at another point, and finally completes the loop through the extracellular medium (see figure I-4.1).† As a result of this current flow, the true transmembrane potentials differ slightly from the Nernst potentials; and these differences will be precisely calculated in subsequent chapters. In addition to the currents described, extracellular current may be imposed on tissue due to the mass firing (production of action potentials) of many neurons (Nicholson & Freeman, 1975) or by an experimental current generator, and these currents may result in transmembrane currents which enter cells at one location and leave at other remote locations.

When electric current flows in a liquid medium containing ions (electrolyte) the flow of charge is due to the movement of ions through the medium. Charge flux or current is defined by (mol sec^{-1} cm^{-2} or amp $sec^{-1} cm^{-2}$)

$$(4.3) \qquad \vec{I} = \vec{J}_C - \vec{J}_A$$

where the flux of cations, $\vec{J}_C$, and of anions, $\vec{J}_A$, are the sum, respectively, of the signed fluxes of each cation and anion in the solution. The symbol $\vec{J}$ will be used to denote a flux which consists of the weighted sum of several ionic fluxes,

---

† The first figure of Section 4 of Chapter I is numbered I-4.1, and so on.

Figure 4.1. The spatial relationships between extracellular K^+ concentration, depolarization/hyperpolarization of biological cell membranes, and the flux of K^+, Na^+, and Cl^- ions results in the transport of K^+ from regions of high to low concentration.

Figure 4.1
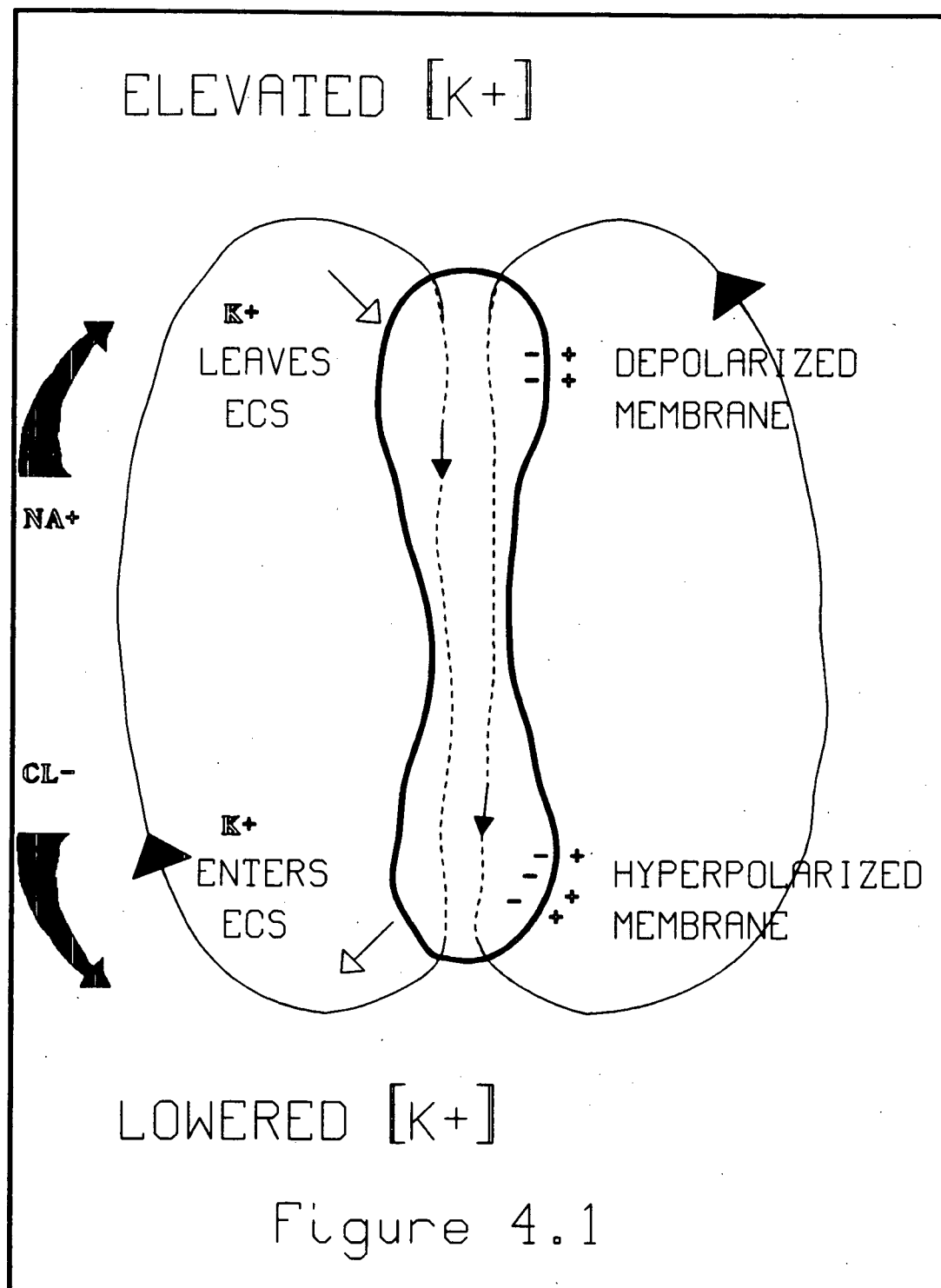
while $\vec{j}$ will be employed to denote a specific ionic flux.

If electric current in an electrolytic medium consisted entirely of the flux of potassium, then by conservation of current, no concentration changes of potassium would occur along the current path. However, only about 1.2% of extracellular currents consist of potassium flux (Gardner-Medwin, 1983). Extracellular currents consist mainly of sodium and chloride fluxes, while transmembrane and intracellular currents consist mainly of potassium flux. Hence, in the current loop described above, a net efflux of potassium occurs from the extracellular space at one location and a net influx occurs at others, with the result that local $[K^+]_o$ is altered. Other sources of extracellular current such as those due to an experimental source may also modify $[K^+]_o$.

Such spatial transport of potassium (or other ions) by electric current will be referred to as electrically mediated spatial transport. Reference to Figure 4.1 shows that when current loops result from spatial gradients of $[K^+]_o$, the effect of electrically mediated spatial transport is to reduce $[K^+]_o$ where it is high and to increase $[K^+]_o$ where it is low. Therefore, this phenomenon is called spatial buffering.

To estimate the magnitude of these effects, A. Gardner-Medwin (1983 a, b; Gardner-Medwin & Nicholson, 1983) performed experiments in which electric current was passed through brain tissue and the consequent movement of K^+ ions was measured. Current was passed perpendicular to the cortical surface through fluid contained in a circular cup placed on the cortical surface. The potassium contents of the cup was monitored during current passage. It was verified by means of intracellular recording and application to the cortex of tetrodotoxin (TTX), a pharmacological agent which suppresses the generation of

action potentials by acting upon sodium channels, that the observed effects were independent of any effect on action potentials of current passage. For some experiments, the extracellular potassium concentration, $[K^+]_o$, was monitored at various depths in the cortex beneath the cup. Finally, the results were interpreted according to a theoretical model. The results were consistent with the conclusion that electrically mediated potassium (spatial buffer) flux is about five times the diffusive flux for potassium distributions varying over distances much greater than 200 μm in the rat brain. The theoretical model was necessary because spatial buffering and diffusion both result from spatial gradients of $[K^+]_o$, so that the results of such an experiment are confounded, and theoretical assumptions must be made in order to attribute a definite fraction of the potassium flux to either diffusion or electrically mediated flux.

The theoretical model for the tissue electrical potentials used by Gardner-Medwin to interpret data was the cable model. It was assumed that intracellular current flowed through a coupled cell population in the cortex, called 'transfer cells', and that intracellular current consisted of potassium flux. However, the cell population which was supposed to be the substrate of the cable equation was not identified. Thus, it was necessary to estimate the parameters of this putative population from the data. This procedure, while useful, does not indicate the relationship between the observations and independent measurements of the microscopic parameters of cell populations.

5.0. NEURAL MODELLING

In this section we summarize Hodgkin and Huxley's model of the action potential. The relation between models for active and for electrotonic properties of nerve is illustrated for the case of Hodgkin and Huxley's model. This is expected

to be instructive in evaluating the present work, though it is well-known to the biological reader. While the Hodgkin-Huxley equations were originally developed for the squid giant axon, they represent the classical physiological model of the action potential, which is assumed (Crill & Schwindt, 1983, 1986) to apply to the neurons in mammalian central nervous system in some possibly generalized form. For example, dendritic membrane exhibits action potentials based on the voltage dependent calcium permeability (Kandel & Schwartz, 1983).

By means of a series of experiments Hodgkin and Huxley, (1952a-d)† were able to formulate quantitative descriptions of the quantities g_i in equation (3.2) for the squid axon. It was found that the transmembrane current could be satisfactorily described as the sum of the capacitive current, I_C, the potassium current I_K, the sodium current, I_{Na}, and the current carried by chloride and other ions, I_l, called the leakage current. Thus, the total transmembrane current I (μmA cm^{-2}) is given by:

$$(5.1) \qquad I = I_C + I_K + I_{Na} + I_l.$$

The ionic conductances of (3.2) satisfy a set of ordinary differential equations with coefficients depending on the membrane potential V.

An action potential is a rapid (lasting ca. 1 msec) regenerative depolarization of the neuronal membrane as a result of a complicated set of changes in the membrane conductances. It is characterized by a rapidly rising phase in which the membrane sodium conductance increases dramatically, and a

---

† For an elementary account, see Aidley, 1978, or many other standard texts. This model contains explicit hypotheses on the non-linear voltage and time dependent 'active' properties of neurons.

somewhat less rapid return to equilibrium in which the sodium conductance decreases and potassium conductance increases. In general, excitable membranes contain voltage dependent sodium channels (Aidley,1978).

From the experimentally determined formulas describing the ionic conductances, it was possible to reconstruct the action potential, assuming that V_K, V_{Na}, and V_l are constant. When the membrane potential V is constant in space, the associated action potential is called 'space clamped' and does not depend on the electrotonic properties of the axon or cell.

To calculate a propagating action potential, a model for the spatial dependence of the potential is needed. For this purpose, Hodgkin and Huxley employed the core conductor model of Hermann (1879), also known as the cable theory† It is assumed that the axon is an elongated cylinder of uniform cross section aligned with the Z axis, and only the axial coordinate is considered. Since the axon is a three dimensional object, radial current flow must occur, so that these assumptions are artificial in some respects.

The model equations of cable theory are:

$$(5.2) \qquad \partial \frac{I^0_t}{\partial z} = i_m$$

$$(5.3) \qquad I^0_t = - I^i_t$$

---

†. The original cable equation of classical physics is due to Kelvin.

(5.4)
$$\frac{\partial \phi^0}{\partial z} = -r_1 I^0_t$$

(5.5)
$$\frac{\partial \phi^i}{\partial z} = -r_2 I^i_t$$

where I^0_t is the axial current flow in the external medium, I^i_t, the axial current flow in the internal medium, i_m is the transmembrane current per unit length, ϕ^0 is the potential in the external medium, ϕ^i is the potential in the internal medium, r_1 is the resistance of the external medium per unit length, and r_2 is the resistance of the internal medium per unit length, A standard argument using (5.2) - (5.5) yields:

(5.6)
$$i_m = \frac{1}{r_1 + r_2} \frac{\partial^2 V}{\partial z^2}$$

where $V = \phi^i - \phi^0$. For a fibre of radius a, $i_m = 2\pi a I$ and $r_2 = R^i / \pi a^2$ where R^i is the specific resistivity of the cytoplasm (Ω cm). The relation between r_1 and R^0 the resistivity of the external medium is complicated because the three-dimensional current flow is not axial. Because R^0 is small however, Hodgkin and Huxley assumed $R^0 = 0$, and thus obtained:

(5.7)
$$I = \frac{i_m}{2\pi a} = \frac{a}{2R^i} \frac{\partial^2 V}{\partial z^2}$$

The validity of the assumptions (5.2) - (5.5) has been investigated experimentally by Hodgkin and Rushton (1946), and Lorente de No (1947),† and mathematically by Clark and Plonsey (1966). It is found that these assumptions are approximately correct for isolated preparations . In addition, the use of the cable model for the intracellular and transmembrane potentials (but not the extracellular potential) can be mathematically justified by a three-dimensional analysis of the electrical potential (Clark & Plonsey, 1966).

A steady propagating action potential must have the form $V = V(z - \theta t)$, where θ is the conduction velocity. The propagating action potential, which satisfies an equation obtained by equating (5.1) and (5.7) has a propagation speed (or wave speed) θ_0 which is determined from the equations by a numerical iteration procedure.

The propagation speed and the dependence of the action potential on $z - \theta t$ depend upon the simplification (5.7) and the values of a, the fibre diameter, and C_M the membrane capacity. Despite the necessity to estimate these parameters, and the various simplifying assumptions, the predicted propagation speed (18.8m/s) of the action potential (Hodgkin & Huxley, 1952d) closely matched the observed speed (21.2m/s). The use of cable theory was an essential step of this calculation, though the cable model for electrotonic properties is simple.

The role of cable theory in the model of the action potential shows that (microscopic) electrotonic properties of neurons play an essential role in their physiology and it may be anticipated that bulk passive properties will be important in the formulation of any macroscopic model.

---

† I am indebted to Dr. E. Puil for pointing out this fundamental early reference.

5.1. Spreading Depression

Spreading depression (SD) was discovered by the physiologist Leão (1944) during studies of experimental epilepsy in the cerebral cortices of rabbits. SD is characterised by a marked and prolonged depression of the spontaneous electrical activity of the brain. Subsequently, SD has been observed in many brain structures and species (Bures et al., 1974). In addition to the electrical changes, later studies revealed large changes in the normal ionic equilibrium of the brain. Kraig and Nicholson (1978) measured changes in the extracellular concentrations of several physiological ions during SD in the cerebellum, namely, an elevation in the concentration of potassium from 4 mM to 40-50 mM , a fall in the concentration of sodium from 80 mM to 60 mM , a fall in the concentration of calcium from 1.2 mM to .12 mM and a fall in the concentration of chloride from 85 mM to 50 mM. Spreading depression has been observed in cerebellum, olfactory bulb, hippocampus, and in vitro in the slice preparation (Somjen & Aiken, 1984).

This section is intended to indicate what factors must be included in any model of SD which accounts for its observable effects. Neither a review of the SD literature nor an evaluation of competing hypotheses is intended. A satisfactory model must include the factors which interact to produce the primary observable effect, but it need not include epiphenomena which accompany the main phenomenon. The factors producing the main phenomenon will be referred to as mediating factors.

Like the nerve impulse, the experimental phenomenon exhibits a wavelike character but with a (much slower) wave speed of 1-9 mm/min. Also it exhibits recovery since the electrical activity and ionic concentrations of the tissue return

to their original levels after several minutes. A detailed comparison of the SD wave and the nerve impulse may be found in Miura (1981).

These changes may be initiated by a variety of stimuli, including electrical stimulation, mechanical stimulation, and the local application of KCl. The pronounced and robust nature of SD affords a unique opportunity to study the interaction of electrical and ionic mechanisms within neural tissue at a macroscopic level.

Several hypotheses have been advanced as to the mediating factors of SD. During the 1950's it was known that extracellular potassium concentrations increased greatly during SD (the magnitude of the increase was later measured to be 40 - 50 mM, in some preparations (Nicholson & Kraig, 1981)). Grafstein (1956) hypothesized that spreading depression was due to the spread of extracellular potassium, which depolarized neurons and caused further potassium release by means of action potentials. At that time, the role of other released factors such as glutamate, which is an important intracellular anion, (Puil, 1981) was not understood. Van Harreveld (1978) postulated that the principal chemical can be potassium, or the neurotransmitter L-glutamate, resulting in two distinct mechanisms for SD. However, the phenomenon does not depend critically on the generation of (sodium) action potentials. The SD wave is not antagonized by treatment of the cortex with tetrodotoxin (TTX) (Sugaya et al., 1975).

Tuckwell and Miura (TM) (1978) formulated a simplified mathematical model for SD,† which accounts for the essential features of the phenomenon

---

† Our calculations are not intended exclusively to extend the SD model. A detailed evaluation and extension of this model from a physiological point of view, would require experimental work, which is beyond the scope of this thesis. Tuckwell and Miura's work is cited here as a paradigm for macroscopic modelling of neurophysiological phenomena.

(depression of spontaneous brain activity, wavelike propagation, ionic concentration changes, and recovery) by incorporating several physiological mechanisms, well-known through microscopic studies, into a set of equations. Tuckwell and Miura hypothesized that conductance changes in post-synaptic membrane rather than action potentials are responsible for the release of potassium by neurons during SD. The increase in extracellular potassium leads to depolarization of neuronal membrane according to equations (3.1) and (3.2). This depolarization leads to the entry of calcium into pre-synaptic terminals which causes release of neurotransmitter (Katz, 1969; Krnjevic, 1974). The neurotransmitter (likely L-glutamate) acts at post-synaptic (and pre-synaptic) receptor sites, changing the conductivities of post-synaptic neurons and leading to further potassium release. It is not necessary to specify the identity of the neurotransmitter within the mathematical model, and it is possible that other neurotransmitters, such as acetylcholine might play the same or a similar role.

According to this model, propagation of the SD wave depends on the spatial transport of potassium from the site of the initial stimulus to remote regions of the extracellular space. The wave speed predicted by this model is about 1mm/min, which is at the lower end of the observed wave speeds of 1-9mm/min in mammalian cortex. This discrepancy is small, given the simplicity of the model, but because many of the other parameters of the model were obtained by fitting the data for the observed wave, the model wave speed might be expected to depend primarily on the diffusion coefficient of potassium, which is accurately known (Horvath, 1985). Hence the discrepancy likely results from the omission of some mediating factor, and not from inaccuracy in the numerical parameters.

Because potassium transport is the basic factor in the propagation of the SD wave in the TM model, refinements of this model might naturally begin with a more complete account of potassium transport in the cortex.

While a tortuosity factor was used to account for the effect of geometry on the effective diffusion coefficient for K^+ the TM model contains no specific assumption (analogous to cable theory) concerning the effect of geometry of the extracellular and intracellular spaces on the transmembrane potential. Therefore, the formulation of a model for this relationship is a second natural refinement of the SD model.

Several empirical correlates of SD are not presently known to be mediating or epiphenomenal. The observations of Nicholson and Kraig, (1981) suggest that SD is accompanied by massive movement of an (unknown) anion from the intracellular space. The mechanism for this putative anion movement is not known and it is possible that this ion may be one of several organic anions, including glutamate. It is found (Van Harreveld & Khattab, 1967) that SD is accompanied by a dramatic reduction of the extracellular space due (at least partly) to swelling of the dendrites in the affected areas. It is likely that this swelling is <u>osmotic</u> and is caused by a net flux of salt (anion and cation) into the intracellular space. Since the <u>osmolarity</u> of intracellular space must be preserved, water enters cells, causing an increase in intracellular volume. At the same time, the electrical resistance of the cortex rises dramatically during SD (Van Harreveld & Ochs, 1957; Ranck, 1964;).

The role of these concomitant factors in SD has not yet been clarified, and some theory would be required to obtain the relation between cell swelling, elevated tissue resistance, transmembrane potentials, and spatial buffering within

the tissue itself. The calculations performed in the present work do not apply to the extreme conditions which prevail during SD, however, they are compatible with the observed correlation between cell swelling and the changes in tissue resistance.

Elevations in the extracellular potassium concentration may produce slow field potentials by depolarizing the membranes of glial cells (Kuffler, 1967; Somjen, 1975). A relation between extracellular potassium, glia, and slow field potentials is strongly suspected on experimental grounds. Extracellular potassium concentration may be involved in certain types of neural signalling (Lebovitz, 1970) and a variety of metabolic effects (Krnjevic & Morris, 1981), even though it may not be the single most critical factor in every case (Somjen, 1984).

A theory of potassium transport and the relation between extracellular, intracellular, and transmembrane potentials is a basic prerequisite for accurate macroscopic modelling of SD and other phenomena, e.g., epilepsy. (Prince, 1978; Crill & Schwindt, 1986; Traub et al., 1985 a,b) in which ion concentrations and extracellular potentials in bulk tissue may play a mediating role.

6.0. OUTLINE OF THESIS

In Section II.1.1† we introduce the Nernst-Planck equation, which is the governing equation for ion transport and electric potential, and specify the jump conditions at the cell membrane. In Section II.2, appropriate scalings for the equations are chosen. This section also deals with the structure of the tissue model and methods for incorporating the jump conditions into formal calculations.

In Chapter III, an asymptotic expansion and averaging procedure is

---

† Chapters are referred to by capital roman numerals and sections by arabic numerals separated by a decimal point. Thus Section II.1.1 refers to subsection 1 of section 1 of Chapter II.

described which reduces the computation of bulk properties to a calculation for a single cell. In Section IV.1, the idea of transport numbers in electrolytic media (Horvath, 1985) is introduced and it is shown that this idea applies to bulk tissue. Coefficient estimates in the averaged equations are computed numerically for a range of microscopic parameter values including cell size, membrane conductance, intracellular conductivity, extracellular space and geometry, in Sections IV.3 - IV.6. An important finding is that theoretical transcellular current, the bulk current flow through disconnected cells, is significant and relatively insensitive to many of these parameters, depending primarily on cell size and membrane conductance.

In Chapter V, the role of electrotonic parameters (the parameters involving electrical constants) in the tissue model is discussed. Section V.1.2 presents a formal analogy between transcellular current and electrostatic polarization as an aid to physical understanding of the transport properties of arrays of disconnected cells. In Section V.2, asymptotic analyses in the electrotonic parameters are performed in order to supplement the numerical solutions with qualitative results, while in Section V.3 it is shown how to build asymptotic assumptions about electrotonic parameters into the model.

In Chapter VI, we discuss biological implications of the analyses from the body of the thesis. The properties of steady solutions to the averaged equations are discussed in Section VI.2 and it is shown that some coefficients of the equations cannot be estimated in a steady experiment. It is argued that the general model proposed here is simpler and more appropriate than (syncytial) cable theory for bulk tissue. For example, Section VI.3.1 concludes that specialized transfer cells are unnecessary to explain transcellular flux and spatial

buffering, while Sections VI.3.2 - VI.3.3 conclude that disconnected cells cannot be neglected, and that tissue structure may be important.

Section VI.4 discusses the significance of current through cells and observed phenomena which may be affected by the length scales which are imposed by experimental observations. Limitations of our approach are discussed in Section VI.5. Finally, Section VI.6 briefly contrasts the present model with previous models.

The present model is chosen to include measurable quantities such as extracellular potential and extracellular K^+ concentration and to be mathematically simple. Since it is shown that the bulk parameters of the model are relatively insensitive to many of the microscopic parameters of the tissue, the resulting governing equations should be applicable to many physiological situations.

GLOSSARY

Action potential , A rapid (lasting ca. 1 msec) regenerative depolarization of the neuronal membrane accompanied by a complicated set of changes in the membrane conductances. In the classical case, it is characterized by a rapidly rising phase in which the membrane sodium conductance increases dramatically, and a somewhat less rapid return to equilibrium in which sodium conductance decreases and potassium conductance increases.

Active properties In Hodgkin-Huxley theory, properties associated with the voltage-sensitive membrane ionic channels.

Active transport Net movement of molecules or ions, often between intracellular and extracellular spaces, which depends on metabolic energy. The use of the term "transport" in this phrase differs from the use of the term in the rest of the thesis.

Anion A negatively charged ion.

Axon An extended tubular process of the neuron which projects to neighbouring neurons, sometimes over a considerable distance (1m or more).

Capacitance The capability of storing electrical energy by the separation of opposite electrical charges.

Cation A positively charged ion.

Central nervous system The higher portion of the nervous system, including the spinal cord, brain stem, cerebellum, basal ganglia, diencephalon and cerebral hemispheres.

Cerebellum A large part of the brain with motor functions, situated near the base of the brain and with a cellular architecture similar to cerebral cortex.

Cerebral cortex The outer layer of gray matter of the cerebral hemispheres, associated with higher perceptual, cognitive and motor functions and having a layered cellular architecture.

Cytoplasm The jelly-like material surrounding the nucleus of a biological cell.

Epilepsy A disorder of the nervous system which results when a large collection of neurons discharge in synchrony. Along with this discharge, stereotyped behaviors may occur, including convulsions.

Excitable Capable of producing action potentials.

Extracellular space The region exterior to biological cells within a tissue.

Gap junctions Intercellular junctions at which cells are connected by transmembrane pores, permitting the exchange of intracellular molecules and electrical charge.

Glia The passive interstitial cells of the central nervous system.

Hippocampus A subcortical brain structure with a distinctive shape (the name is from the Greek for seahorse) and regular cellular architecture. It is associated with memory in man.

Ion An electrically charged atom or group of atoms.

Intracellular space The regions interior to biological cells within a tissue, taken together.

In vitro A phrase used to characterize biological experiments made under artificial conditions, and not in a living animal.

In vivo A phrase used to characterize biological experiments or conditions in a living animal; as opposed to in vitro.

Invertebrate The biological phylum consisting of animals which lack backbones, such as the squid, leech, insects, etc..

Membrane A thin flexible sheet composed of lipid molecules which forms the surface of biological cells or organelles, and which separates intracellular and extracellular regions.

Metabolic Pertaining to the chemical processes occurring within a biological cell.

Motor cortex A region of the cerebral cortex associated with motor function.

Myelin Layers of lipid and protein substances composing a sheath around nerve fibers.

Neuron The primary cell type of the nervous system, which is capable of producing action potentials. It consists of the nerve cell body and its processes, the axon, and other processes called dendrites.

Olfactory bulb A region of the cerebral cortex associated with the sense of smell.

Osmolarity The sum of the total concentrations of all solutes in a solution, so called because of the importance of this quantity for osmotic phenomena.

Osmotic Pertaining to the process by which two different solutions which are mechanically separated (for example, by a membrane) tend to equalize their respective total solute concentrations by the flow of solvent from one to the other.

Organelle A membrane-enclosed structure with a specific biochemical function within a biological cell.

Passive A technical term referring to membrane properties which are not voltage dependent, as opposed to the active voltage- and time-dependent conductances of the Hodgkin-Huxley model.

Peripheral nervous system The parts of the nervous system outside the central nervous system.

Permeability The relative ease with which an ion passes through membrane pores. This may be measured by a mathematical coefficient.

Preparation Part of an organism which is "prepared" in some way (in vivo or in vitro) which facilitates physiological study, e.g., of squid axon, frog muscle, etc..

Processes Continuous anatomical extensions of a biological cell body, which may be tubular or sheetlike.

Resting transmembrane potential The transmembrane potential across excitable membrane in the absence of stimulation, when action potentials are not occurring.

Squid giant axon A physiological preparation of the axon of the squid Loligo , used because its large size facilitates experiments.

Slice preparation A thin section of tissue, often from the cerebral cortex or hippocampus which preserves cellular architecture and function in vitro .

Soma The cell body of a neuron, containing the nucleus of the cell.

Synapse A specialized contact zone at which two neurons are closely apposed and where communication occurs by electrical or (typically) chemical transmission.

Synaptic transmission The process by which the information of the action potential is transmitted from one neuron to another, typically through the release of a chemical factor which diffuses across the synapse.

II. THE MODEL EQUATIONS

1.0. INTRODUCTION

In this chapter the mathematical problem for determination of electrical and ion transport properties from a model of neural tissue containing two types of cell (neurons and glial cells) is specified precisely. The objectives of this mathematical formulation are to calculate the averaged electrical and ion transport properties of the tissue in a systematic way and to exhibit the dependence of macroscopic tissue properties on the the microscopic properties of cells. This provides a theoretical connection between studies of microscopic cellular properties, such as those described by Turner and Schwartzkroin (1984), and studies of macroscopic tissue properties such as those by Ranck (1963,1964) and Gardner-Medwin (1983 a, b).

1.1. Transport Equations in Electrolyte Solution

We now sketch the physical chemistry thought to apply to ion transport in solution (Horvath, 1985; Carnie & Torrie, 1984; Fuoss & Accasina, 1959) and justify the transport equations to be used in the remainder of this thesis. † This section is intended to justify the use of these equations here, rather than to derive them, since these derivations are described in elementary textbooks or in the voluminous literature of classical chemistry. The discussion of transport given in this section refers to electrolyte solutions such as those of the extracellular medium in neural tissue. In these basic electrochemical equations, averages are

---

† As stated in Chapter I the term "transport" refers here to the flux of some conserved quantity such as net electric charge or an ionic species, in response to a gradient of intensity (e.g., potential, concentration) of that conserved quantity (cf. Batchelor, 1974).

taken over length scales of $10 - 100$ A$^\circ$ rather than $10 - 100$ μm as in the tissue equations I.(4.1) - I.(4.2). It is assumed that no convective transport occurs and the discussion is restricted to transport due only to diffusion and electrical forces.

From a theoretical point of view, the simplest transport process is diffusion. If there are neither electrical forces nor concentration gradients, then ionic and solvent molecules undergo brownian motions due to thermal energy, but have no average relative motion. In the presence of an ionic concentration gradient these random motions result in movement (diffusion) of ions from regions of high concentration to regions of low concentration. The result of the individual motions of the molecules and average flux in aqueous solution (Robinson & Stokes, 1955) is precisely described by Fick's law:

$$(1.1) \qquad \vec{j}_D = -D_i \nabla C_i,$$

where C is the ionic concentration (mol cm^{-3}), $\vec{j}_D$ is the ionic flux vector in mol sec^{-1}cm^{-2}, and D_i is the diffusion coefficient (cm^2 sec^{-1}) for the ith ionic species.

The description of ionic flux in an electric field requires some assumptions, however. For reasons discussed below, it will be assumed that the sum of the total concentration of cations multiplied by their valence is equal to the sum of the total concentration of anions multiplied by their valence in any non-zero volume. This assumption is referred to as 'electroneutrality' because it implies zero net charge within any non-zero volume. Since variations in the D_i's are unlikely to be important under physiological conditions of moderate variation in temperature and concentration, the diffusion constants D_i will be treated as

empirical constants depending on the identities of solvent and solute, and independent of concentration. Using electroneutrality this assumption implies that $\Sigma z_i D_i \nabla C_i = 0$, where z_i is the valence of the ith ionic species, so that the net electric flux due to diffusion is zero throughout the solution.†

When both electrical and concentration gradients exist, we assume that the total flux $\vec{j}_i$ (mol sec^{-1} cm^{-2}) of the ith ion is given by the classical Nernst-Planck equation

$$(1.2) \qquad \vec{j}_i = -D_i \{ \nabla C_i + z_i C_i \frac{F}{RT} \nabla \phi \},$$

The first term on the right-hand-side of (1.2) is a flux proportional to concentration gradient and, therefore, will be referred to as the diffusive transport term. The second term on the right-hand-side of (1.2) is proportional to an electric potential gradient and will be referred to as the electrical transport term.

Using the above assumptions, summation of (1.2) gives the total diffusive mass flux vector:

$$(1.3) \qquad \vec{J}_D = -\sum_{i=1}^{3} D_i \nabla C_i,$$

where the flux $\vec{J}_D$ (mol sec^{-1}cm^{-2}) is a sum of diffusive fluxes. Multiplication of

---

† Since Fick's law is valid for electrolytes, the coefficients D_i, $i=1,...n$, must be consistent with the possibility that (electrical current) $z_c D_c \nabla C_c + z_a D_a \nabla C_a = 0$ at the boundary for a solution composed of a single cation and anion, where C_c is the concentration of cations and C_a the concentration of anions, and z_c and z_a are, respectively, the valences of cation and anion. Because of electroneutrality, $z_c \nabla C_c + z_a \nabla C_a = 0$ throughout the solution. Combining the latter two equations implies either $D_c = D_a$, or $\nabla C_a = \nabla C_c = 0$, so that the above result is true throughout the solution.

(1.2) by the valence z_i and summation gives the net current in mol $sec^{-1} cm^{-2}$

$$(1.4) \qquad \vec{I} = - \frac{F}{RT} \sigma \nabla \phi,$$

where $\sigma := \Sigma z_i^2 D_i C_i$ (mol $sec^{-1} cm^{-1}$) will be referred to as mass conductivity where 'mass' refers to the dimensions of this quantity. It is shown below that this quantity, σ, is proportional to the electrical conductivity of the solution. When the electrolyte considered consists only of uni-valent ions, $\nabla \sigma$ is just the total diffusive flux of ions.

Thus, the form of the Nernst-Planck equations is simplified by assuming electroneutrality. Equation (1.4) asserts that under the stated assumptions, a spatially dependent conductivity $\kappa = \kappa(\vec{x})$, (mS cm^{-1}) may be assigned to electrolyte solutions of given composition. The electric current $\vec{i}$ may be written in the local form of Ohm's law as;

$$(1.5) \qquad \vec{i} = - \kappa \nabla \phi,$$

where $\kappa := F^2 \sigma / RT$ has the dimensions of conductivity.

1.2. Limitations of the Nernst-Planck Equations

While the Nernst-Planck equations (1.2) are taken as the model equations, it is important to note that this entails some compromise. The Nernst-Planck equations (1.2) give each ionic flux independently of the others. For low concentrations or strong electrolytes, this prediction is born out empirically and is known as Kohlrausch's law of independent migration of ions. Equation (1.5)

asserts that an electrolyte solution behaves ohmically and the effective conductivity is a linear function of the concentrations of each ion. The ohmic behavior has considerable support while the status of the linearity assumption is less certain. There is considerable experimental evidence (Horvath, 1985) that electrolyte solutions are ohmic ($\vec{i} = \kappa \nabla \phi$); however, at low concentrations ($<<$ .1M), electrolyte solutions exhibit conductivities given asymptotically by;

$$(1.6) \qquad \kappa = C(\Lambda_0 - b\sqrt{C})$$

where C is the ionic strength and Λ_0 and b are constants independent of concentration.

In addition to (1.6), there are a large number of other semi-empirical non-linear formulas applicable to particular electrolyte types (Horvath, 1985). It is not clear which if any of these formulas are applicable in the physiological context. At physiological concentrations, the dependence of the conductivity of a strong electrolyte on concentration is approximately linear.

As C $\longrightarrow 0$ in (1.6), $\kappa \longrightarrow C\Lambda_0$, where κ was defined in Section 1.1, so that Λ_0 is the limiting molar conductivity at infinite dilution. The quantity Λ_0 may be approximately calculated from thermodynamic arguments. The theoretical value appears in the Nernst-Planck equations (1.2) and may be calculated using (1.4), (1.5), and (1.6). For example, for a solution of a single uni-univalent electrolyte (such as KCl):

$$(1.7) \qquad \Lambda_0 = 2 \frac{F^2}{RT} D$$

where D is the diffusion coefficient for the electrolyte, and Λ_0 is computed using the definition of σ with two uni-valent ions.

For self-consistency of the model, the assumed diffusion coefficients will be the effective coefficients at physiological temperatures and concentrations, and solution conductivities will be computed from these values. The resulting conductivities will be less than the tabulated infinite dilution conductivities (Robinson & Stokes, 1955) but this procedure should produce more accurate approximations to the solution conductivity than the use of infinite dilution data, since it incorporates an empirical correction for concentration.

In principle, the individual ionic fluxes should be governed by non-linear formulas analogous to (1.6) and, due to non-linearity, each flux must be a function of the local concentration of all the solute ions. However, in contrast to the experimental data leading to (1.6), these more detailed data are not available. In view of this situation, it is assumed in our model that the local ion fluxes are predicted by the Nernst-Planck equations. Because the conductivity of physiological solutions is determined largely by strong electrolytes, the non-linear correction which is neglected should be small.

A theoretical account of the observed deviations of transport properties from those predicted by (1.2) is complicated. First, the Nernst-Planck equations (1.2) do not specify the electric potential ϕ. Since this equation describes the motions of charged particles (ions), a completely satisfactory model would determine ϕ so that it included the effect of the ionic charges. The correct resolution of this problem, using the principles of statistical mechanics is the subject of current research (N. Patey, personal communication).

The use of Poisson's equation to compute ϕ is inappropriate because it

assumes that a smooth, stationary charge density is a valid approximation to the collective effect of individual charges. Ionic charges of opposite sign rapidly cluster around one another, however, in an effect known as charge screening, so that the charge density is not smooth or stationary in time. In this thesis, we have accepted, with others (Plonsey, 1969; Carnie & Torrie, 1984), a classical treatment of this problem known as the Gouey-Chapman theory (Gouey, 1910; Chapman, 1911). Gouey-Chapman theory consists of studying the properties of the Poisson-Boltzmann equation:

$$
(1.8) \qquad \nabla^2 \phi = -\frac{q_e}{\epsilon_b} \sum_{i=1}^{3} z_i C_i e^{-z_i q_e \phi / RT}
$$

where q_e is the charge of an electron, and ϵ_b is a dielectric permittivity (farads cm^{-1}). The Poisson-Boltzmann equation assumes the chemical solution has a bulk dielectric permittivity, ϵ_b, and identifies the electrostatic potential with the corresponding thermodynamic potential. The reader is referred to Plonsey (1969) for mathematical details, and to Carnie and Torrie (1984) for the relationship of Gouey-Chapman theory to other theories. Physically, the theory asserts that charge separation cannot occur over a large region because charge separation requires energies which are large compared to the available thermal energy. Gouey-Chapman theory predicts electroneutrality of the solution over any length scale larger than the Debye shielding distance. This distance is 9.6 A^{o} units in .1 molar uni-univalent electrolyte solution (McGillivray & Hare, 1969; Plonsey, 1969). Thus, in this work the concentrations of anion and cation are taken as equal in any volume element, and no charge separation occurs in the bulk

solution. †

2.0. THE NON-DIMENSIONAL MODEL EQUATIONS

2.1. Scaling of the Transport Equations

In order to prepare the transport equations for asymptotic and numerical analyses, it is useful to choose non-dimensional variables which reflect the magnitudes of the physical quantities of interest. These choices are made both for reasons of numerical convenience, and in order to identify small non-dimensional parameters which may be used to construct asymptotic approximations to the full equations.

We begin with a brief description of the electrical and ionic environment within nervous tissue. In a common experimental preparation (mammalian brain slice) typical extracellular concentrations of physiological ions are as shown in Table 2.1 (Llinas & Sugimori, 1980). For comparison, typical concentrations of physiological ions in human cerebrospinal fluid (CSF) (Davson, 1976) are also shown. Magnesium, Mg^{2+}, and calcium, Ca^{2+}, are also present in the brain, in cerebrospinal fluid, and are included in experimental bathing solutions, at about 1 4 mM concentration, but they will play no role in our transport equations because these ions contribute little to solution conductivity. The Ca^{2+} ion may play some role in determining the resting membrane potentials of some neurons, however, this omission is not expected to qualitatively affect the conclusions of the present work with respect to potassium and electrical potential.

Intracellular concentrations of ions are less certain but may be estimated

---

† This assumption is not satisfied for ionic fluxes across biological membranes, and the treatment of flux across membranes involves model equations different from those given here (Shultz, 1980; Plonsey, 1969).

Table 2.1. Extracellular Ionic Concentrations.

Ion	Slice	CSF
Na^+	150 mM	147 mM
K^+	6.2 mM	2.86 mM
Cl^-	131 mM	113 mM
HCO_3^-	26 mM	23.3 mM

(mM = milli-molar)

as Na^+ (30 mM), K^+ (130 mM), Cl^- (10 mM), and organic anions (150 mM) (Llinas et al., 1980), which consist mainly of glutamate and aspartate (Puil, 1981). Hence the intracellular concentration of potassium, $[K^+]_i$, exceeds the extracellular concentration, $[K^+]_o$, by a factor of 20-40, and the extracellular concentration of sodium, $[Na^+]_o$, exceeds the intracellular concentration $[Na^+]_i$ by a factor of 5. Differences also occur for the other physiological ions. The concentration $[K^+]_o$ may vary considerably during abnormal physiological states, reaching 12 mM during epileptic activity (Prince, 1978) and 40-50 mM during spreading depression (Nicholson & Kraig, 1981). Spreading depression is also accompanied by large changes in the concentrations of Na^+, Cl^-, and Ca^{2+}.

Tabulated conductivity data for electrolyte solutions give an estimate for the conductivity of the extracellular fluid of 20 mS cm^{-1} at 37C^o which is in agreement with the observed conductivity of cerebrospinal fluid (Nicholson, 1980). Correct values of the intracellular conductivity are considerably less certain owing to the complicated morphology of neurons and the fact that axoplasm is not a simple electrolyte solution. Typical measured values are between 1 to 4 times the resistivity predicted by the composition of the intracellular medium (Barrett &

Crill, 1974; Carpenter et al., 1971, 1973; Schanne & Ruiz P.-Ceretti, 1978). Using the concentrations cited above, this leads to an estimate for the internal resistivity, r_i, between 67-268 Ωcm, while the resistivity of somatic cytoplasm is even more variable (Schanne & Ruiz P.-Ceretti, 1978). Extracellular electrical potential gradients are usually between $|\nabla\phi| = 1$ mV to 250 mV cm^{-1} (Somjen, 1979). Typical length scales for cells in brain tissue are L $\simeq$ 10 μm to 100 μm. For example, dendrites may be 1 μm in diameter, the cell body of a Purkinje cell may have a radius of 10 μm, astrocyte processes may extend 40 μm to 50 μm, while the complete arborization of a Purkinje cell may extend for 500 μm (Hounsgaard & Nicholson, 1983).

At physiological temperatures and concentrations, diffusion coefficients for KCl and NaCl are approximately 1.7 x 10^{-5} and 1.3 x 10^{-5} cm^{2}sec^{-1}, respectively, and at the physiological temperature, T= 37C, RT/F is 27mV.

Non-dimensional variables are chosen so that under typical conditions the magnitudes of relevant quantities are close to unity. A convenient (though arbitrary) choice is to take the non-dimensional voltage gradient to be near unity. The scaled spatial coordinate is defined as $\tilde{x}_j = x_j / L$ and the scaled voltage $\nu\tilde{\phi}$ = Fϕ/RT where νRT/F is the typical voltage variation over the length L and ν is a non-dimensional constant. Denoting a typical ionic concentration by $\overline{C}$, we obtain the non-dimensional concentrations; $\tilde{C}_i = C_i / \overline{C}$, which will differ between intracellular and extracellular environments.

For the case of potassium, K$^+$, the magnitudes of the terms in the Nernst-Planck equations may be roughly deduced as follows. Each nerve impulse releases K$^+$ at approximately 2 x 10^{-9} m mole cm^{-2} sec^{-1} (Orkand, 1980), at a frequency between 1 Hz and 100 Hz. At 100 Hz the flux associated with this

release rate corresponds to a current density of 2 x 10^{-5} amp cm^{-2}. In contrast, an extracellular potential gradient of .1 V cm^{-1} (Somjen, 1981) at an effective conductivity † of .31mS leads to a current density of 3.1 x 10^{-5} amp cm^{-2}. Hence, the diffusive and electrical terms are of comparable magnitudes.

Dimensionless variables are selected so that typical concentrations and voltage gradients will be of order unity. Thus, it is appropriate in the case of the potassium ion, K^+, to take L = 50 μm, D_i = .85 x $10^{-5}cm^2$ sec^{-1}, $\overline{C}$ = 5 mM, and $\nu RT/F$ = .5mV (that is .5mV/50μm =100mV/1cm) which implies ν = .0185. Since ν is small, the flux associated with a voltage gradient of order unity is small compared to the flux associated with a concentration gradient of order unity. No special use will be made of this fact, but it is necessary for later calculations that the electrical flux be at most of the order of the diffusive flux. It is important to note, however, that the magnitudes of the characteristic electric potential gradients on long and short length scales may differ because of fine structure in the tissue conductivity induced by the presence of cells.

A similar choice of scalings is appropriate for equations (1.1) - (1.5). It is convenient to scale σ by $\overline{\sigma} = \Sigma D_i \overline{C}$, while the variables x and ϕ are scaled as before.

2.2. Asymptotic Assumptions

In this work, we focus on results which are independent of detailed considerations of cell geometry and placement, because such results are more likely to be applicable to a variety of different preparations. It is assumed for

---

† The approximate effective partial conductivity due to potassium in the extracellular medium.

convenience that the tissue contains a large number of periodically arranged cells. The periodic domains correspond to the smallest repeating subunits of the periodic structure of the tissue model, which will be called crystallographic unit cells.†
The assumption of periodicity and other assumptions made later about cell shape are convenient for computation. While the mathematical model employed could be used in two or three dimensions, it is convenient to perform the numerical calculations in two dimensions.

It is expected that the properties of this abstract model, and properties of the real tissue, will depend in similar ways on characteristic dimensionless parameters related to the extracellular space fractional volume, electrical properties of the intracellular and extracellular media, and cell size, since these model parameters can be matched to the real ones.

It is assumed that there are two fine characteristic length scales; a fine length scale, L_1 which is characteristic of neuron size and a finest length, L_2 which is characteristic of glial cell size, (see Figure 2.1). Since it will not be assumed that neuronal membrane has properties distinct from glia in this model, the 'neuronal' cell population could be any asymptotically larger cell population. This two-tier structure is chosen to model the structure of real tissue, which contains both coarse and fine structures of various kinds. For example, dendrites, and glial cell bodes and processes are expected to have finer spatial dimensions than neuronal cell bodies and axons (Peters et al., 1976). The asymptotic expansion in Chapter III will be constructed using this assumption (referred to as a two-tier model). The calculation for a simple periodic array (one-tier model) forms a part of the two-tier calculation and this simpler model is considered in

---

† This term is borrowed from elementary chemistry.

Figure 2.1. Periodic arrays of model cells can be arranged in different ways to match the properties of biological tissue. Possible shapes for the biological cell are shown, and assumptions about the spatial length scales L_0, L_1, and are illustrated. The model tissue used later will be in two dimensions (compare Figures IV-3.1 and IV-6.3).

Tissue models

Model neurons
Order epsilon length

Crystallographic
unit cell

L_0

Alternate unit cells

ECS

Model glia
Order epsilon
squared length

L_2

TORTUOUS
ECS paths increased
in length

SYNCYTIAL
continuous
tissue sheet
(hatched)
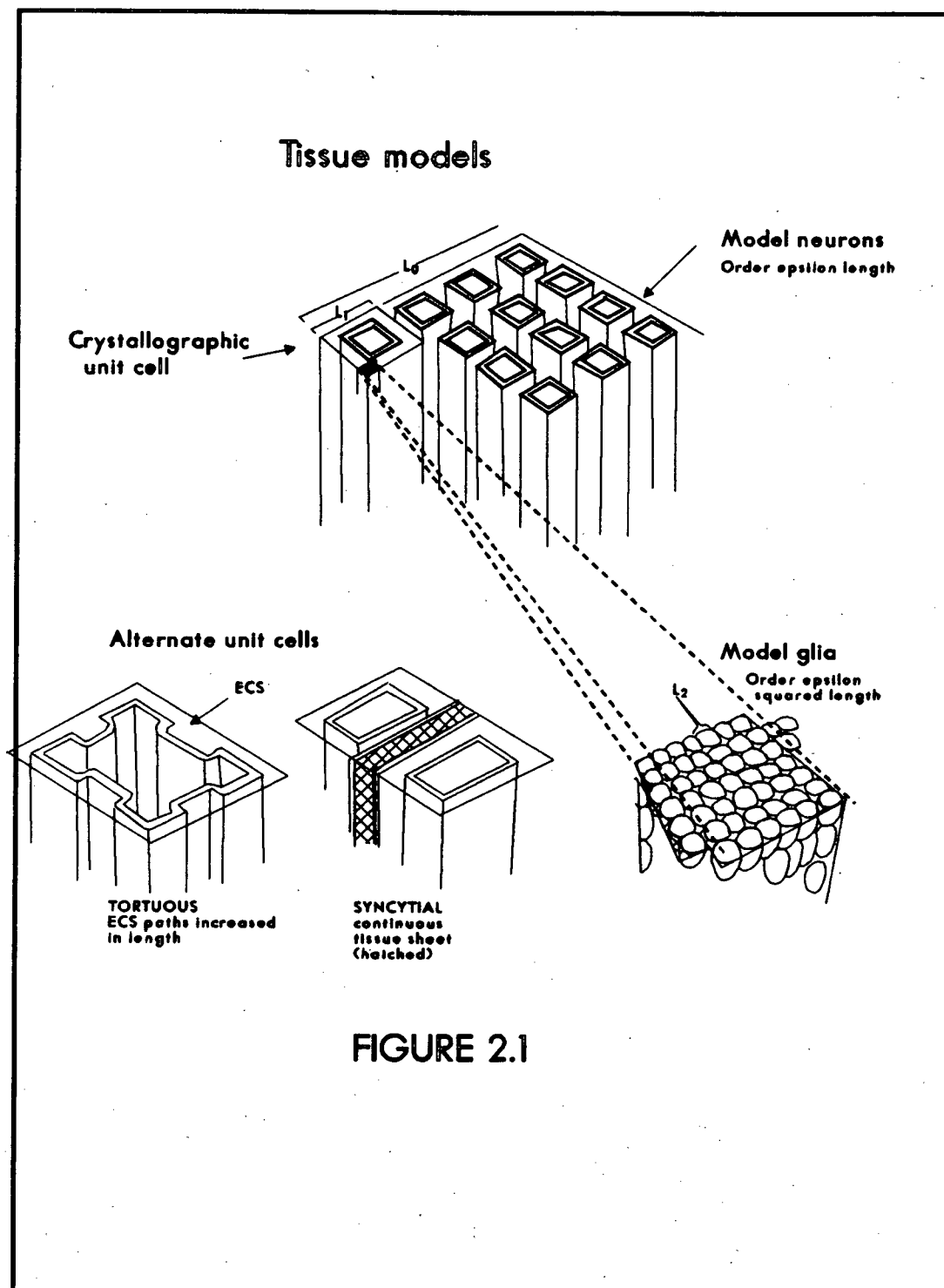
FIGURE 2.1

many of the numerical calculations.

While our results show that the two-tier model may be useful, further experimental data would be required to justify more detailed study of this model. Figure 2.1 illustrates the hypothesis that larger cells are aligned anisotropically, while finer cells are aligned isotropically. Such an alignment might be expected because neurons and glia have complicated branching structures, so that the finer structures tend to have less spatial organization. To completely justify this model however, it will be necessary to gather detailed quantitative data on the relative size, shapes, and positions of cells in neural tissue.

In order to determine relationships between macroscopic and microscopic properties of tissue, we calculate the macroscopic properties of this tissue model over a coarse length scale, $L = L_0$. The notation L_0, L_1, and L_2 will denote asymptotic length scales which may correspond to various physical quantities. It will always be assumed that $L_1/L_0 = \epsilon$ and $L_2/L_0 = O(\epsilon^2)$ where $O(\cdot)$ is the usual order notation. The extracellular and intracellular media are assumed to include only the uni-valent ions, Na^+, K^+, and Cl^-. Neuronal and glial membrane are assumed to be permeable only to K^+ ions. This is correct for glial membrane and is approximately correct for resting neuronal membrane (Kandel & Schwartz, 1983, p40). The electric potential, ϕ, and concentration, C_i, are discontinuous across the cell membranes.

The time-dependent equations for the electrical and ion transport properties of tissue are more complicated than those formulated here. Such equations would have included capacitive current and the time dependence of the membrane conductances. However, appreciable ion transport takes place only over times on the order of a second or longer. Thus, the time scale of interest (several

seconds) is long compared to the time constant (a few milliseconds) for charging of the membrane capacity, or the time constant(s) for relaxation of the membrane conductances toward their steady state values. It may be shown by an elementary calculation that the charge or ion transport associated with charging of membrane capacity and relaxation of conductances is smaller (by a factor of about 1000) than the net charge and ion transport which can occur over several seconds. A characteristic time, t_c, of this order will be chosen and will appear in the definitions of the non-dimensional variables. Thus, in computing the electrical and ion transport properties of neural tissue it will be assumed that the membrane charge and conductances have attained their steady state values. The extracellular ion concentrations will be (slowly) time dependent, and the equations specifying this time dependence will be given. Thus, a quasi-steady non-linear averaged equation for the evolution of the extracellular potassium concentration is derived. The present analysis is different from previous analyses (see Chapter I) because it does not assume that the tissue is syncytial, includes more than one type of cell, and explicitly treats electrodiffusion of ions in the extracellular medium according to equation (1.2).

2.3. Model Equations

Table 2.2 shows the dimensional parameters and Table 2.3, the dimensionless parameters to be used in the model equations.

Table 2.4 gives the definitions of dimensionless variables used in the model equations. The tilde ~ denotes dimensionless variables in Tables 2.2 - 2.4, and will be dropped in the text. Displayed equations are always given using the dimensionless variables of Table 2.4.

Table 2.2. Characteristic Dimensional Parameters.

Parameter	Description
L	length
L_0	measurement length
L_1	fine tissue structure length
L_2	finest tissue structure length
$\overline{C}$	concentration
$\overline{\sigma} = \Sigma D_j \overline{C}$	mass conductivity
t_c	time
$\overline{S} = \overline{\sigma} F^2 / RT$	conductivity / cm

Table 2.3. Dimensionless Parameters.

Parameter	Description
ν	voltage gradient parameter
$\tau = L^2 \overline{C} / t_c \overline{\sigma}$	time constant parameter
$\theta_j = D_j / \Sigma D_k$	ionic diffusion parameters

Table 2.4. Dimensionless Variables

Parameter	Description
$\widetilde{x}_j = x_j / L$	space coordinate
$\widetilde{t} = t / t_c$	time
$\widetilde{C}_i = C_i / \overline{C}$	concentration

$\tilde{\phi} = F\phi / \nu RT$ electric potential

$\tilde{\sigma} = \sigma / \overline{\sigma}$ conductivity

$\tilde{q}_i = L^2 q_i / \overline{\sigma}$ concentration source density

$\tilde{Q}_1 = \Sigma L^2 q_i / \overline{\sigma}$ ionic source density

$\tilde{Q}_2 = \Sigma L^2 z_i q_i / \overline{\sigma}$ charge source density

$\tilde{V} = F V / \nu RT$ transmembrane potential

$\tilde{V}_r = F V_r / \nu RT$ resting transmembrane potential

$\tilde{g}_i = L g_i / \overline{S}$ membrane conductance

$\tilde{p}_i = L p_i / F\overline{\sigma}$ active transport ionic flux

$\tilde{P}_1 = \Sigma \tilde{p}_i$ active transport ionic flux

$\tilde{P}_2 = \Sigma z_i \tilde{p}_i$ active transport charge flux

If $\vec{j}_i$ is the flux of the ith ionic species given by the Nernst-Planck equation and each ionic species is conserved, it is shown (by a derivation identical to that for the diffusion equation (Carrier & Pearson, 1976) with $\vec{j}_i$ substituted for the diffusive flux) that:

$$(2.1) \qquad -\nabla_x \cdot \vec{j}_i = \frac{\partial C_i}{\partial t} + q_i$$

where ∇_x is the gradient operator with respect to $\vec{x}$ and q_i is a source density (mol / sec cm^{-3}). The ionic source q_i is zero in the intracellular and extracellular media unless ions are introduced experimentally. Equation (2.1) and all following equations hold in the interiors of the extracellular and intracellular regions. The

quantities $\vec{j}_i$, C_i, q_i, are functions of the spatial coordinates $\vec{x}$.

Using the Nernst-Planck equations (1.2), the dimensionless form of (2.1) becomes:

$$(2.2) \qquad \theta_i \nabla^2_x C_i + \nu z_i \theta_i \nabla_x \cdot (C_i \nabla \phi) = \tau \frac{\partial C_i}{\partial t} + q_i, \quad i = 1,2,...,N$$

where the variables and parameters are defined in Tables 2.2 - 2.4. Note that since $\theta_i = D_i / \Sigma D_k$, the sum $\Sigma \theta_i C_i$ is σ.

Summing (2.2) over i gives:

$$(2.3) \qquad \nabla^2_x \sigma = \tau \sum_{i=1}^{3} \frac{\partial C_i}{\partial t} + Q_1$$

where $Q_1 := L^2 \Sigma_i q_i / \overline{\sigma}$. Multiplying (2.2) by z_i, the ionic valence, and summing over i gives:

$$(2.4) \qquad \nu \nabla_x \cdot (\sigma \nabla_x \phi) = Q_2$$

where the new quantity Q_2 is defined (Table 2.4) as $Q_2 := \Sigma_i L^2 z_i q_i / \overline{\sigma}$. The time derivatives on the right-hand-side of (2.2) sum to zero by electroneutrality.

2.4. Jump Conditions and Boundary Conditions

Sign conventions are illustrated in Table 2.5. The abbreviations ECS and ICS denote the extracellular and intracellular spaces, respectively. The normal $\vec{n}$ to the cell membrane is outward pointing. The signs of the ion fluxes, $\vec{j}_i$, imply

Table 2.5. Corresponding Sign Conventions at Membrane.

Name	ECS	ICS	Symbol
		Direction	
Normal Vector		<	$\vec{n}$
Membrane Potential	+	-	$V := \phi^i - \phi^o < 0$
Current		>	$\vec{I} \cdot \vec{n} < 0$
Potential Gradient		<	$\nabla\phi \cdot \vec{n} > 0$
Cation Flux		>	$\vec{j}_i \cdot \vec{n} < 0$

that cations flow in the same direction as electric current. Thus, the electric potential, ϕ, is defined so that cation flux is in the direction of decreasing potential and diffusive flux (the first term of (1.2)) is in the direction of decreasing concentration. As a result of these conventions, the values of V and $\sigma\nabla\phi \cdot \vec{n}$ have opposite sign.

Using equation I.(3.3) for the transmembrane current, and the definition of $\vec{j}_i$, the jump conditions for ϕ and C_i at cell membranes are:

$$(2.5) \qquad -\theta_i\nabla_x C_i \cdot \vec{n} - \nu z_i \theta_i C_i \nabla\phi \cdot \vec{n} = \nu z_i g_i (V_r - V_i) + p_i$$

where p_i is an active transport or 'pump' term and the transmembrane potential V is defined by $V := \phi^i - \phi^o$ where ϕ^i and ϕ^o are the intracellular and extracellular potential, respectively, at adjacent points across the cell membrane. The electrical potential ϕ, concentrations C_i, and their spatial derivatives, are discontinuous at the cell membranes. The quantity V_r is the membrane resting

potential given by the Goldmann-Hodgkin-Katz formula (equation (1.2) of Chapter I) and the surface integral is evaluated over the membrane of a single cell. The dimensionless Nernst potentials, V_i, are given by:

$$(2.6) \qquad \nu V_i = \frac{1}{z_i} \ln(C_i^0 / C_i^i)$$

where C_i^0 denotes extracellular and C_i^i intracellular ionic concentrations.

The jump conditions (2.5) hold intracellularly and extracellularly, and so (2.5) specifies two equations. Conditions of the same form hold at the cell membranes of both the smaller and the larger cell populations. In addition, boundary conditions are prescribed on the boundary of a region which is large compared to both cell lengths (order one in the L_0 scale).

The pump term p_i is chosen so that no net ionic flux occurs between intracellular and extracellular space. This is physiologically correct under normal conditions over many seconds. It is assumed that:

$$(2.7) \qquad \int_M \{\nu z_i g_i(V_r - V_i) + p_i\}dS = 0$$

Summation of (2.5) produces, using electroneutrality:

$$(2.8) \qquad -\nabla_x \sigma \cdot \vec{n} = \sum_{i=1}^{3} \nu z_i g_i(V - V_i) + P_1$$

and (2.8) - (2.9) hold at the cell membranes. Multiplication of (2.5) by z_i and summation results in:

(2.9)
$$-\nu\sigma\nabla_x\phi\cdot\vec{n} = \sum_{i=1}^{3} \nu g_i(V - V_i) + P_2.$$

When $g_i = 0 = p_i$ for i such that $\text{sgn}(z_i) = \text{const}$, the membrane is permeable to only cations or only anions and a useful simplification ensues. For example if the membrane is permeable only to cations; $\sum_{i=1}^{3} \{\nu g_i(V - V_i) + z_i p_i\}$ $= \sum_{i=1}^{3} \{\nu z_i g_i(V - V_i) + p_i\}$ so that from (2.8) - (2.9).

(2.10)
$$\nabla_x\sigma\cdot\vec{n} = \nu\sigma\nabla_x\phi\cdot\vec{n},$$

at the membrane. This condition will be applied at the membrane of model glial cells since they are permeable only to potassium, K^+. †

Because the quantities g_i, P_i, and q_i contain the dimension of length, independent assumptions must be made about the asymptotic orders of the corresponding dimensionless quantities, just as assumptions must be made about the asymptotic orders of cell lengths. Different assumptions correspond to tissue models with different physical properties. It should be noted that the definitions of $\tilde{g}_i$ and $\tilde{p}_i$ imply that the dimensionless quantities may become large as $L \longrightarrow \infty$.

---

† The model equations remain fully coupled because of the time derivative occurring in (2.3).

2.5. Continuity and Smoothness Conventions

The dependent variables are differentiable everywhere, except possibly at the cell membrane, where jumps may occur. It is assumed that the dependent variables ϕ, and C_i, containing transmembrane jumps take some bounded values inside the membrane, but only the transmembrane jumps will enter the calculation. The ionic and charge fluxes are continuous, and given by (2.2) and (2.4) respectively, away from the membrane. When the electric potential and ion concentrations jump across the membrane, the derivatives of these quantities do not exist at the membrane. Thus, the intracellular and extracellular solutions are coupled through the jump conditions (2.5) at the membrane.

While the above conditions completely specify the solutions, it is still necessary to evaluate averages of the spatial derivatives of the electrical potential and ionic concentrations over the complete unit cell, including the membrane, during the formal calculation of bulk properties. One straightforward approach to this computation would be to replace the membrane by a thin region of low conductivity and to take limits as the thickness of the region and its conductivity jointly tend to zero. To avoid such lengthy analytic arguments in the course of the asymptotic calculation, however, it is useful to extend the interpretation of the spatial derivatives and to use an extension of the divergence theorem, discussed in this section. While similar results could be obtained in three dimensions, we only need the two-dimensional result in later chapters.

The divergence theorem may be extended to functions with jump discontinuities along a piecewise smooth curve in two dimensions as follows. Let $\vec{F}$ be a vector field to which the divergence theorem applies on two disjoint open regions, R_1 and R_2, with boundaries, ∂R_1 and ∂R_2, where R_1 and R_2 are

separated by a curve, M, which lies in ∂R_1 and ∂R_2. A jump discontinuity in $\vec{F}$ occurs on M, and the divergence operator $\nabla \cdot$ is interpreted so that (cf. Royden, 1968):

$$(2.11) \qquad \lim_{\delta \to 0} \int_{M_\delta} \nabla \cdot \vec{F} dA = \int_M \{\vec{F}_2 - \vec{F}_1\} \cdot \vec{n}_M ds,$$

where $\vec{F}_r$, $r = 1, 2$, are the values of $\vec{F}$ in R_r adjacent to M, $\vec{n}_M$ is a unit normal to M pointing into R_1 and M is traversed once. The right-hand-side may be computed as the limit as $\delta \to 0$ of a sequence of functions $\vec{F}_\delta$ where each $\vec{F}_\delta$ changes smoothly from $\vec{F}_1$ to $\vec{F}_2$ in the neighbourhood of M, M_δ. Then:

$$\int_{R \cup M} \nabla \cdot \vec{F} dA = \int_{int R_1} \nabla \cdot \vec{F} dA + \int_{int R_2} \nabla \cdot \vec{F} dA + \lim_{\delta \to 0} \int_{M_\delta} \nabla \cdot \vec{F} dA$$

$$(2.12) \qquad = \int_{\partial R_1 - M} \vec{F} \cdot \vec{n} \, ds + \int_M \vec{F}_1 \vec{n}_M \, ds + \int_{\partial R_2 - M} \vec{F} \cdot \vec{n} \, ds$$

$$- \int_M \vec{F}_2 \cdot \vec{n}_M \, ds + \int_M \{\vec{F}_2 - \vec{F}_1\} \cdot \vec{n}_M \, ds$$

$$= \int_{\partial R - M} \vec{F} \cdot \vec{n} \, ds$$

where $\vec{n}$ is an outward pointing unit normal on $\partial R_1 \cup \partial R_2 - M$, boundary arcs are traversed counterclockwise, and $R = R_1 \cup R_2$. This is the same formal result as the divergence theorem except that $\vec{F}$ is discontinuous.

To illustrate the extended divergence theorem, let $S(\vec{x})$ be defined by:

$$S(\vec{x}) = \begin{cases} S^1(\vec{x}) & \text{for } \vec{x} \text{ in ECS} \\ S^0(\vec{x}) & \text{for } \vec{x} \text{ in M} \\ S^2(\vec{x}) & \text{for } \vec{x} \text{ in ICS} \end{cases}$$

(2.13)

where S^r, $r = 0, 1, 2$, are continuous in their respective domains, ECS denotes the extracellular space, ICS the intracellular space, and M the separating membrane. For example, the function $S(\vec{x})$ could be the conductivity function, σ. Let $\vec{G}$ be continuous except for a jump across the membrane. The function $\vec{G}$ corresponds to a dependent variable ϕ or C_i.

Using the extended divergence theorem (2.12) on R = (ICS)U(ECS)U(M), we obtain

$$\int_R \nabla \cdot S\vec{G} \ dA = \int_{\partial R - M} S\vec{G} \cdot \vec{n} \ dS$$

(2.14)

which is zero when there are periodic boundary conditions on R - M. A similar calculation for the integral:

$$\int_R S\nabla \cdot \vec{G} \ dA = \int_{R-M} S\nabla \cdot \vec{G} \ dA + \int_M S(\vec{G}^2 - \vec{G}^1) \cdot \vec{n} \ dS$$

(2.15)

yields two terms.

When $\vec{G}$ is the gradient of concentration or electric potential, the first integral of the right-hand-side of (2.15) represents the average flux of the

associated quantity and the second integral is proportional to the net transmembrane flux. Thus, if the associated quantity is conserved within the cell, the second integral is zero.

These results are used later to simplify expressions of the form of the left hand sides of (2.14) - (2.15), by removing the need to integrate over the membrane.

2.6. The Mathematical Approach

The equations, non-dimensionalizations, and assumptions presented in this Chapter complete the specification of the mathematical model for bulk tissue properties. This model corresponds mathematically to a non-linear initial-boundary-value problem with coefficients rapidly varying in space. In Chapter III it will be shown that computation of the macroscopic properties of this model can be reduced, using the method of multiple scales, to a sequence of numerical boundary-value problems on periodic domains (Keller, 1977; Bensoussan et al., 1978). These problems are called 'cell' problems in Bensoussan et al., and are called 'canonical' problems here to avoid confusion. Whereas the solution of the original problem when ϵ is small is an ill-conditioned and complicated computational problem (Traub et al., 1985 a,b; Babuska, 1976), the numerical solution of the canonical problem is straightforward. The application of the method of multiple scales to the computation of averaged properties of inhomogeneous media is called 'homogenization' (Babuska, 1976; Bensoussan et al., 1978; Sanchez-Palencia, 1980).

III. ASYMPTOTIC EXPANSION

1.0. INTRODUCTION

The dependent variables ϕ, σ, and C_i are functions of time and the spatial coordinates, $\vec{x}$. In order to apply the method of multiple scales, additional scaled spatial coordinates are defined by, $\vec{u} := \vec{x} / L_0$, $\vec{v} := \vec{x} / L_1$, $\vec{w} := \vec{x} / L_2$.

The conductances, g_i, appearing in the jump conditions II.(2.5) are each defined by scaling with respect to an arbitrary length L in Table II.2.4. Because we are interested in the bulk properties of cell arrays, the scaled conductance is equal to the entry in Table II.2.4 with $L=L_0$, where L_0 is long compared to the cell length. An additionally scaled value of g_i is defined as follows. Since experimental data (Turner & Schwartzkroin, 1984) show that neuronal electrotonic length scales (length scales formed from the electrical parameters) and the cell length are of similar magnitude, the scaled value of g_i with $L=L_1$ is O(1). Hence, we define a new g_i using $L=L_1$ and rewrite the scaled conductance as $\epsilon^{-1} g_i$ where the new g_i is O(1). A similar argument is used to define rescaled pump fluxes. The pump fluxes must have the same order as g_i in order to balance the transmembrane fluxes as described in Chapter II.

Since the asymptotically larger population might not be neurons, other rescalings of g_i are possible. However, the above assumption is the least-order assumption about membrane conductance which allows O(1) flux through this population. The role of electrotonic parameters in tissue models is discussed in more detail in Chapter V.

In the asymptotically finer 'glial' population, g_i is rescaled in the same way as above, and we rewrite the scaled conductance as $\epsilon^{-1} g_i$ where the new

g_i is O(1). Thus, electrotonic length scales have been assumed to be the same in the two populations, so that the membranes and intracellular and extracellular media of the finer population are assumed to have the same properties as in the coarser population. This assumption is made because there is relatively little data about membrane properties of very fine tissue structures. Because the leading-order equations up to O(1) will contain no time derivatives, the time dependence is suppressed.

1.1. Expansion

With the above definition of the scaled spatial coordinates, we have the formal correspondence:

$$\nabla_x \longrightarrow \epsilon^{-2}\nabla_w + \epsilon^{-1}\nabla_v + \nabla_u$$

$$(1.1) \qquad := \sum_{m=-2}^{0} \epsilon^m \vec{D}_m \ .$$

It is assumed that ϕ, σ, and C_i may be expanded in the form: $\phi = \sum_{n=0}^{\infty} \epsilon^n \phi_n$, $\sigma = \sum_{n=0}^{\infty} \epsilon^n \sigma_n$, and $C_i = \sum_{n=0}^{\infty} \epsilon^n C_{in}$. Details of the expansion of operators and boundary conditions are given in Appendix III.A.

Collecting the equations from (A.4) - (A.6) for ϕ_0, σ_0, and C_{i0} we have:

$$\nabla_w \cdot (\sigma_0 \nabla_w \phi_0) = 0,$$

$$(1.2) \qquad \nabla_w^2 \sigma_0 = 0,$$

$$\nabla_w \cdot (\theta_i \nabla_w C_{io}) + \nu z_i \nabla_w \cdot (\theta_i C_{io} \nabla_w \phi_0) = 0.$$

The jump conditions in $\vec{w}$ are applied at glial membrane. Since the membrane is permeable only to K^+, we use the simplification (II.2.10) to obtain explicitly;

$$\sigma_0 \nabla_w \phi_0 \cdot \vec{n} = 0,$$

(1.3) $$\nabla_w \sigma_0 \cdot \vec{n} = 0,$$

$$\theta_i \nabla_w C_{io} \cdot \vec{n} = 0.$$

These conditions together with periodicity in $\vec{w}$ specify ϕ_0, σ_0, and C_{io}, intracellularly and extracellularly, though not the transmembrane jump. Because the equations (1.2) are potential equations and the jump conditions (1.3) are homogeneous Neumann conditions, σ_0 is a function of $\vec{u}$ and $\vec{v}$ alone. Thus ϕ_0 is a function of $\vec{u}$ and $\vec{v}$ alone. Using these observations it is concluded that C_{io} is a function of $\vec{u}$ and $\vec{v}$ alone. The jump across the membrane will be determined later using (A.8) - (A.10).

Gathering equations for ϕ_1, σ_1, and C_{i1}, in the expansions (A.4) - (A.6) produces:

$$A^{\sigma}_{-3} \phi_0 + \nabla_w \cdot (\sigma_0 \nabla_w \phi_1) = 0,$$

(1.4) $\quad A_{-3}\sigma_0 + \nabla_w^2\sigma_1 = 0,$

$$\theta_i A_{-3} C_{io} + \nabla_w \cdot (\theta_i \nabla_w C_{i1}) + \nu z_i \{\theta_i A_{-3}^C \phi_0 + \nabla_w \cdot (\theta_i C_{io} \nabla_w \phi_1)\} = 0,$$

where $A_{-3}^f = \nabla_v \cdot (f_0 \nabla_w) + \nabla_w \cdot (f_0 \nabla_v) + \nabla_w \cdot (f_1 \nabla_w)$, and from (A.8) - (A.10):

$$-\nu\sigma_0\{\nabla_w\phi_1\cdot\vec{n} + \nabla_v\phi_0\cdot\vec{n}\} = \sum_{i=1}^{3} g_{io}(\nu V_0 - \nu V_i) + P_2,$$

(1.5) $\qquad -\nabla_w\sigma_1\cdot\vec{n} - \nabla_v\sigma_0\cdot\vec{n} = \sum_{i=1}^{3} z_i g_{io}(\nu V_0 - \nu V_i) + P_1,$

$$-\theta_i\{\nabla_w C_{i1}\cdot\vec{n} + \nabla_v C_{io}\cdot\vec{n}\} = z_i(1 - \theta_i C_{io}/\sigma_0)g_{io}(\nu V_0 - \nu V_i) + p_i.$$

The integral of the transmembrane fluxes (1.5) over the cell membrane must be zero, where the integral over 'glial' membrane is performed in the $\vec{w}$ coordinate. Since the O(1) solution of (1.2) - (1.3) implies that the right hand sides are functions of $\vec{u}$ and $\vec{v}$ alone, this implies that the right hand sides of (1.5) are identically zero.

The definition of A_{-3}^f and the form of ϕ_0, σ_0, and C_{io} in $\vec{w}$ imply that A_{-3}^f annihilates each of the operands in (1.4). The equations (1.4) for ϕ_1, σ_1, and C_{i1} in the intracellular and extracellular media are thus identical to those for ϕ_0, σ_0, and C_{io}.

Equations (1.4) reduce to potential equations because of the form of ϕ_0, σ_0, and C_{io} in $\vec{w}$. However, the jump conditions depend on ϕ_0, σ_0, and

C_{io} which are arbitrary functions of $\vec{v}$. For example, because ϕ_0 is an arbitrary function of $\vec{v}$, each derivative $\nabla_v \phi_0$ is an arbitrary function in the solution for ϕ_1. It may be verified by direct substitution into (1.4) and (1.5) that if ϕ_1, σ_1, and C_{i1}, respectively, have the form; $\phi_1 = \vec{\chi} \cdot \nabla_v \phi_0 + \overset{\cdot}{\phi}_1$, $\sigma_1 = \vec{\eta} \cdot \nabla_v \sigma_0 + \overset{\cdot}{\sigma}_1$, and, $C_{i1} = \vec{\kappa}_i \cdot \nabla_v C_{io} + \hat{C}_{i1}$, where $\overset{\cdot}{\phi}_1$, $\overset{\cdot}{\sigma}_1$, and $\hat{C}_{i1}$ are arbitrary functions of $\vec{u}$, and $\vec{\chi}$, $\vec{\eta}$ and $\vec{\kappa}$ satisfy the vector equations:

$$\vec{\nabla}_w \cdot (\sigma_0 \vec{\nabla}_w \vec{\chi}) = 0,$$

(1.6) $$\vec{\nabla}_w \cdot \vec{\nabla}_w \vec{\eta} = 0,$$

$$\vec{\nabla}_w \cdot (\theta_i \vec{\nabla}_w \vec{\kappa}_i) = 0,$$

with jump conditions at 'glial' membrane:

$$\vec{\nabla}_w \vec{\chi} \cdot \vec{n} = -\vec{n},$$

(1.7) $$\vec{\nabla}_w \vec{\eta} \cdot \vec{n} = -\vec{n},$$

$$\vec{\nabla}_w \vec{\kappa}_i \cdot \vec{n} = -\vec{n},$$

then a solution is obtained.

Because (1.4) reduce to potential equations, no other non-trivial $\vec{w}$ dependence is possible, by applying the same argument that was used at order

one to the difference of two solutions.

It is only necessary to know the general form of ϕ_2, σ_2, and C_{i_2} in the computation of the $\vec{u}$-dependence of ϕ_0, σ_0, and C_{i_0}. The computation which specifies ϕ_2, σ_2, and C_{i_2} is given in Appendix III.B. It is shown that the intracellular and extracellular equations for these quantities are potential equations and the solutions assume a simple form analogous to that of ϕ_1, σ_1, and C_{i_1}.

2.0. AVERAGING

2.1. Introduction

The symbol $M_w(\cdot)$ denotes the average over the $\vec{w}$ unit cell;

$$(2.1) \qquad M_W(F) = \frac{1}{|W|} \int_{W-M} F \, dA_w$$

where W denotes the $\vec{w}$ unit cell, $dA_w = dw_1 dw_2$, and

$$(2.2) \qquad |W| = \int_{W-M} F \, dA_w.$$

The interpretation of averaging for our asymptotic solutions is now given, and the asymptotic size of the averaging region is specified precisely. This clarifies the relationship between the periodic average given by (2.1) - (2.2) and the average over a 'sufficiently large' region in the unscaled spatial variable, often referred to in the physical literature (Garland & Tanner, 1978) without mathematical definition.

Suppose that a formal flux vector, $\vec{J}(\vec{x},\vec{X})$, is given by the multiple scales

procedure where $\vec{x} = (x_1, x_2)$ are the space coordinates, $\vec{X} = (X_1, X_2) :=$ $(x_1/\epsilon, x_2/\epsilon)$, and $\vec{J}$ is doubly periodic in (X_1, X_2) and a smooth function of $\vec{x}$. Then the spatial flux vector is defined by $\vec{j}\ (\vec{x}, \epsilon) := \vec{J}\ (\vec{x}, \vec{x}/\epsilon)$.

It will be shown that a smooth flux vector $\vec{J}_A$ can be defined at each point $\vec{x}_0 := (x_{10}, x_{20})$ by averaging $\vec{j}(\vec{x}, \epsilon)$ over a square region, R_μ, of side μ centered at $\vec{x}_0$, assuming that $\mu = \epsilon^\rho$ for some ρ, $0 < \rho < 1$ as $\epsilon \to 0$, and recalling that the cells have length $O(\epsilon)$. The result $\vec{J}_A(\vec{x}_0)$ is independent of the choice of ρ, $0 < \rho < 1$. A property which holds locally will hold within an asymptotic region of this size. Also, it will be shown that averages over R_μ are functions only of the first set of arguments of $\vec{J}$ (coarse variables), and may be evaluated by integrating over a single period of the second set of arguments (fine variables).

The above statements follow from computing the average of $\vec{j}$ over R_μ, a square area element of side $\mu = \epsilon^\rho$, centered at $\vec{x}_0$:

$$(2.3) \qquad \vec{j}_R(\epsilon, \vec{x}_0) = \frac{1}{|R_{\epsilon^\rho}|} \int_{R_{\epsilon^\rho}} \vec{j}(\vec{x}_0, \vec{x}_0/\epsilon)\ dA,$$

where $|R_{\epsilon^\rho}| = \epsilon^{2\rho}$. Then the average flux vector will be the limit of (2.3) as $\epsilon \to 0$, i.e., $\vec{J}_A = \lim_{\epsilon \to 0} \vec{j}_R(\epsilon, \vec{x}_0)$.

To evaluate the limit it is useful to make the change of variables in the integrand: $\bar{x}_1 = \epsilon^{-1}(x_1 - x_{10})$ and $\bar{x}_2 = \epsilon^{-1}(x_2 - x_{20})$, or in vector form $\vec{\bar{x}} = \epsilon^{-1}(\vec{x} - \vec{x}_0)$. It then follows that $dA = dx_1 dx_2 = \epsilon^2\ d\bar{x}_1\ d\bar{x}_2 = \epsilon^2\ d\bar{A}$ and the regions of integration transform $R_{\epsilon^\rho} \longrightarrow \bar{R}_{\epsilon^{\rho-1}}$ where

$$R_{\epsilon\rho} = \{(x_1, x_2): x_{10} - \epsilon^\rho/2 < x_1 < x_{10} + \epsilon^\rho/2; \ x_{20} - \epsilon^\rho/2 < x_2 < x_{20} + \epsilon^\rho/2\}$$

(2.4)

$$\overline{R}_{\epsilon\rho-1} = \{(x_1, x_2): -\epsilon^{\rho-1}/2 < \overline{x}_1 < \epsilon^{\rho-1}/2; \ -\epsilon^{\rho-1}/2 < \overline{x}_2 < \epsilon^\rho/2\}.$$

The vector $\vec{J}_A$ may now be expressed as an integral over the fine variables (X_1, X_2) since as $\epsilon \to 0$:

$$\vec{J}_A = \lim_{\epsilon \to 0} \vec{j}_R(\epsilon, \vec{x}_0) = \lim_{\epsilon \to 0} \frac{1}{\epsilon^{2\rho}} \int_{R_{\epsilon\rho}} \vec{j}(\vec{x}_0 - \epsilon\vec{x}, \ \vec{x}_0/\epsilon - \vec{x}) dA$$

(2.5)
$$= \lim_{\epsilon \to 0} \epsilon^{\frac{1}{2\rho-2}} \int_{\overline{R}_{\epsilon\rho-1}} \vec{j}(\vec{x}_0 + \vec{O}(\epsilon^\rho), \ \vec{x}_0/\epsilon - \vec{x}) d\overline{A}$$

$$= \lim_{T,S \to \infty} \frac{1}{4ST} \int_{-T}^{T} \int_{-S}^{S} \vec{j}(\vec{x}, \vec{X}) \ dX_1 dX_2$$

where the last equality is obtained from the multi-periodicity of $\vec{J}(\vec{x}, \cdot)$, setting $S = T = \epsilon^{\rho-1}/2$, $X_1 = -\overline{x}_1 + x_{10}/\epsilon$, and $X_2 = -\overline{x}_2 + x_{20}/\epsilon$. For fixed (x_{10}, x_{20}), the periodicity of $\vec{J}$ implies that the average in (2.5) may be evaluated over a single period. Thus, for regions of appropriate asymptotic size, an average flux vector $\vec{J}_A$ is defined even though $\vec{J}$ may not be continuous, and $\vec{J}_A(\vec{x})$ is a function of the coarse variables alone.

2.2. Averaging Procedure

In this section the specification of the average governing equation at coarse length scales is completed. The $\vec{v}$-dependence of ϕ_0, σ_0, C_{i0}, is deduced from a necessary condition for the existence of a bounded solution for ϕ_3, σ_3, and C_{i3}, namely the Fredholm Alternative applied to a constant function at $O(\epsilon^{-2})$ in (A.4) - (A.6). This condition is equivalent to the physical observation that there can be no steady periodic solution to the potential equation unless (charge or concentration) is conserved, so that the periodic source density must have zero integral over each period. This leads to the conditions:

$$\int_W \{A_{-2}\sigma_0 + A_{-3}\sigma_1\}dA_W = 0$$

(2.6)

$$\int_W \{A^{\sigma}_{-2}\phi_0 + A^{\sigma}_{-3}\phi_1\}dA_W = 0$$

$$\int_W \theta_i\{A_{-2}C_{i0} + A_{-3}C_{i1} + \nu z_i\theta_i(A^C_{-2}\phi_0 + A^C_{-3}\phi_1)\}dA_W = 0$$

where $A^f_{-2} = \nabla_u \cdot (f_0\nabla_w) + \nabla_w \cdot (f_0\nabla_u) + \nabla_v \cdot (f_1\nabla_w) + \nabla_w \cdot (f_1\nabla_v) + \nabla_v \cdot (f_0\nabla_v) + \nabla_w \cdot (f_2\nabla_w)$, and the integrals are interpreted as described in Section II.2.5. Thus, using the extended divergence theorem, the integrals of ∇_w applied to discontinuous $\vec{w}$-periodic quantities are zero.

To obtain the $\vec{u}$-dependence of ϕ_0 , σ_0 , and C_{i0} , the same necessary condition for the existence of bounded ϕ_4 , σ_4 , and C_{i4} is applied to the $O(1)$ equations from the expansion of Appendix III.A. These equations are integrated over $\vec{w}$ and $\vec{v}$ to give:

$$\int_{WV} \{A_0 \sigma_0 + A_{-1} \sigma_1 + A_{-2} \sigma_2\} dA_V dA_W = \int_{WV} \{Q_1 + \tau \sum_i \frac{\partial C_{i0}}{\partial t}\} dA_V dA_W$$

$$(2.7) \quad \int_{WV} \{A_0^\sigma \phi_0 + A_{-1}^\sigma \phi_1 + A_{-2}^\sigma \phi_2\} dA_V dA_W = \int_{WV} Q_2 \, dA_V dA_W$$

$$\int_{WV} \theta_i \{A_0 C_{i0} + A_{-1} C_{i1} + A_{-2} C_{i2}\} dA_V dA_W$$
$$+ \nu z_i \theta_i \int_{WV} \{A_0^C \phi_0 + A_{-1}^C \phi_1 + A_{-2}^C \phi_2\} dA_V dA_W$$
$$= \int_{WV} \{q_i + \tau \frac{\partial C_{i0}}{\partial t}\} dA_V dA_W$$

where WV is the unit cell in $\vec{v}$ space and $A_0^f = \nabla_u \cdot (f_0 \nabla_u) + \nabla_u \cdot (f_1 \nabla_v) + \nabla_v \cdot (f_1 \nabla_u) + \nabla_u \cdot (f_2 \nabla_w) + \nabla_w \cdot (f_2 \nabla_u) + \nabla_v \cdot (f_3 \nabla_w) + \nabla_w \cdot (f_3 \nabla_v) + \nabla_w \cdot (f_4 \nabla_w)$.

This averaging procedure, as applied to the computation of bulk properties of inhomogeneous materials is discussed by Bensoussan et al., (1978) but has not previously been applied to any non-linear equation with jump conditions in the interior of the domain. However, the main objective here is the application of the analysis, rather than mathematical novelty. These equations provide an alternative to the cable model in computing the bulk properties of brain tissue and this treatment differs from those of Ranck (1964) and Havstad (1976) by the use of a systematic averaging procedure and the incorporation of ion transport into the model.

The resulting averaged equations have an extracellular and intracellular part. In order to apply the averaged equations it is necessary to determine the

extracellular and intracellular parts. Thus we now investigate the specific form of the solutions to (2.6) (2.7). This part of the calculation appears to be new.

It is assumed that a geometry has been chosen in which the averaged coefficients reduce to scalars. In this case, the averaged equations (2.6) become

$$e\nabla_v^2 \sigma_0 \;=\; 0,$$

$$(2.8) \qquad \nabla_v \cdot (a\sigma_0 \nabla_v \phi_0) \;=\; 0,$$

$$\nabla_v \cdot (\theta_i e_i \nabla_v C_{i0}) \;=\; 0,$$

with periodic boundary conditions on the $\vec{v}$ unit cell (neuronal scale) and the jump conditions at neuronal membrane:

$$-e\nabla_v \sigma_0 \cdot \vec{n} \;=\; P_1 \;+\; g_{20}\{\nu V_0 - \nu V_k\}$$

$$(2.9) \qquad -\nu a\sigma_0 \nabla_v \phi_0 \cdot \vec{n} \;=\; P_2 + g_{20}\{\nu V_0 - \nu V_k\}$$

$$-e_i C_{i0} \nabla_v \phi_0 \cdot \vec{n} \;-\; \theta_i e_i \nabla_v C_{i0} \cdot \vec{n} \;=\; p_i \;+\; z_i g_{i0}\{\nu V_0 - \nu V_k\}$$

where $\nu V_K := \ln(C_{20}^0 / C_{20}^i)$ and the definitions of a, e, and e_i are given in Appendix III.C with the more general calculation. The right-hand-sides of these equations are zero by an argument similar to that given for the right-hand-sides of equations (1.5). These equations have continuous intracellular and extracellular

solutions ϕ_0, σ_0, C_{io}, where $\phi_0^i = \phi_0^0 + V_K$ while σ_0^i and C_{io}^j are constants.

After averaging in $\vec{w}$ (described in Appendix III.C) the $O(\epsilon)$ equations are:

$$e\nabla_v^2 \sigma_1 = 0,$$

$$(2.10) \qquad \nabla_v \cdot (a\sigma_0 \nabla_v \phi_1) = 0,$$

$$\nabla_v \cdot (\theta_i e_i \nabla_v C_{i_1}) + \nu z_i \nabla_v \cdot (\theta_i e_i C_{io} \nabla_v \phi_1) = 0,$$

with jump conditions at 'neuronal' membrane:

$$-e\{\nabla_v \sigma_1 \cdot \vec{n} + \nabla_u \sigma_0 \cdot \vec{n}\} = g_{20}\{\nu V_1 + (\frac{C_{21}^i}{C_{20}^i} - \frac{C_{21}^0}{C_{20}^0})\},$$

$$(2.11) \quad -a\sigma_0\{\nabla_v \phi_1 \cdot \vec{n} + \nabla_u \phi_0 \cdot \vec{n}\} = g_{20}\{\nu V_1 + (\frac{C_{21}^i}{C_{20}^i} - \frac{C_{21}^0}{C_{20}^0})\},$$

$$-\theta_i e_i\{\nabla_v C_{i_1} \cdot \vec{n} + \nabla_u C_{io} \cdot \vec{n}\} = z_i(1-\theta_i e_i C_{io}/a\sigma_0)g_{20}\{\nu V_1 + (\frac{C_{21}^i}{C_{20}^i} - \frac{C_{21}^0}{C_{20}^0})\},$$

and periodic boundary conditions on the unit cell. The periodic boundary conditions follow from the periodic structure of the tissue. These equations (2.11) hold intracellularly and extracellularly.

The equations (2.10) - (2.11) are linear and the solutions may be obtained by the substitutions

$$\sigma_1 = \nu(\vec{\eta}_p \cdot \nabla_u \phi_0 + \vec{\eta}_v \cdot \nabla_u V_0) + \vec{\eta}_c \cdot \nabla_u C_{io} + \vec{\eta}_s \cdot \nabla_u \sigma_0 + \hat{\sigma}_1,$$

$$(2.12) \quad \nu\phi_1 = \nu(\vec{\chi}_p \cdot \nabla_u \phi_0 + \vec{\chi}_v \cdot \nabla_u V_0) + \vec{\chi}_c \cdot \nabla_u C_{io} + \vec{\chi}_s \cdot \nabla_u \sigma_0 + \hat{\phi}_1,$$

$$C_{i1} = \nu C_{io}(\vec{\kappa}_p \cdot \nabla_u \phi_0 + \vec{\kappa}_v \cdot \nabla_u V_0) + C_{io}(\vec{\kappa}_c \cdot \nabla_u C_{io} + \vec{\kappa}_s \cdot \nabla_u \sigma_0) + \hat{C}_1.$$

where $\vec{\chi}_p$, $\vec{\chi}_v$, $\vec{\chi}_c$, $\vec{\chi}_s$, $\vec{\eta}_p$, $\vec{\eta}_v$, $\vec{\eta}_c$, $\vec{\eta}_s$, $\vec{\kappa}_p$, $\vec{\kappa}_v$, $\vec{\kappa}_c$, and $\vec{\kappa}_s$ are to be determined. We write $\tilde{\sigma}_0 = a\sigma$, $\tilde{\theta}_i = e_i \theta_i$ and drop the tildes in what follows. Substituting as described into (2.10) - (2.11), it is found that the variables to be determined in (2.12) satisfy the potential equation extracellularly and intracellularly, with jump conditions at the cell membrane given by:

$$-\frac{e}{a}\nabla_v \eta_{p1} \cdot \vec{n} = g_{20}\{\chi^i_{p1} - \chi^0_{p1} + \kappa^i_{p1} - \kappa^0_{p1}\},$$

$$(2.13) \qquad -\sigma_0\{\nabla_v \chi_{p1} \cdot \vec{n} + n_1\} = g_{20}\{\chi^i_{p1} - \chi^0_{p1} + \kappa^i_{p1} - \kappa^0_{p1}\},$$

$$-\theta_i C_{io} \nabla_v \kappa_{p1} \cdot \vec{n} = g_{io}(1 - \theta_i C_{io}/\sigma_0)\{\chi^i_{p1} - \chi^0_{p1} + \kappa^i_{p1} - \kappa^0_{p1}\},$$

$$-\frac{e}{a}\nabla_v \eta_{v1} \cdot \vec{n} = g_{20}\{\chi^i_{v1} - \chi^0_{v1} + \kappa^i_{v1} - \kappa^0_{v1}\},$$

(2.14)

$$-\sigma_0^0 \nabla_v \chi_{v1}^0 \cdot \vec{n} = -\sigma_0^i \{\nabla_v \chi_{v1}^i \cdot \vec{n} + n_1\} = g_{20}\{\chi_{v1}^i - \chi_{v1}^0 + \kappa_{v1}^i - \kappa_{v1}^0\},$$

$$-\theta_i C_{io} \nabla_v \kappa_{v1} \cdot \vec{n} = g_{io}(1-\theta_i C_{io}/\sigma_0)\{\chi_{v1}^i - \chi_{v1}^0 + \kappa_{v1}^i - \kappa_{v1}^0\},$$

$$-\frac{e}{a}\{\nabla_v \eta_{s1}^0 \cdot \vec{n} + n_1\} = g_{20}\{\chi_{s1}^i - \chi_{s1}^0 + \kappa_{s1}^i - \kappa_{s1}^0\},$$

(2.15)

$$-\sigma_0 \nabla_v \chi_{s1} \cdot \vec{n} = g_{20}\{\chi_{s1}^i - \chi_{s1}^0 + \kappa_{s1}^i - \kappa_{s1}^0\},$$

$$-\theta_i C_{io} \nabla_v \kappa_{s1} \cdot \vec{n} = g_{io}(1-\theta_i C_{io}/\sigma_0)\{\chi_{s1}^i - \chi_{s1}^0 + \kappa_{s1}^i - \kappa_{s1}^0\},$$

$$-\frac{e}{a} \nabla_v \eta_{c1}^0 \cdot \vec{n} = g_{20}\{\chi_{c1}^i - \chi_{c1}^0 + \kappa_{c1}^i - \kappa_{c1}^0\}$$

(2.16)

$$-\sigma_0 \nabla_v \chi_{c1} \cdot \vec{n} = g_{20}\{\chi_{c1}^i - \chi_{c1}^0 + \kappa_{c1}^i - \kappa_{c1}^0\}$$

$$-\theta_i C_{io} \nabla_v \kappa_{c1} \cdot \vec{n} = -\theta_i\{C_{io}^0 \nabla_v \kappa_{c1}^0 \cdot \vec{n} + n_1\}$$
$$= g_{io}(1-\theta_i C_{io}/\sigma_0)\{\chi_{c1}^i - \chi_{c1}^0 + \kappa_{c1}^i - \kappa_{c1}^0\}$$

where the subscript 1 denotes the first components of the quantities $\vec{\chi}$, $\vec{\eta}$, and $\vec{\kappa}$. Later it is shown that the canonical problem for each component is the same and thus, that these coefficients reduce to scalars under appropriate geometrical

assumptions.

Since the variables $\vec{\eta}$ do not appear on the right-hand-side of (2.11), it is possible to solve (2.10) - (2.11) by first solving for χ_p, χ_v, χ_c, χ_s, κ_p, κ_v, κ_c, and κ_s because they are independent of the η solutions. In addition, as described in Chapter IV, it is assumed that $\nabla_u \sigma_0 = 0$. Hence the η solutions do not appear in the expressions for ϕ_1, σ_1, and C_{i_1} and need not be computed. The χ and κ solutions, which are calculated numerically in Chapter IV, will be substituted into the averaging conditions (2.7) to obtain the average governing equations which are the goal of this chapter.

Substitution of the χ and κ solutions into (2.7) gives the equations:

$$D_1 \nabla_u^2 \phi_0 + E_1 \nabla_u^2 V_0 + F_1 \nabla_u^2 C_0 = Q_2$$

(2.17)

$$D_2 \nabla_u^2 \phi_0 + E_2 \nabla_u^2 V_0 + F_2 \nabla_u^2 C_0 = q + \tau \frac{\partial C_0}{\partial t}$$

where C_0 is the potassium ionic concentration and the coefficients are defined using (2.1) - (2.2) by

$$D_1 = \sigma_0 M_V \{ t_\sigma (1 + \nabla_v \chi_{p1}) \},$$

$$E_1 = \sigma_0 M_V \{ t_\sigma (t_\beta + \nabla_v \chi_{v1}) \},$$

$$F_1 = \sigma_0 \nu^{-1} M_V \{ t_\sigma \nabla_v \chi_{c1} \},$$

(2.18)

$$D_2 = \sigma_0 M_V \{ t_K t_\sigma (1 + \nabla_v \chi_{p1}) + \nabla_v \kappa_{p1} \},$$

$$E_2 = \sigma_0 M_V \{ t_K t_\sigma ((t_\beta + \nabla_v \chi_{v1}) + \nabla_v \kappa_{v1}) \},$$

$$F_2 = \nu^{-1} \{ M_V \{ (\theta C_0 \nabla_v \kappa_{c1} + \theta) + \sigma_0 t_K t_\sigma \nabla_v \chi_{c1} \} \},$$

where t_β is unity intracellularly and zero otherwise, and $t_\sigma = \sigma_0 / \sigma_0^0$.

The periodic problems for the η, χ, and κ variables depend on σ_0, g_{20}, and C_{io} through (2.13) - (2.16) and thus are, in general, functions of $\vec{v}$. Thus an infinite number of the canonical periodic problems must be solved in order to obtain the (variable) coefficient functions of (2.17). This is because the original mathematical problem was non-linear. It is shown in Chapter IV that it is appropriate to approximate (2.17) by a system with constant coefficients obtained from a single set of canonical problems in which $\nabla_u \sigma = 0$. As it is impractical to solve numerically for the variable coefficients this is a useful simplification. The coefficients D_1, D_2, E_1, E_2, F_1, and F_2 are tabulated in Chapter IV using this assumption.

The calculations of this chapter show that the coefficients of the average governing equation are different depending on the length scale. This has implications in the interpretation of data from experiments on the bulk properties of brain tissue, and some specific comparisons of one-tier with two-tier models are made later.

APPENDIX III.A. OPERATOR EXPANSIONS

Using the correspondence (1.1) it follows that:

$$\nabla_x^2 \longrightarrow \epsilon^{-4}\nabla_w^2 + \epsilon^{-3}(\nabla_v \cdot \nabla_w + \epsilon^{-2}(\nabla_u \cdot \nabla_w + \nabla_w \cdot \nabla_u + \nabla_v^2)$$

$$(A.1) \qquad + \epsilon^{-1}(\nabla_u \cdot \nabla_v + \nabla_v \cdot \nabla_u) + \nabla_u^2$$

$$:= \sum_{m=-4}^{0} \epsilon^m A_m,$$

where mixed partials such as $\nabla_u \cdot \nabla_v$ and $\nabla_v \cdot \nabla_u$ must be distinguished from each other in view of the discontinuity at the cell membrane. While the boundary-value problem is formulated using jump conditions at the membrane, it is still necessary to interpret expressions such as $\nabla_u \cdot (\sigma\nabla_w\phi)$ and $\nabla_w \cdot (\sigma\nabla_u\phi)$ in performing averages of derivatives over the unit cell R (intracellular and extracellular spaces and membrane).

Thus if $f = \sum_{n=0}^{\infty} \epsilon^n f_n,$

$$f\nabla_x \longrightarrow \epsilon^{-2}f_0\nabla_w + \epsilon^{-1}(f_0\nabla_v + f_1\nabla_w)$$

$$(A.2) \qquad + \sum_{n=0}^{\infty} \epsilon^n(f_n\nabla_u + f_{n+1}\nabla_v + f_{n+2}\nabla_w)$$

$$:= \sum_{n=-2}^{\infty} \epsilon^n \vec{D}_n^f.$$

In general

$$\nabla_x \cdot (f \, \nabla_x) \longrightarrow (\, \epsilon^{-2} \nabla_w \; + \; \epsilon^{-1} \nabla_v \; + \nabla_u) \cdot (\sum_{n=-2}^{\infty} \epsilon^n \vec{D}_n^f \,)$$

$$(A.3) \qquad\qquad := \sum_{n=-4}^{\infty} \epsilon^n A_n^f \, .$$

So that the model equation (II.2.3) becomes:

$$(A.4) \qquad \sum_{m=-4}^{0} \sum_{n=0}^{\infty} \epsilon^{m+n} A_m \sigma_n \; = \; Q_1 \; + \; \tau \sum_{n=0}^{\infty} \sum_{i=1}^{3} \epsilon^n \frac{\partial C_{in}}{\partial t}$$

and (II.2.4) becomes:

$$(A.5) \qquad \nu \sum_{m=-4}^{0} \sum_{n=0}^{\infty} \epsilon^{m+n} A_m \sigma \phi_n \; = \; Q_2 .$$

We define the operator $\theta_i A_m^C := A_m^f$, where $f = \theta_i C_i$. The differential equations (II.2.2) for C_i become:

$$\sum_{m=-4}^{0} \sum_{n=0}^{\infty} \epsilon^{m+n} \theta_i A_m C_{in} + \nu z_i \sum_{m=-4}^{\infty} \sum_{n=0}^{\infty} \epsilon^{m+n} \theta_i A_m^C \phi_n$$

$$(A.6)$$

$$= \sum_{n=0}^{\infty} \sum_{i=1}^{3} \epsilon^n \frac{\partial C_{in}}{\partial t} + q_i .$$

The jump conditions are now expanded in the new variables. These conditions are to be applied at the asymptotic scales corresponding to the

assumptions about cell sizes. The condition for 'glial' membrane is applied in the $\vec{w}$ variable and the condition for 'neuronal' membrane is applied in the $\vec{v}$ variable.

We define g_{in} by expanding: $g_i(\sum_{n=0}^{\infty} \epsilon^n V_n) = \sum_{n=0}^{\infty} \epsilon^n g_{in}$, so that $g_{i0} = g_i(V_0)$, $g_{i1} = g'_i(V_0)V_1$, $g_{i2} = \frac{1}{2}\{g''_i V_1^2 + 2g'_i V_2\}$ where the prime ' denotes $dg_i(V)/dV$ and define h_{in} by expanding $\nu g_i(V-V_i) = \sum_{n=0}^{\infty} \epsilon^n h_{in}$ so that:

$$h_{i0} = g_{i0}\{\nu V_0 - \frac{1}{z_i}\ln(C_{io}^0 / C_{io}^i)\},$$

(A.7)

$$h_{i1} = g_{i1}\{\nu V_0 - \frac{1}{z_i}\ln(C_{io}^0 / C_{io}^i)\} + g_{i0}\{\nu V_1 - \frac{1}{z_i}\{\frac{C_{i1}^i}{C_{io}^i} - \frac{C_{i1}^0}{C_{io}^0}\}\},$$

etc.

Then the jump conditions (II.2.5) become:

$$-\sum_{m=-2}^{0} \sum_{n=0}^{\infty} \{\epsilon^{m+n}\theta_i \vec{D}_m C_{in} \cdot \vec{n} + \nu z_i \epsilon^{m+n}\theta_i \vec{D}_m C_n \phi_n \cdot \vec{n}\}$$

(A.8)

$$= \sum_{n=0}^{\infty} \epsilon^{n-1} z_i h_{in} + \epsilon^{-1} p_i$$

at the 'glial' and 'neuronal' membranes, where the scaling of p_i was discussed in the introduction to this chapter. The equation (II.2.8) transforms to:

(A.9)
$$-\sum_{m=-2}^{0} \sum_{n=0}^{\infty} \vec{D}_m(\epsilon^{n+m}\sigma_n) \cdot \vec{n} = \sum_{n=0}^{\infty} \epsilon^n z_i h_{in} + P_1$$

and (II.2.9) to:

$$(A.10) \qquad -\nu \sum_{m=-2}^{\infty} \sum_{n=0}^{\infty} \vec{D}_m^{\sigma}(\epsilon^{n+m}\phi_n)\cdot\vec{n} = \sum_{n=0}^{\infty} \epsilon^n h_{in} + P_2$$

at the glial membrane.

APPENDIX III.B. SECOND ORDER PERTURBATIONS OF THE DEPENDENT VARIABLES

To $O(\epsilon^{-2})$ (A.4) - (A.6) imply that ϕ_2, σ_2, and C_{i2} satisfy:

$$A_{-2}^{\sigma}\phi_0 + A_{-3}^{\sigma}\phi_1 + \nabla_w\cdot(\sigma_0\nabla_w\phi_2) = 0,$$

$$(B.1) \quad A_{-2}\sigma_0 + A_{-3}\sigma_1 + \nabla_w^2\sigma_2 = 0,$$

$$\theta_i A_{-2i}C_{i0} + \theta_i A_{-3i}C_{i1} + \nabla_w\cdot(\theta_i\nabla_w C_{i2})$$
$$+ \nu z_i\{\theta_i A_{-2i}^C\phi_0 + \theta_i A_{-3i}^C\phi_1 + \nabla_w\cdot(\theta_i C_{i0}\nabla_w\phi_2)\} = 0,$$

where $A_{-2}^f = \nabla_u\cdot(f_0\nabla_w) + \nabla_w\cdot(f_0\nabla_u) + \nabla_w\cdot(f_1\nabla_v) + \nabla_v\cdot(f_1\nabla_w) + \nabla_w\cdot(f_2\nabla_w)$, while the jump conditions at glial membrane become:

$$-\sum_i h_{i1} = -g_{20}\{\nu V_1 + (\frac{C_{21}^i}{C_{20}^i} - \frac{C_{21}^0}{C_{20}^0})\} = \nu\sigma_1\{\nabla_w\phi_1\cdot\vec{n} + \nabla_v\phi_0\cdot\vec{n}$$
$$+ \nu\sigma_0\{\nabla_w\phi_2\cdot\vec{n} + \nabla_v\phi_1\cdot\vec{n} + \nabla_u\phi_0\cdot\vec{n}\} ,$$

(B.2) $\quad -\sum_i z_i h_{i1} = -g_{20}\{\nu V_1 + (\dfrac{C_{21}^i}{C_{20}^i} - \dfrac{C_{21}^0}{C_{20}^0})\} = \nabla_w \sigma_2 \cdot \vec{n} + \nabla_v \sigma_1 \cdot \vec{n} + \nabla_u \sigma_0 \cdot \vec{n} \;,$

$\quad -h_{i1} = -g_{20}(1 - \theta_i C_{io}/\sigma_0)\{\nu V_1 + (\dfrac{C_{21}^i}{C_{20}^i} - \dfrac{C_{21}^0}{C_{20}^0})\} = \theta_i \{\nabla_u C_{io} \cdot \vec{n} + \nabla_v C_{i1} \cdot \vec{n} + \nabla_w C_{i2} \cdot \vec{n}\} \;.$

The definition of A_{-2}^f and the form of ϕ_0, σ_0, and C_{io} imply that A_{-2}^f reduces to $\nabla_w \cdot (f_1 \nabla_v) + \nabla_v \cdot (f_0 \nabla_v)$, when applied to the O(1) terms in (B.1). No similar reduction is possible for A_{-3}^f but the equations (B.1) - (B.2) may be simplified by substitution of the known forms for ϕ_1, σ_1, C_{i1}. By an explicit calculation, we obtain the equivalent equations for ϕ:

$$-\nabla_w \cdot (\sigma_0 \nabla_w \phi_2) = 2\vec{\nabla}_w \vec{\chi} \cdot \vec{\nabla}_v (\nabla_v \phi_0) + \nabla_v \sigma_0 \cdot \vec{\nabla}_w \vec{\chi} \cdot \vec{\nabla}_w \vec{\eta} \cdot \nabla_v \phi_0$$

(B.3) $$+ \nabla_v \sigma_0 \cdot \vec{\nabla}_w \vec{\eta} \cdot \nabla_v \phi_0 + \sigma_0 \nabla_v^2 \phi_0 + \nabla_v \sigma_0 \cdot \nabla_v \phi_0 \;.$$

The equations for σ are (cancelling θ_i):

(B.4) $$-\nabla_w^2 \sigma_2 = 2\vec{\nabla}_w \vec{\eta} \cdot \vec{\nabla}_v (\nabla_v \phi_0) + \nabla_v^2 \sigma_0 \;,$$

while the equations for C_i are:

$$\nabla_w^2 C_{i2} + 2\vec{\nabla}_w \vec{\kappa} \cdot \vec{\nabla}_v (\nabla_v C_{io}) + \nabla_v^2 C_{io} + \nu z_i \{\nabla_w \cdot (C_{io} \nabla_w \phi_2)$$

(B.5) $\quad + 2C_{io}\vec{\nabla}_w\vec{\chi}\cdot\vec{\nabla}_v(\nabla_v\phi_0) + \nabla_vC_{io}\cdot\vec{\nabla}_w\vec{\chi}\cdot\vec{\nabla}_w\vec{\eta}\cdot\nabla_v\phi_0$

$$+ \nabla_vC_{io}\cdot\vec{\nabla}_w\vec{\kappa}\cdot\nabla_vC_{io} + C_{io}\nabla_v^2\phi_0 + \nabla_vC_{io}\cdot\nabla_v\phi_0\} = 0.$$

where $\vec{\chi}$, $\vec{\eta}$, and $\vec{\kappa}$ are defined in (1.6) - (1.7).

By the solution to (1.4) - (1.5), the first term in the definition of h_{i1} is zero, so that the jump condition for ϕ in equation (B.1) has been simplified to:

$$-g_{20}\{\nu V_1 - (C_1^i / C_0^i - C_1^0 / C_0^0)\} = \nu\sigma_1(\nabla_w\phi_1\cdot\vec{n} + \nabla_v\phi_0\cdot\vec{n}) + \nu\sigma_0(\nabla_w\phi_2\cdot\vec{n}$$
$$+ \nabla_v\phi_1\cdot\vec{n} + \nabla_u\phi_0\cdot\vec{n}).$$ Also, equations (1.6) - (1.7) imply that the terms proportional to σ_1 vanish in the latter expression. Hence the expression reduces to:

$$\nu\sigma_0\{\nabla_w\phi_2\cdot\vec{n} + (\vec{\chi}\cdot\nabla_v)\cdot\nabla_v\phi_0\cdot\vec{n} + \nabla_v\phi_1\cdot\vec{n} + \nabla_u\phi_0\cdot\vec{n}\}$$

(B.6) $\qquad = -g_{20}\{\nu V_1 + (\dfrac{C_{21}^i}{C_{20}^i} - \dfrac{C_{21}^0}{C_{20}^0})\}$.

Similarly:

$$\nu\sigma_0\{\nabla_w\sigma_2\cdot\vec{n} + (\vec{\eta}\cdot\nabla_v)\cdot\nabla_v\sigma_0\cdot\vec{n} + \nabla_v\phi_1\cdot\vec{n} + \nabla_u\phi_0\cdot\vec{n}\}$$
$$= -g_{20}\{\nu V_1 + (\dfrac{C_{21}^i}{C_{20}^i} - \dfrac{C_{21}^0}{C_{20}^0})\},$$

(B.7)

$$\theta_i\{\nabla_w C_{i2}\cdot\vec{n} + (\vec{\kappa}\cdot\nabla_v)\cdot\nabla_v C_{io}\cdot\vec{n} + \nabla_v C_{i1}\cdot\vec{n} + \nabla_u C_{io}\cdot\vec{n}\}$$
$$= -g_{20}(1 - \theta_i C_{io}/\sigma_0)\{\nu V_1 + (\dfrac{C_{21}^i}{C_{20}^i} - \dfrac{C_{21}^0}{C_{20}^0})\}.$$

Since ϕ_0, σ_0, and C_{i_0} do not depend on $\vec{v}$, under the specific assumptions made here, the functions ϕ_1, σ_1, and C_{i_1} do not depend on $\vec{v}$ by (2.8) - (2.9). Thus, inspection of (B.3) - (B.7) shows that the intracellular and extracellular equations for ϕ_2, σ_2, and C_{i_2} are potential equations and the solutions assume simple forms analogous to those for ϕ_1, σ_1, and C_{i_1}. This observation simplifies the computation of the $\vec{u}$-dependence of ϕ_0, σ_0, and C_{i_0}.

APPENDIX III.C. GENERAL AVERAGING

In this appendix, the averaging calculations are carried out in the general case. Without special assumptions about the geometry, the computed average coefficients do not reduce to scalars, even though the microscopic parameters, solution conductivity, and diffusion coefficients are constant. Because the objective of this calculation is only the general form of the average coefficients, it is not necessary to separately consider the extracellular and intracellular parts of the solutions.

Substitution into (2.6) of the previously derived forms for ϕ_1, σ_1, and C_{i_1} yields the averaged equations at 'neuronal' length scales:

$$\sum_{j,k} \frac{\partial}{\partial v_j} \left\{ e_{jk} \frac{\partial \sigma_0}{\partial v_k} \right\} = 0,$$

(C.1)
$$\sum_{j,k} \frac{\partial}{\partial v_j} \left\{ \sigma_0 a_{jk} \frac{\partial \phi_0}{\partial v_k} \right\} = 0,$$

$$\sum_{j,k} \frac{\partial}{\partial v_j} [\{\theta_i e_{jki} \frac{\partial C_{io}}{\partial v_k}\} + \nu z_i \frac{\partial}{\partial v_j} \{\theta_i C_{io} a_{jk} \frac{\partial \phi_0}{\partial v_k}\}] = 0$$

where $a_{jk} = M_W(\delta_{jk} + \partial \chi^k / \partial W_j)$, $e_{jk} = M_W(\delta_{jk} + \partial \eta^k / \partial W_j)$, $e_{jki} = M_W(\delta_{jk} + \partial \kappa^k / \partial W_j)$, and δ is the Kronecker delta, $\delta_{jk} = 1$ when $j=k$ and 0 otherwise.

It is shown in Chapter IV that for the geometries assumed here; $a_{jk} = a(\vec{u})$, $e_{jk} = e(\vec{u})$, $e_{jki} = e_i(\vec{u})$.

The quantities ϕ_0 , σ_0, and C_{io} satisfy jump conditions obtained by averaging fluxes of order ϵ^{-1} at 'neuronal' membrane since (1.1) implies that $\sigma \nabla_v \phi$ is associated with a flux of this order. These conditions are:

$$-\sum_{j,k} e_{jk} \frac{\partial \sigma_0}{\partial v_k} n_j = g_{20}\{\nu V_0 - \nu V_k\} + P_1$$

(C.2)

$$-\sum_{j,k} \nu \sigma_0 a_{jk} \frac{\partial \phi_0}{\partial v_k} n_j = g_{20}\{\nu V_0 - \nu V_k\} + P_2$$

$$-\sum_{j,k} \theta_i e_{jki} \frac{\partial C_{io}}{\partial v_k} n_j = g_{20}(1 - \theta_i C_{io}/\sigma_0)\{\nu V_0 - \nu V_k\} + p_i$$

The $\vec{v}$-dependence of ϕ_1 , σ_1, and C_{i1} is deduced from a necessary condition for the existence of a bounded solution for ϕ_3 , σ_3 , and C_{i3} , namely, the Fredholm Alternative applied at order ϵ^{-1}; yielding

$$\int_W \{A_{-1}\sigma_0 + A_{-2}\sigma_1 + A_{-3}\sigma_2\} dA_W = 0$$

(C.3) $$\int_W \{A^\sigma_{-1}\phi_0 + A^\sigma_{-2}\phi_1 + A^\sigma_{-3}\phi_2\} dA_W = 0$$

$$\int_W \theta_i\{A_{-1}C_{io} + A_{-2}C_{i_1} + A_{-3}C_{i_2}\} + \nu z_i\theta_i(A^C_{-1}\phi_0 + A^C_{-2}\phi_1 + A^C_{-3}\phi_2)\} dA_W = 0$$

where $A^f_{-1} = \nabla_u \cdot (f_0\nabla_v) + \nabla_v \cdot (f_0\nabla_u) + \nabla_u \cdot (f_1\nabla_w) + \nabla_w \cdot (f_1\nabla_u) + \nabla_v \cdot (f_2\nabla_w) + \nabla_w \cdot (f_2\nabla_v) + \nabla_w \cdot (f_3\nabla_w)$.

Hence, these averages yield (corresponding to 2.10):

$$\sum_{j,k} \frac{\partial}{\partial v_j}\{e_{jk}\frac{\partial\sigma_1}{\partial v_k}\} = 0$$

(C.4) $$\sum_{j,k} \frac{\partial}{\partial v_j}\{\sigma_0 a_{jk}\frac{\partial\phi_1}{\partial v_k}\} = 0$$

$$\sum_{j,k}[\frac{\partial}{\partial v_j}\{\theta_i e_{jki}\frac{\partial C_i}{\partial v_k}\} + \nu z_i\frac{\partial}{\partial v_j}\{\theta_i C_{io}a_{jk}\frac{\partial\phi_1}{\partial v_k}\}] = 0$$

with jump conditions:

$$-\sum_{j,k} e_{jk}\{\frac{\partial\sigma_1}{\partial v_k}n_j + \frac{\partial\sigma_0}{\partial u_k}n_j\} = g_{20}\{\nu V_1 + (\frac{C^i_{21}}{C^i_{20}} - \frac{C^0_{21}}{C^0_{20}})\}$$

$$(C.5) \quad -\nu\sigma_0 \sum_{j,k} a_{jk}\{\frac{\partial\phi_1}{\partial v_k}n_j + \frac{\partial\phi_0}{\partial u_k}n_j\} = g_{20}\{\nu V_1 + (\frac{C_{21}^i}{C_{20}^i} - \frac{C_{21}^o}{C_{20}^o})\}$$

$$-\theta_i \sum_{j,k} e_{jki}\{\frac{\partial C_{i1}}{\partial v_k}n_j + \frac{\partial C_{io}}{\partial u_k}n_j\} = z_i g_{io}(1-\theta_i C_{io}/\sigma_0)\{\nu V_1 + (\frac{C_{21}^i}{C_{20}^i} - \frac{C_{21}^o}{C_{20}^o})\}$$

This is a system similar to (1.5) - (1.6) except that the coefficients now contain averages and the boundary conditions are applied at 'neuronal' membrane. The explicit form of the solutions when the coefficients are scalar is given in equations (2.10) - (2.15).

Finally, to obtain the $\vec{u}$-dependence of ϕ_0, σ_0, and C_{io}, the necessary condition, equation (2.7), for bounded ϕ_4, σ_4 and C_{i4} is applied to the $\vec{w}$-averaged equation at $O(1)$ which yields, using the previously computed $\vec{v}$ dependence of ϕ_0, σ_0, C_{io}, ϕ_1, σ_1, and C_{i1}:

$$\sum_{j,k} \frac{\partial}{\partial u_j}\{\hat{e}_{jk}\frac{\partial\sigma_0}{\partial u_k}\} = Q_1 + \tau\sum_i \frac{\partial C_{io}}{\partial t}$$

$$(C.6) \quad \sum_{j,k} \frac{\partial}{\partial u_j}\{\sigma_0\hat{a}_{jk}\frac{\partial\phi_0}{\partial u_k}\} = Q_2$$

$$\sum_{j,k} [\frac{\partial}{\partial u_j}\{\theta_i\hat{e}_{jki}\frac{\partial C_{io}}{\partial u_k}\} + \nu z_i\frac{\partial}{\partial u_j}\{\theta_i C_{io}\hat{a}_{jk}\frac{\partial\phi_0}{\partial u_k}\}] = \tau\frac{\partial C_{io}}{\partial t} + q_i,$$

where $\hat{a}_{jk}$, $\hat{e}_{jk}$, and $\hat{e}_{jki}$ are defined in a manner analogous to a_{jk}, e_{jk}, and e_{jki}, by taking $\vec{v}$-averages over $\vec{v}$-unit cells of canonical problems with $\vec{w}$

averaged coefficients, in the same way that (C.1) were obtained by averaging over $\vec{w}$ unit cells.

IV. CANONICAL PROBLEMS AND THE COMPUTATION OF BULK PROPERTIES

1.0. INTRODUCTION

The physical theory of ion transport is based on ideal assumptions which are useful for obtaining the qualitative features of such transport (Horvath, 1985). It is desirable to incorporate these idealizations into our model because most relevant experimental work on ion transport in biology is described with reference to this (transport number) theory (Horvath, 1985; Gardner-Medwin, 1983; Barry & Hope, 1969 a, b). More generally, the physical applications of results from homogenization theory have been relatively neglected, (I. Rubenstein, personal communication) and much of the theoretical work has only reproduced results already known to experimentalists or derivable through other techniques (Batchelor 1974; Lehner, 1979). It is expected that the incorporation of physical theory will facilitate new physical insights as well as applications.

Thus, in this chapter, we are concerned with the relationship between the expansion procedure of Chapter III and the existing physical theory of ion transport. It is shown that this transport number theory applies to bulk tissue, and a further simplification of the canonical problems of Chapter III is made for consistency with the physical theory. Finally, bulk properties of the tissue model are computed for a variety of parameters.

1.1. Transport Numbers in Electrolyte

It is observed experimentally that when a steady electric current is passed through an electrolyte solution, the current $\vec{I} = \sum_i z_i \vec{j}_i$ is approximately divided into constant fractions, t_i, depending only on the composition of the electrolyte

(Horvath, 1985). These transport numbers, t_i, have been justified within the thermodynamic literature and tabulated (Robinson & Stokes, 1955). The theory of transport numbers assumes that (ideally) ionic fluxes are proportional to electric current with a single constant of proportionality over space and that the electric current is specified by a linear equation with constant coefficients. If these assumptions are true, it is simple to predict the effect of current passing experiments on the concentrations of ions. The appropriateness of this idealization for a simple electrolyte solution is now discussed.

While our model equations (II.1.2) represent a simplification of a more complete thermodynamic treatment (see Chapter I), they still give rise to non-linear governing equations. Thus, in general, the transport number is not constant under this model. If we assume that (II.1.2) is correct and electroneutrality holds, then we have in the steady state away from sources:

$$\nabla^2 \sigma = 0,$$

(1.1) $$\nabla \cdot (\sigma \nabla \phi) = 0,$$

$$-\nabla \cdot \vec{j}_i = \nabla \cdot (\theta_i \nabla C_{io}) + \nu z_i \nabla \cdot (\theta_i C_i \nabla \phi) = 0$$

Thus, when σ is known, the computation of the electrical potential ϕ is straightforward. When C_i are constant, this implies that $\nabla C_i = 0$, the diffusive term is zero in (II.1.2), and $\sigma =$ constant because of its definition (Section II.1.1). In this case the ion transport vector has the simple form:

(1.2)
$$-\vec{j}_i \;=\; \nu z_i \theta_i C_i \nabla\phi \;=\; \nu t_i z_i \sigma \nabla\phi,$$

where $t_i = \theta_i C_i / \sigma$. Under these conditions, $\Sigma_i t_i = 1$. The numbers t_i are the theoretical transport numbers measured by passing current through electrolyte solutions (Horvath, 1985).†

Since C_i is not constant in general, this assumption concerning the transport properties of electrolyte solution is an idealization which is reasonable as long as variations in C_i are not large. The diffusive portion of the ionic flux is assumed to remain unchanged.

Because the intracellular regions have transport properties different from the extracellular medium, the definition of bulk tissue transport numbers is more complicated than the definition of transport numbers in electrolyte.

1.2. Discontinuous Ionic Flux in Bulk Tissue

The idealization of constant transport number in electrolyte solution is useful and accepted in physical theory. Fortunately, no further assumptions are necessary in order to derive bulk transport properties for tissue which are similar to those for electrolyte solution. That is, potassium transport in bulk

---

† It is important to note that these are not the only conditions under which $\vec{j}_i$ may be linearly related to electric current. For example, if $\sigma = $ constant and $C_i \nabla\phi$ is small: $\nu \nabla \cdot (\theta_i C_i \nabla\phi) \simeq 0$ holds, and the electric potential satisfies, and C_i nearly satisfies, the potential equation. If, on the boundary of some region, the potential ϕ and the concentration C_i satisfy boundary conditions of the form $\partial\phi / \partial n = K \; \partial C_i / \partial n$, then ∇C_i will be proportional to $\nabla\phi$ everywhere in the region and so $\vec{j}_i \simeq \theta_i \nabla C_i + \nu t_i z_i \sigma \nabla\phi$ is proportional to $\vec{I}$ the electric current. A physical situation similar to this one, with more complicated boundary conditions, occurs in bulk tissue and is reflected in the mathematical form of averaged coefficients in Sections 1.3 and 6.6.

tissue is a linear function of the electric current, and the electric current is specified by a constant coefficient potential equation. The physical basis for the transport number theory in bulk tissue is now described.

In the extracellular medium, K^+ ions have a relatively low tabulated transport number of about .012, while Na^+ has a transport number of about 0.4, and Cl^- of about 0.6. In contrast, because glial and resting neuronal membrane are primarily permeable to K^+ (Dietzel et al., 1980) the transport number for K^+ across such membranes is close to unity.

It is difficult to estimate the transport number for K^+ inside glia or neurons because the intracellular medium is different from standard electrolyte solutions, containing cell organelles and a variety of organic molecules. However, since $[K^+]_i$ is considerably higher than $[K^+]_o$, the intracellular transport number of K^+ must be closer to unity and the flux of K^+ must be a larger fraction of the intracellular electrical current than in the extracellular current. Therefore, it will be assumed that the intracellular transport number for K^+ is unity. This assumption about intracellular transport number is not crucial (though it simplifies calculation), but since we will assume simple geometry it seems appropriate to make simple assumptions about transport numbers in this section.

The above idealization permits a conceptually simple description of electrically mediated spatial potassium transport. Because of these assumptions, the K^+ flux vector is nearly unaffected by the electric field in the extracellular medium, but is proportional to the electric current vector in the intracellular medium.

The situation can be visualized by imagining that the electrical streamlines (charge paths) passing through the inhomogeneous medium consisting of

intracellular and extracellular compartments are coloured. Some of these streamlines will pass through one or more cells. If current streamlines are coloured blue extracellularly and red where they pass through cell interiors then relatively more electrical potassium transport occurs along the red segments of streamlines, and relatively little along the blue segments because of the difference in intracellular and extracellular transport numbers.† If there are no initial concentration gradients, then the average of the red flux is the average K^+ flux at the instant the electric field is turned on. In the steady state, the average K^+ flux is the spatial average of the red intracellular flux and the diffusive flux due to extracellular concentration gradients.

1.3. Local Transport Number in Bulk Tissue

Formal expressions for the fluxes of electric charge $\vec{I}$ (current) and potassium $\vec{j}_K := \vec{j}_2$ are obtained from the multiple scales procedure. To define a local average transport number it must first be shown that average electric current is determined by a linear equation with constant coefficients over a region which includes a large number of cells. This requirement concerning the equation for ϕ follows from the form of the multiple scales expansion and the discussion of averaging in Chapter III. As was described earlier, 'local' means, over a length scale μ which includes many cells but is small compared to the measurement scale, L_0, for example, $\mu = \epsilon^\rho$ for $\rho < 1$. We denote such a region   by

---

† In the extracellular medium, K^+ moves primarily by diffusion (in this idealization). Because the extracellular medium contains high concentrations of other current carrying ions, Na^+ and Cl^-, there is no inconsistency in the specification of ϕ. Diffusion does not cancel the electrical transport because, unlike the electric flux, it has no preferred direction in free space or in cortical tissue (Nicholson & Phillips, 1981).

R_μ.

A linear relationship between bulk current and potassium flux follows from an appropriate interpretation of the averaged coefficients occurring in the expansion since, physically, the averaged coefficients are equivalent to averaged fluxes. The linear relationship of averaged current and average ionic flux implies that the local transport number theory carries over to tissue.

Bulk transport numbers describe any local linear relation between an electrical and ionic flux. It is simple to define them physically. We denote the extracellular and intracellular transport numbers by t_K^o and t_K^i respectively. There are at least two approximate ways to define bulk transport numbers which are useful. In general, the relation between $\vec{j}_K$ and $\vec{I}$ will be a matrix function instead of a simple proportionality.

The first definition assumes that $\vec{j}_K$ is zero in the extracellular space and thus the average of $\vec{j}_K$ involves an integral only over the intracellular space.

$$(1.3) \qquad M_W(\vec{j}_K) := \frac{1}{|\overline{W}|} \int_{ICS} t_K^i \vec{I} dA,$$

where W denotes the unit cell. Equation (1.3) defines a local linear operator applied to $\vec{I}$. Since any such linear operator is associated with a matrix, this defines a matrix of 'local transport numbers'.

The second definition assumes that $\sigma = $ constant, $\nu \nabla \cdot (C_2 \nabla \phi) \simeq 0$ and no average change in concentration occurs over the unit cell. This case is a modification of the situation described in the footnote of Section 1.1. The average of $\vec{j}_K$ is given approximately by:

$$(1.4) \quad M_W(\vec{J}_K) := \frac{1}{|\vec{W}|}\{ \int_{ICS} t^i_K \vec{I} dA + \frac{1}{|\vec{W}|} \int_{ECS} t^0_K \vec{I} dA + \nu \int_{ECS} \sigma \nabla \psi_J dA \},$$

where ψ_J satisfies membrane jump conditions of the form $\vec{I} \cdot \vec{n} = \nu \sigma \nabla \psi_J \cdot \vec{n}$ and periodic boundary conditions on the unit cell. The function ψ_J corresponds to the flux due to concentration gradients set up by the jump conditions. Despite the periodic boundary conditions, the average of $\nabla \psi_J$ is not zero because of the presence of the biological cell. Because ψ_J depends linearly on $\vec{I}$ through the jump condition, equation (1.4) defines a linear operator applied to $\vec{I}$ and this defines a matrix of 'local transport numbers'.

Thus, assuming the transport number theory is valid in electrolyte, it may be deduced that bulk tissue has transport properties which parallel those of electrolyte solution, though the transport numbers are not, in general, scalars.

2.0. FINAL SIMPLIFICATION OF THE BULK EQUATION

Inspection of the governing equations for ϕ_0, σ_0, and C_{i0} (III.2.8) -(III.2.9) shows that these quantities are constant extracellularly and constant intracellularly over R_μ for $\mu = \epsilon^\rho$. Thus, the coefficients of the equations for the dependence of ϕ_1, σ_1, and C_{i1} on the fine variables are constant both extracellularly and intracellularly over R_μ. Hence, locally, to leading order, the transport number theory is valid intracellularly and extracellularly over R_μ.

It is now assumed, in addition, that the transport number theory is valid over asymptotically larger regions R_μ, $\mu = \epsilon^0$, consistent with the transport number theory of the physical literature. Mathematically, this assumption means that we assume $\nabla \sigma_0 = 0$ and that $\theta_i C_i$ is replaced by $t_i \sigma_0$ in the expression for

electrical ionic flux. In the calculations which follow, a geometry has been selected in which matrix coefficients reduce to scalars.

It has been shown that a bulk transport number theory is valid locally. The assumption that transport numbers are constant throughout the extracellular and intracellular spaces, therefore, implies a bulk transport number theory which is valid throughout the tissue. While this assumption is <u>ad hoc</u> in a mathematical sense, it is important to note that the assumption σ = constant is a consistent assumption because σ does not appear on the right-hand-sides of (III.2.11). Also these assumptions are supported by experimental studies (Gardner-Medwin, 1983 a, b; Havstad, 1976) which found no evidence that such non-linear effects qualitatively affected bulk properties.

The idealization that the (electrolyte) transport numbers in the extracellular space and intracellular space are constant will convert the variable-coefficient averaged equation into an equation with constant coefficients. This is useful because the coefficients of the averaged equation have to be computed numerically and the numerical computation of the values of variable coefficients is impractical here. At the same time, the dependence of the membrane potential on K^+ concentration and the presence of intracellular and extracellular compartments will make the averaged equations different from those which hold in electrolyte solution.

Inspection of (III.2.11) shows that it is not consistent to assume that the concentration C is constant in computing ϕ. However, some comparisons will be made with such a model because it is simple, and, as we show by direct computation, qualitatively correct in some respects.

3.0. COMPUTATION OF COEFFICIENT ESTIMATES

3.1. Introduction

In order to apply the results from Chapter III and the present chapter to ion transport in tissue, it is necessary to solve the canonical microscopic boundary-value problems for the variables χ_p, χ_v, χ_c, χ_s, κ_p, κ_v, κ_c, and κ_s, to be determined in (III.2.12). These quantities satisfy Laplace's equation intracellularly and extracellularly, periodic boundary conditions on a fundamental domain W, and the jump conditions (III.2.13) - (III.2.16) which have the form:

$$-\sigma_0\{\nabla_v \chi_{p_1} \cdot \vec{n} + n_1\} = g\{\chi_{p_1}^i - \chi_{p_1}^0 + \kappa_{p_1}^i - \kappa_{p_1}^0\},$$

(3.1)

$$-\theta C_0 \nabla_v \kappa_{p_1} \cdot \vec{n} = g(1-\theta C_0/\sigma_0)(\chi_{p_1}^i - \chi_{p_1}^0 + \kappa_{p_1}^i - \kappa_{p_1}^0),$$

$$-\sigma_0^0\nabla_v \chi_{v_1}^0 \cdot \vec{n} = -\sigma_0^i\{\nabla_v \chi_{v_1}^i \cdot \vec{n} + n_1\} = g\{\chi_{v_1}^i - \chi_{v_1}^0 + \kappa_{v_1}^i - \kappa_{v_1}^0\},$$

(3.2)

$$-\theta C_0 \nabla_v \kappa_{v_1} \cdot \vec{n} = g(1-\theta C_0/\sigma_0)\{\chi_{v_1}^i - \chi_{v_1}^0 + \kappa_{v_1}^i - \kappa_{v_1}^0\},$$

$$-\sigma_0 \nabla_v \chi_{c_1} \cdot \vec{n} = g\{\chi_{c_1}^i - \chi_{c_1}^0 + \kappa_{c_1}^i - \kappa_{c_1}^0\},$$

(3.3)

$$-\theta C_0 \nabla_v \kappa_{c_1} \cdot \vec{n} = -\theta\{C_0^0\nabla_v \kappa_{c_1}^0 \cdot \vec{n} + n_1\}$$
$$= g(1-\theta C_0/\sigma_0)\{\chi_{c_1}^i - \chi_{c_1}^0 + \kappa_{c_1}^i - \kappa_{c_1}^0\},$$

where $g := g_2$ at the cell membrane. Solutions must be obtained for a range of values of membrane and intracellular conductivity values.

Since it is impractical, numerically, to obtain many solutions of these boundary-value problems in three dimensions, solutions were computed in two dimensions. Although bulk conductivity and other properties should depend on whether the calculations are carried out in two or in three dimensions, the values we obtain are consistent with the experiments. Also, the discussion in Chapter V of transcellular conductance (average current flowing through cells per unit voltage drop) when membrane resistance is extremely high or low will suggest that the qualitative behavior of this conductance does not depend on the number of dimensions in which the computations are conducted. Therefore, a two-dimensional computation should suffice to estimate the order of magnitude of the coefficients in (III.2.17) and to determine the nature of their dependence on a number of important physiological parameters such as cell size, membrane conductance, intracellular conductivity, the extracellular space fraction, and the relative positions of the cells.

For convenience in computation, cells are assumed to have straight boundaries. It is assumed that cells are square, although rectangular, or other rectilinear cell shapes would pose no special difficulties. Below, it is shown that this assumption reduces $\vec{\chi}$ and $\vec{\kappa}$ to scalars.

3.2. General Properties of Solutions

The unit cells W employed in straight and staggered arrays are shown in Figure 3.1 surrounded by dashed lines. The jump conditions (3.1) - (3.3) in which n_1 appears are equivalent to a set of line sources at the membrane surfaces (indicated in Figure 3.1 by ±). Because of the source distributions and geometry, solutions are odd functions about the lines O and even functions about the lines E.

Typical solution surfaces for χ_p, χ_c, χ_v, κ_c, κ_p, and κ_v, which satisfy Laplace's equation, periodic boundary conditions and jump conditions (3.1) - (3.3), are shown in Figures 3.2a-f. The horizontal axes are in units of h = (1/72)L where $L := \epsilon L_2 / L_1$, is the length of the unit cell, h is the numerical space step for this solution, and the vertical axis is dimensionless. The numerical values of the solution surface will depend on the conductivity distribution intracellularly, extracellularly, and at the membrane, and the intracellular and extracellular transport numbers, t_K^i and t_K^0 It is seen that the solution surfaces are discontinuous across the membranes. This jump apparently occurs over a length (1/72)L in the pictures, because it is convenient to represent the membrane as a region of reduced conductivity between mesh points. † There is an apparent non-uniqueness in the solution of (III.2.10) - (III.2.11), because the proportional boundary conditions in (III.2.11) give rise to an arbitrary constant in the jump across the membrane. In addition, when the intracellular transport number, t_K^i is unity, the κ quantities are given by an arbitrary constant intracellularly. This non-uniqueness is resolved by the hypothesis in Chapter II

---

† In a centred finite difference scheme the difference between the finite difference solution at adjacent mesh points represents the true solution derivative (flux) half-way between the mesh points.

Figure 3.1. Two-dimensional biological cells can be arranged in straight or staggered periodic arrays. The crystallographic unit cells in each case (indicated by dashed lines) are different. Plus (+) and minus (−) signs correspond to the signs of the virtual sources associated with the jump conditions 3.1 - 3.2 at the membrane.

Figure 3.1a — Straight Unit Cell
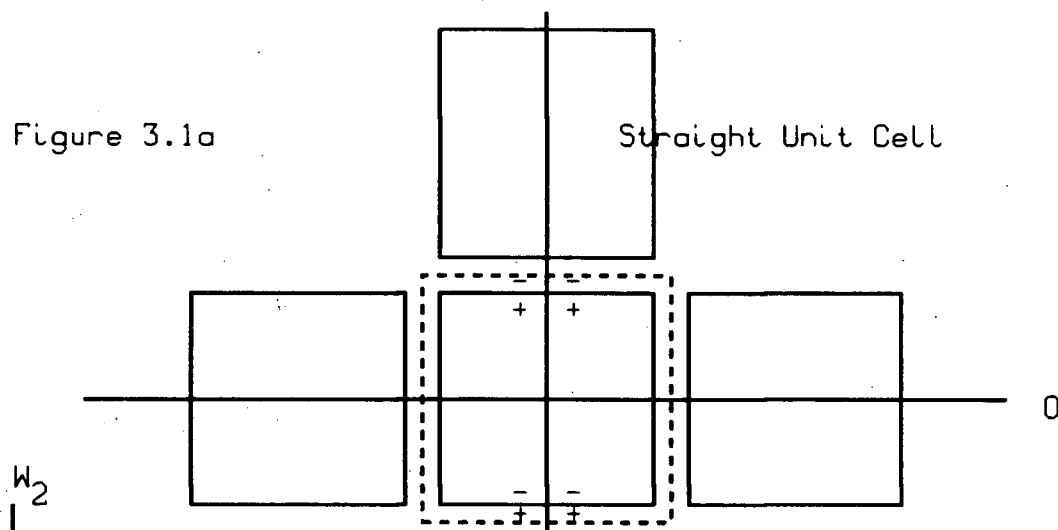
Figure 3.1b — Staggered Unit Cell
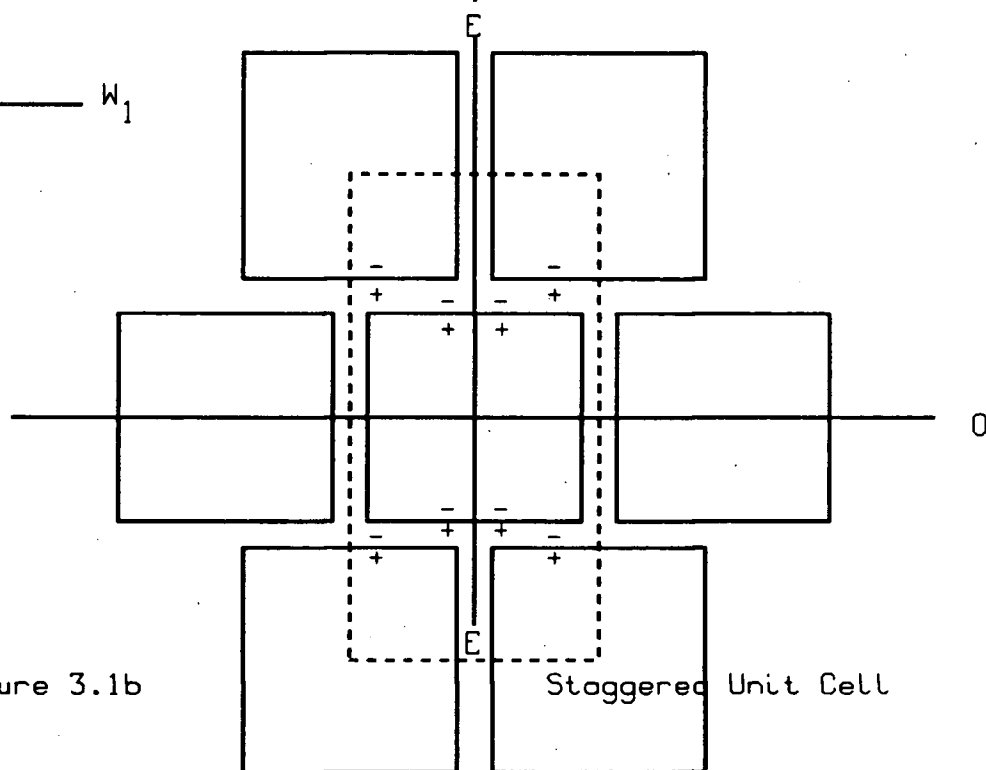
Array Geometries

Figure 3.2. Typical (L=72.1 μm) solution surfaces for canonical solutions χ_p, χ_c, χ_v, κ_c, κ_p, and κ_v are shown in Figure 3.2.a -3.2.f, while solution surfaces for staggered arrays are shown in Figures 3.2.g 3.2.l. These solutions satisfy Laplace's equation, periodic boundary conditions, and the jump conditions (3.1) - (3.2). Each solution was computed on a 72 x 72 grid with an extracellular space fraction of 23%. These solutions represent, respectively, the $O(\epsilon)$ perturbations indicated in each figure title. A description of the main features of these solutions is given in Section 3.2.

χ_p: Perturbation in $\varphi \propto \varepsilon \, \nabla \varphi_0$
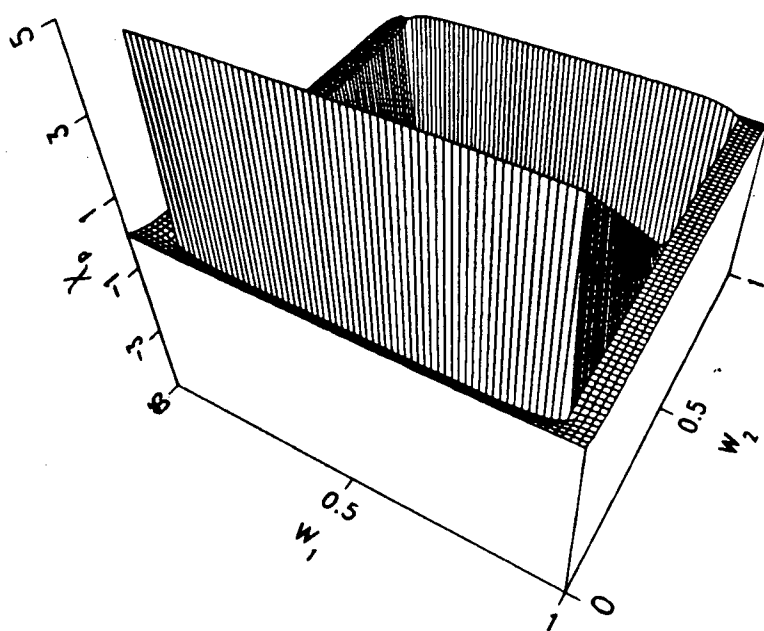
FIGURE 3.2.a

L = 72.1μ Straight Array

$$\chi_c: \text{ Perturbation in } \varphi \propto \varepsilon \, \nabla C_0$$
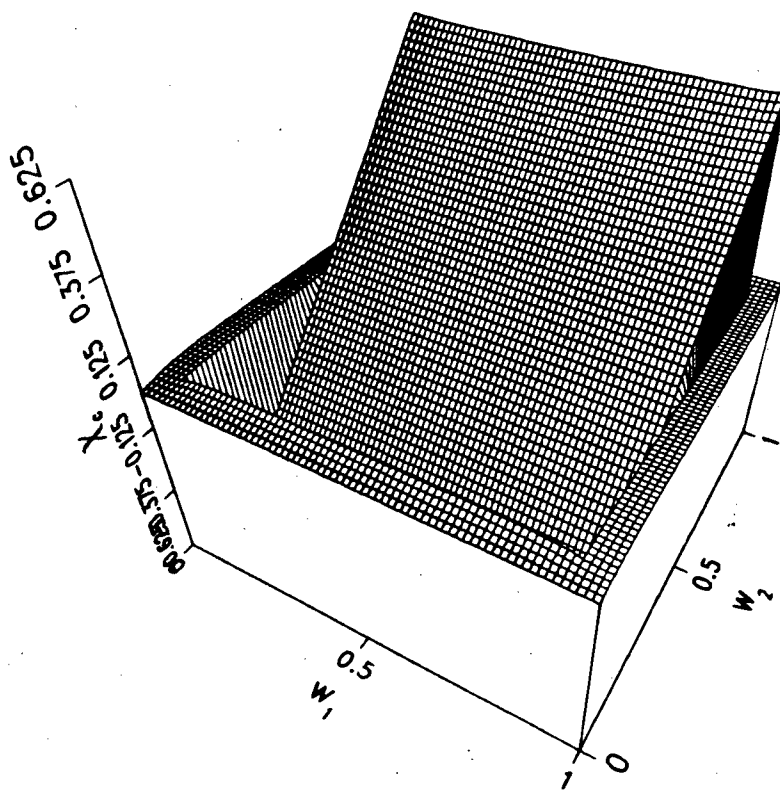
FIGURE 3.2.b

L = 72.1μ Straight Array

χ_v: Perturbation in $\varphi \propto \varepsilon \, \nabla V_0$
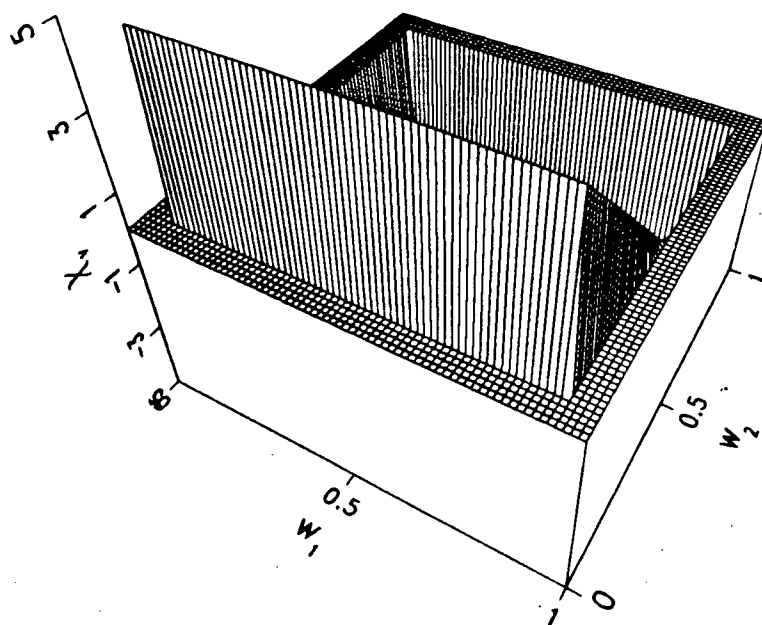
FIGURE 3.2.c

L = 72.1μ Straight Array

$\mathcal{K}_c$: Perturbation in $C \propto \varepsilon \, \nabla C_0$
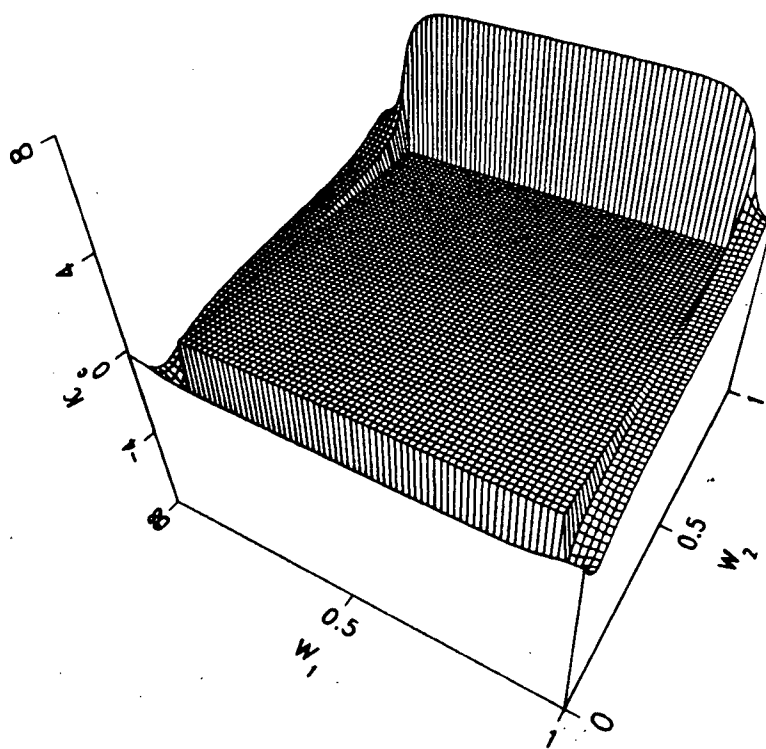
FIGURE 3.2.d

L = 72.1μ Straight Array

$\mathcal{K}_p$: Perturbation in $C \propto \varepsilon \, \nabla \varphi_0$
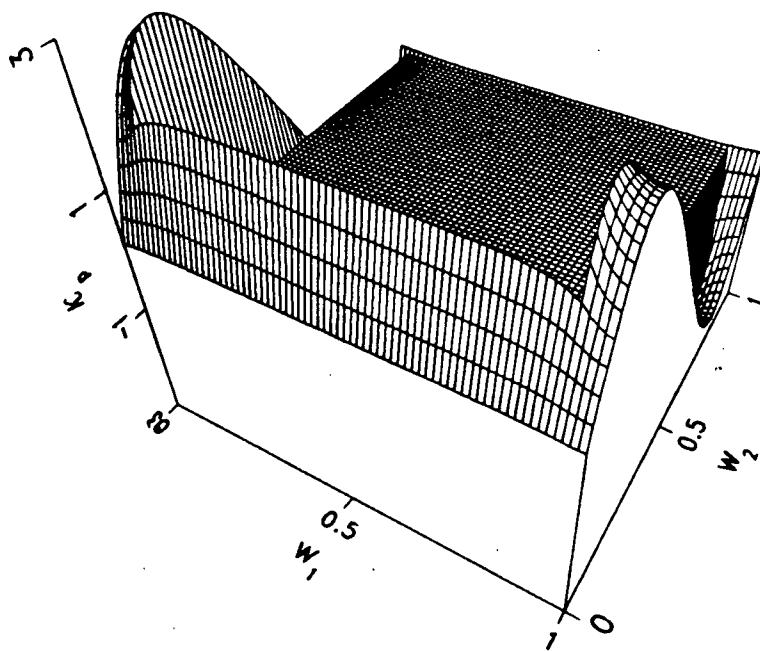
FIGURE 3.2.e

$L = 72.1 \mu$ Straight Array

$$\mathcal{K}_v: \text{ Perturbation in } C \propto \varepsilon \, \nabla V_0$$
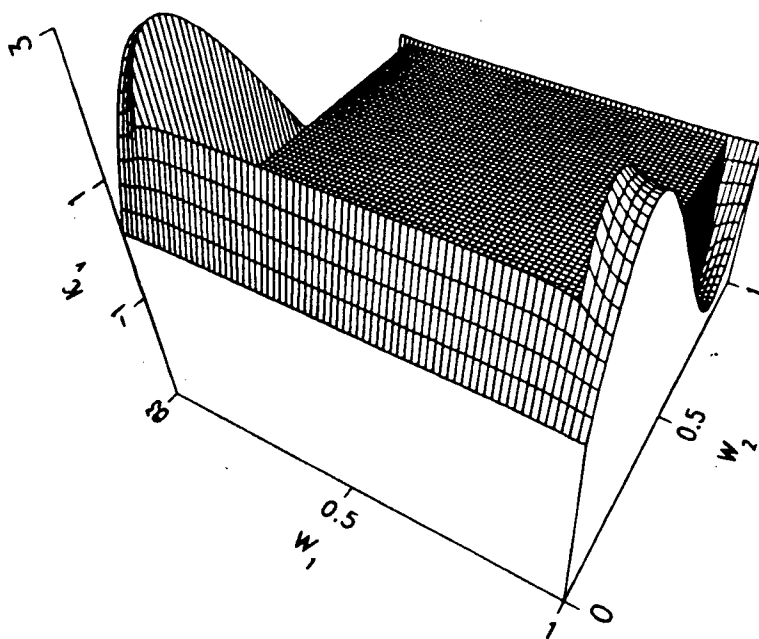
FIGURE 3.2.f

L = 72.1μ Straight Array

χ'_p: Perturbation in $\varphi \propto \varepsilon \, \nabla\varphi_0$

FIGURE 3.2.g

L = 72.1μ Staggered Array

χ_c: Perturbation in $\varphi \propto \varepsilon \, \nabla C_0$
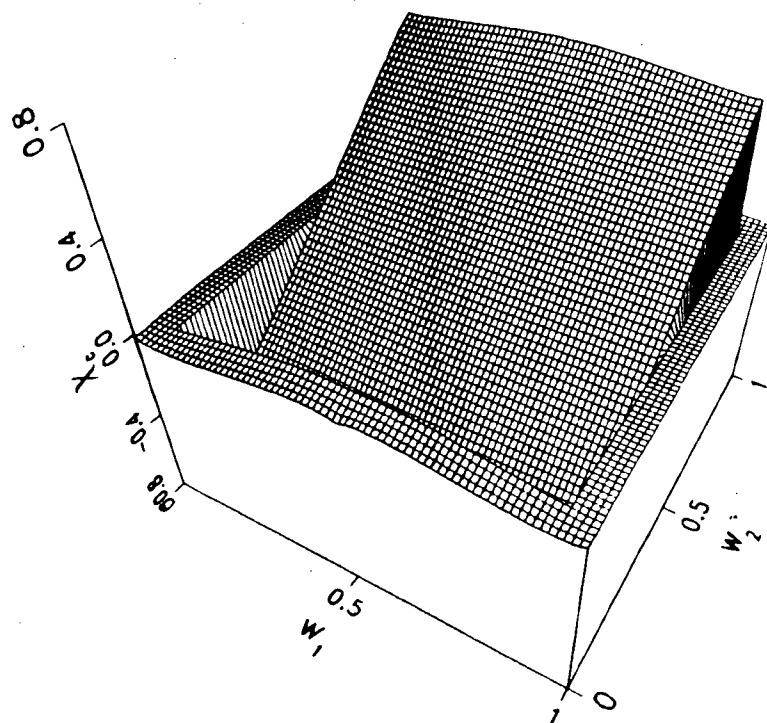
FIGURE 3.2.h

L = 72.1μ Staggered Array

χ_v: Perturbation in $\varphi \propto \varepsilon \nabla V_0$
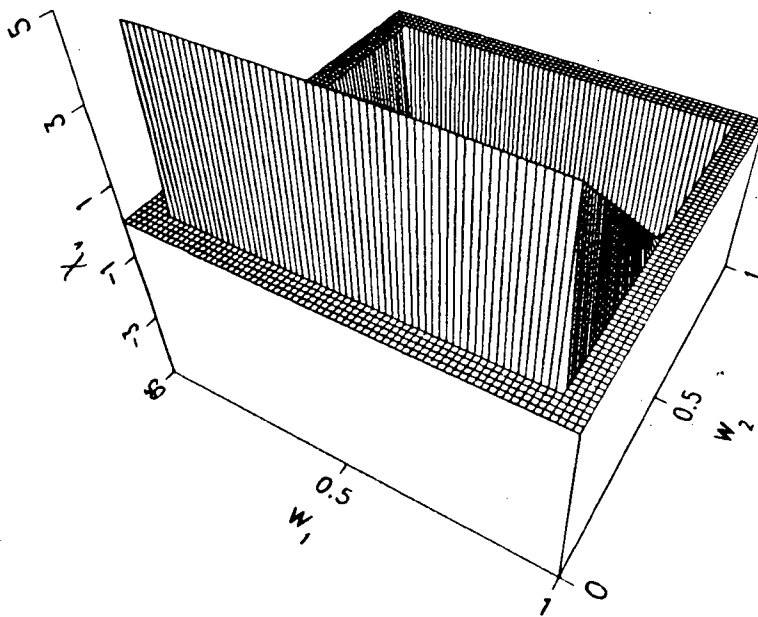
FIGURE 3.2.i

L = 72.1μ Staggered Array

$\mathcal{K}_c$: Perturbation in $C \propto \varepsilon \, \nabla C_0$
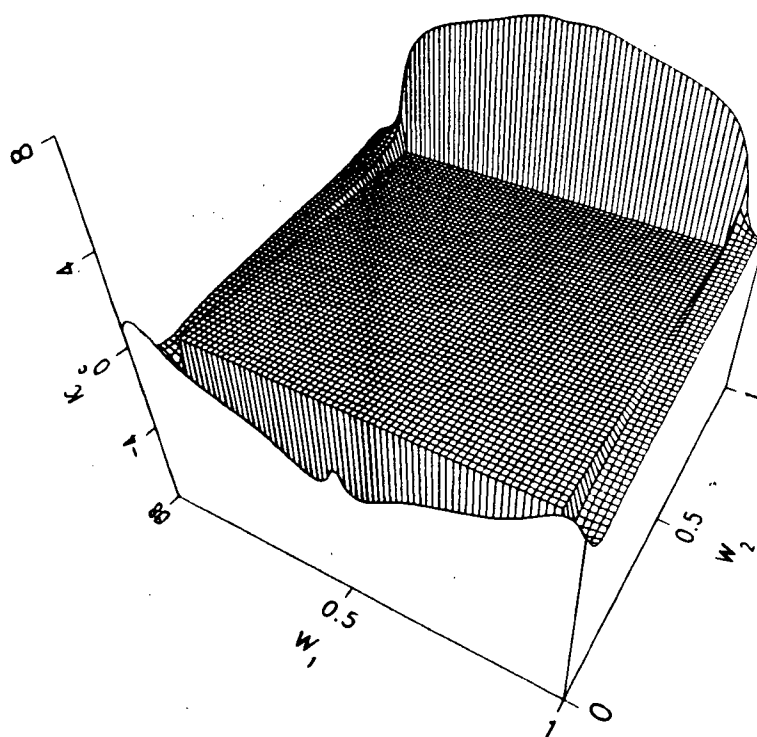
FIGURE 3.2.j

L = 72.1μ Staggered Array

$\mathcal{K}_\rho$: Perturbation in $C \propto \varepsilon \nabla \varphi_0$

FIGURE 3.2.k

L = 72.1μ Staggered Array

K_γ: Perturbation in $C \propto \varepsilon \nabla V_0$
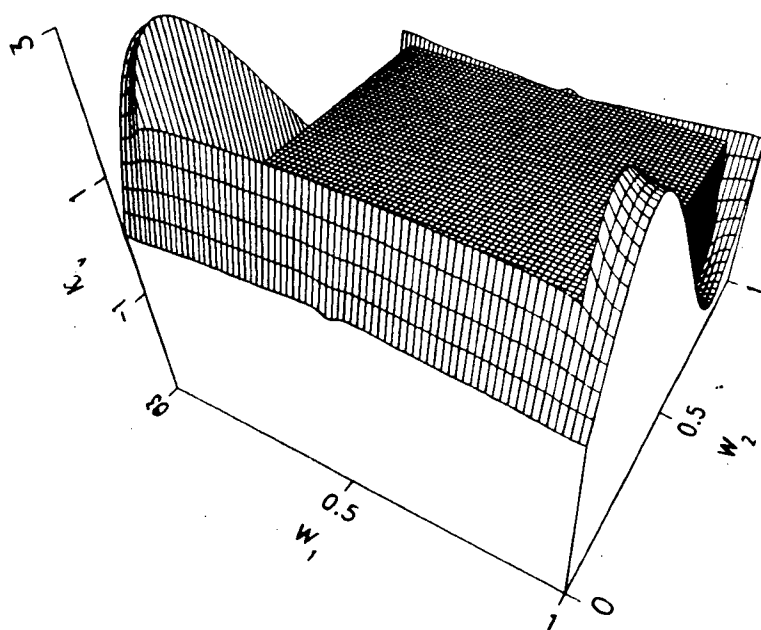
FIGURE 3.2.1

L = 72.1μ Staggered Array

that the pump fluxes force the net ionic flux and electric current to be zero over the cell membrane.

Most of the unit cell is occupied by the biological cell, which is surrounded by a narrow extracellular gap. Solutions are zero along the two opposite ends of the unit cell which are axes of odd symmetry and have zero normal derivative along the sides of the unit cell which are axes of even symmetry. The solutions have two types of appearance; one type of solution is nearly a planar segment intracellularly, which is non-zero and tilted because of the presence of source terms, and the second type of solution is non-zero because of flux conditions at the membrane and exhibits considerably more curvature. Solution maxima ranged from approximately .15 to 50, depending on the parameters and type of solution.

4.0. NUMERICAL METHODS

4.1. Choice of Numerical Method

The canonical microscopic problems specified by (III.2.10) - (III.2.15), have been solved using finite differences. Details of the numerical algorithm are discussed later in this section. It is shown here that the features of the biological modelling problem make our choice of numerical method more suitable than other possible choices. It is not suggested that other methods could not be applied, but that finite differences is a simple and appropriate method in view of the special features of the modelling problem.

Two special features of this biological problem are the low membrane conductance, and the relatively small extracellular space fraction necessary to

simulate the biological problem. First, it is easily verified that when the membrane conductance $g \to 0$, the problems (III.2.10) - (III.2.15) have no unique solution and the intracellular and extracellular solutions differ by an arbitrary constant. Thus, it is expected that at $g = 0$ the coefficient matrix associated with any numerical method will be singular and for small g it will be ill-conditioned and difficult to invert numerically. If g were zero, an arbitrary constraint could be added to the equations to make the solution unique, but physiological values of g are small, so that some other approach is necessary. Second, it is desirable to be able to determine the dependence of solutions on the extracellular space fraction independent of the shape of the extracellular space and to employ biologically relevant extracellular space fractions less than 0.2. These features make certain classical methods for solving the potential equation, those involving integral equations, and those involving separation of variables, difficult to apply.

One approach to solving the potential equation in an array of periodic inclusions assumes that a separation of variables solution is available for the potential equation in the intracellular and extracellular domains.† McPhedran & McKenzie (1978) used this technique to compute the average conductivity of an infinite array of spheres with conductivity k_1 imbedded in a medium of conductivity k_2. Although the biological problem here differs from their problem, in that cells are surrounded by membrane, and our equations are coupled, the same techniques are applicable. The technique consists of equating the values of the periodic separation of variables solutions centred at different cells to obtain an infinite system of linear equations for the series coefficients. This infinite system is truncated at some large M, where M is the row dimension of the

---

† This technique was anticipated by Maxwell (1878), exactly 100 years earlier.

coefficient matrix, and solved exactly.

Also, the use of a separation of variables solution depends on the availability of such solutions in the form of classical special functions, for example, those available on elliptical regions. The use of elliptical regions in two dimensions has drawbacks, however, because the largest packing fraction (fractional area occupied by cells) which can be attained in an array which is not staggered is $\pi/4 = 0.785$. Since the usual extracellular space fraction is about 0.2, it becomes necessary to use unit cells with geometries close to this theoretical packing fraction. At the theoretical limit ($\pi/4$) the extracellular space has zero width where the cells touch and the width of this gap controls bulk conductivity. For example, if the conductivity of the inclusions is zero, bulk conductivity is zero when they touch; while if the inclusions are perfect conductors, bulk conductivity is infinite when they are in contact.

Therefore, if cells are elliptical, it is difficult to study the effect of small extracellular space fractions. Because this can only be achieved by rearranging the cells, the effects of rearrangement and extracellular space fraction changes cannot be separated. Unfortunately, most obvious cell shapes for which separation of variable solutions are available have similar drawbacks.

Other methods for solving the potential equation involve integral equations. We denote typical solutions of the canonical problems by ψ. Since $\Delta\psi = 0$ intracellularly and extracellularly, the solution of such a boundary-value problem is determined by the normal derivative $\partial\psi/\partial n$ of the solution at the cell membrane, using a Green's function. Solution techniques for the potential equation based on Green's functions when the conductivity is piecewise constant have been described by Geselowitz (1967). Such an approach is possible for any cell shape

including the square cell shape assumed here. However, the near singularity of the numerical problem for small values of the membrane conductance, g, is a difficulty for this method since the coefficient matrices which arise do not have any useful structure.

For these reasons it seemed desirable to choose a rectilinear shape for the inclusions and to solve the canonical problems using a finite-difference method. The choice of a square or rectangular shape creates additional difficulties because such domains contain corners at which the spatial derivatives do not exist. Thus, numerical methods based on the existence of these derivatives suffer a loss of accuracy near the corners.

For the potential equation in which the solution (but not its derivatives) is continuous at the corners, this is not a serious difficulty. Near a two-dimensional corner, with angle a radians, the solution ψ of the potential equation (where $\partial \psi / \partial n$ but not ψ is discontinuous at the corner) takes the form:

$$(4.1) \qquad Re\{A(z - z_0)^{1 + a/2\pi}\} + f(z),$$

where z is a complex variable, f(z) is analytic, z_0 is the location of the corner in the complex plane, and A is a real constant. This formula becomes asymptotically correct near the corner so that at mesh points adjacent to the corner the solution has the form $f(z) + O(h^{1 + a/2\pi})$ as $h \longrightarrow 0$. The finite-difference formula produces an approximation to f(z) which is second order away from a boundary or jump locus. Finite difference methods are less accurate at boundaries (Mitchell, 1969), however. If a method with second-order accuracy in space is used, for example, accuracy near a boundary (or jump locus) is first

order. That is, the local truncation error of the finite-difference formula near the boundary is O(h) where h is the space step. Hence, the accuracy of the finite-difference formula near the corner, which is $O(h^{1+a/2\pi})$, is as good as the usual accuracy at boundary points. The magnitude of the global error may be estimated by variation of the mesh size.

4.2. Numerical Algorithm

The finite difference approximation to the Laplacian:

$$(4.2) \qquad \delta^2_{w_1} \delta^2_{w_2} U_{ij} = U_{i,j+1} + U_{i,j-1} + U_{i+1,j} + U_{i-1,j} - 4U_{ij}$$

was employed in the interior of each (intracellular and extracellular) domain. From a computational point of view it was convenient to model the jump conditions as discontinuities in the coefficients of the original potential equation. Thus, the region M_h in the Figure 4.1 is assigned a conductivity σ_{mh} (mS) with the property that as $h \longrightarrow 0$ the approximation to the transmembrane current may be written equivalently as

$$(4.3) \qquad \sigma_{mh}(\psi^i - \psi^0)/h = \sigma_m(\psi^i - \psi^0)$$

where σ_m is in mS cm^{-1}. In this way the same numerical scheme could be used throughout intracellular and extracellular domains and across the membrane. This is an advantage because this means that the stability properties of an iterative numerical scheme are preserved.

The line sources at the membrane surfaces which are equivalent to the

Figure 4.1. In the finite difference approximation, the membrane is represented by a region M_h of thickness h and conductivity σ_{mh} (mS). Conductivities in the extracellular and intracellular spaces are σ^o and σ^i, respectively. The unit cell is bounded by the dashed lines.
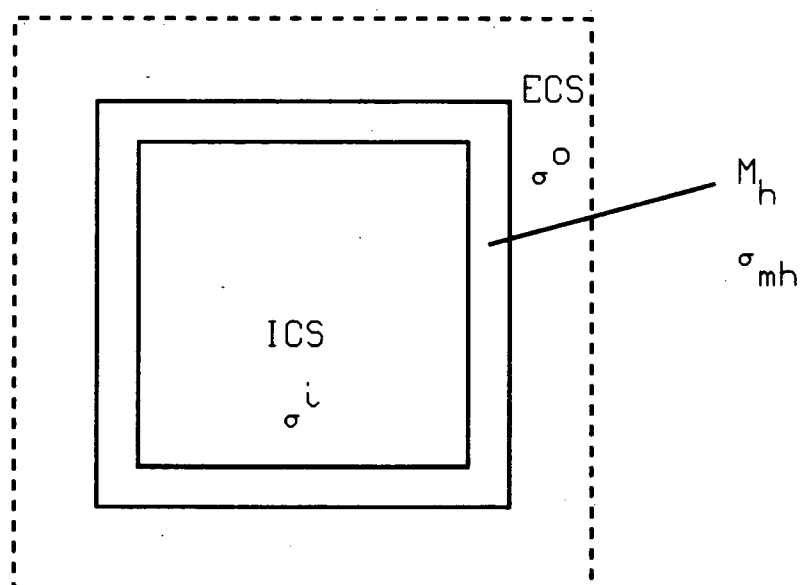
Conductivity Distribution

in Unit Cell

Figure 4.1

jump conditions (3.1) - (3.3) are of magnitude $|\sigma^0 - \sigma_{mh}|$ extracellularly and $|\sigma^i - \sigma_{mh}|$ intracellularly. The line sources are discretized, and represented by point sources. The intensities of the individual point sources on the source loci depend on h, since the sum of the point sources equals the total intensity of the line source. The difference equations for the model system adjacent to the membrane are

$$(4.4) \quad U_{i,j-1} + U_{i,j+1} + U_{i-1,j} + \lambda^r U_{i+1,j} - (3+\lambda^r)U_{ij} + F(\lambda^r - 1) + q_{ij} = 0, \quad r = 1,2,$$

where q_{ij} is a source density. This difference formula is zero when (i,j) are on membrane loci of the form pictured in Figure 4.2.A within the same tolerance, where F is a source strength, $\lambda^1 := hg/\sigma^0$, and $\lambda^2 := hg/\sigma^i$. Thus, λ^r is proportional to the mesh size h, reflecting the fact that while $U_{i,j+1} - U_{i,j}$ goes to zero as $h \to 0$ intracellularly and extracellularly, the transmembrane jump tends to a non-zero value.

At inside corners (4.4) was modified to (Figure 4.2.B)

$$(4.5) \quad U_{i,j-1} + U_{i+1,j} + \lambda^2(U_{i-1,j} + U_{i,j+1}) - 2(1+\lambda^2)U_{ij} + F(1-\lambda^2) + q_{ij} = 0,$$

and at outside corners:

$$(4.6) \quad U_{i,j+1} + U_{i,j-1} + U_{i+1,j} + U_{i-1,j} - 4U_{ij} + F(\lambda^0 - 1) + q_{ij} = 0.$$

In some cases λ^r was taken as small as $.5 \times 10^{-4}$.

Figure 4.2. The locations of the points (i-1,j-1), (i-1,j), (i,j-1), (i,j), etc., in the difference formulas (IV.4.4) - (IV.4.6), is shown near the membrane locus, indicated by the solid lines (compare Figure 4.1).
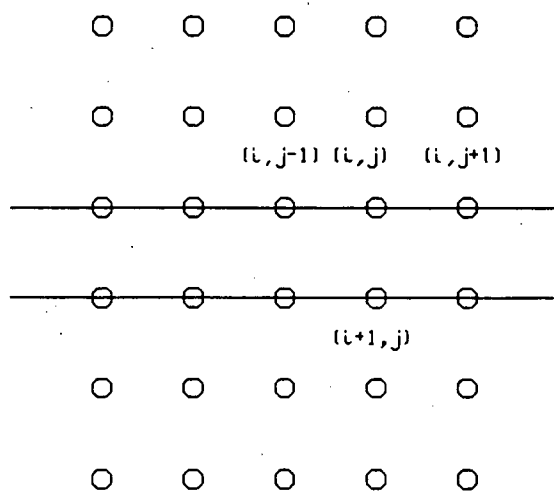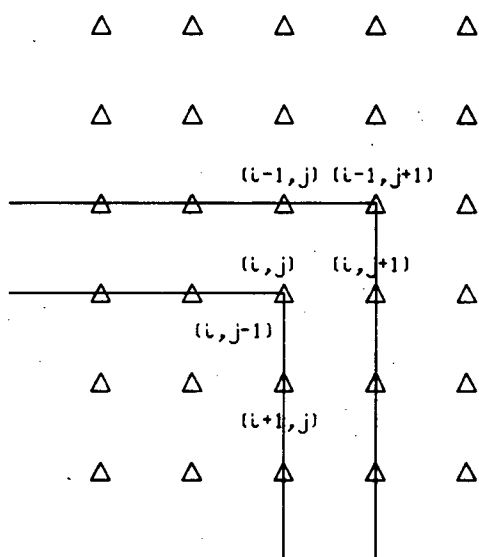
Location of points

in difference formulas

Figure 4.2

While the boundary-value problem being solved is ill-conditioned for small g, the corresponding initial-value problem contains no such difficulty. This suggests that certain types of iterative methods will not be affected by this type of ill-conditioning. For this reason, a commercial iterative solver for the two-dimensional potential equation with variable coefficients (NAG library D03UAF) was employed. This solver performed a single iteration of the strongly implicit procedure described by Ames (1965).

Making use of the symmetries, the minimum area over which a numerical solution had to be obtained was one quadrant of the unit cell, bounded by the lines O, E, and the dashed lines in Figure 3.1. Because the staggered unit cell array was more complicated, the use of symmetry was less effective in reducing the size of the numerical problem for a fixed extracellular space gap. Because of the symmetry in the problem solved here, appropriately chosen Dirichlet and Neumann conditions were equivalent to periodic boundary conditions. The symmetry was necessary in order to apply the present numerical method, since Dirichlet, Neumann, or Robin conditions were required as input to the solver.

The numerical iteration was started with an initial guess for (χ_p^0 , κ_p^0). Coupling of the pairs of dependent variables (χ_p, κ_p), (χ_c, κ_c), (χ_v, κ_v), was acheived by using each variable to generate a source term in the iterations performed on the other. For example, k_i iterations of the solver are performed toward the solution for κ_{p1}^{n+1} in

$$\nabla^2 \kappa_{p1}^{n+1} = 0,$$

(4.7)

$$-\theta C_0 \nabla_v \, \kappa_{p1}^{n+1} \cdot \vec{n} \;=\; g(1 - \theta C_0/\sigma_0)\{ \chi_{p1}^{n,i} - \chi_{p1}^{n,o} + \kappa_{p1}^{n+1,i} - \kappa_{p1}^{n+1,o} \},$$

followed by l_i iterations of the solver toward the solution for χ_{p1}^{n+1} in

$$\nabla^2 \chi_{p1}^{n+1} \;=\; 0,$$

(4.8)

$$-\sigma_0 \{ \nabla_v \chi_{p1}^{n+1} \cdot \vec{n} + n_1) \;=\; g\{ \chi_{p1}^{n+1,i} - \chi_{p1}^{n+1,o} + \kappa_{p1}^{n+1,i} - \kappa_{p1}^{n+1,o} \},$$

where (k_i, l_i) are a sequence of pairs of integers.

A cyclic sequence for (k_i, l_i), $i = 1,...,6$; given by $(20,1),(1,2),(1,2),(2,1),(2,1),(1,20)$ was found by trial to be effective, and produced much faster convergence than $(k_i, l_i) = (1,1)$, $i = 1,...,N$. However, iterations in the above sequence were terminated at a preset error tolerance and the overall solution algorithm terminated when the residuals in the finite difference equations were $< 10^{-5}$, and the solutions had not changed by more than 10^{-5}. In addition, it was necessary to use large values of an internal D03UAF parameter APARAM, to reliably avoid failure (blowup) of the iteration procedure. We took APARAM=10 in the χ iteration and APARAM=100 in the κ solutions. Solutions at neighbouring values of λ^1 were used to start the iteration for new values, a procedure called continuation. The results of varying mesh size are described in Appendix IV.A, but the results from the finest grid used (72 x 72) will be reported.

With continuation, some 100-300 iterations were required to obtain the accuracy described. It was convenient to implement this procedure on the Floating

Point Systems processor model 164 (FPS-164/MAX) attached to the general purpose Amdahl computer at the University of British Columbia.

To assess the effect of the coupling between the concentration and potential equations, some solutions of an 'uncoupled' version of the χ_p system, in which the κ terms were omitted in the first equation of (3.1) are described in Appendix IV.B. Solving the uncoupled equations was less time consuming than solving the coupled equation with jump conditions (3.1) - (3.3). However, there was some indication that the uncoupled equations were more difficult to solve, since continuation and parameter selection required greater care than the coupled case when the NAG routine was used. A finite difference method similar to that described for the coupled case was used to obtain the uncoupled solutions.

5.0. BIOLOGICAL PARAMETER SELECTION

Because the geometry selected for the cellular matrix does not model the real geometry and because exact microscopic parameter values are not known in some cases, it is necessary to choose length scales and membrane conductances so that they approximate the characteristic values prevalent in the neural tissue and to explore the dependence of the solutions on these parameters in order to obtain qualitative results. Results which are not sensitive to the geometry and parameters chosen may be assumed to hold in vivo .

As will be shown in Chapter V, for purposes of analysis, cell size and membrane conductance may be combined into a single parameter, analogous to the electrotonic length of cable theory. This fact was used in the choice of the order of the jump conditions in Chapter III. In what follows, it is assumed that the cells under discussion have membrane resistivity equal to 320 Ωcm^2, which is Havstad's (1976) estimate of glial membrane conductance. Deduced parameters

then depend on the characteristic size of the cells and their surface/volume ratio (discussion below). For other cells (neurons), membrane resistivity might be 3000 to 5000 Ωcm^2, based on the resistivity of dendritic membrane. In this case the parameters employed in numerical studies correspond to cells which are larger by a factor equal to g_g/g_d (or its square root, as we describe below) where g_g and g_d are glial and dendritic membrane conductances, respectively.

In choosing biologically relevant parameters, we followed Gardner-Medwin (1983) in taking into account the surface/volume ratio for cells in the brain. This has been estimated at 5 μm^{-1} (Horstmann & Meves, 1959) on the average, or 5 μm^2 of membrane per μm^3 of tissue. The (two-dimensional) cells are square and, as discussed in Section 3.3, the choice of straight cell boundaries was made to facilitate the study of the effect of realistic extracellular space fraction values, as well as for ease in computation. The dimensional length of the unit cell is denoted by l and the biological cell will have length fl, where f is a fixed fraction close to unity. For an extracellular space fraction of $a=23\%$, the value of f is .875. Had these elements been extended normal to the W-plane, the resulting square shafts would have had surface volume ratio $4lf/l^2 = 4f/l$. The parameter λ^r can be written as $\lambda^1 = hg/\sigma^0 = lg/24\sigma^0$ and $\lambda^2 = hg/\sigma^i = lg/24\sigma^i$ for a mesh which is 24 x 24. The value of g in two dimensions may be deduced from the assumption that these extended shafts have the membrane conductance observed experimentally. For each characteristic size l, it was assumed that the effective membrane conductance was increased by a factor equal to that necessary to make the surface volume ratio of the unit cell equal to 5 μm^{-1}, say $l=l_1$. The formulas for λ^1 when the surface-volume ratio is taken into account and when it is not are:

$$\lambda^1 = l_0 g / 24 \sigma^0,$$

(5.1)

$$\lambda^1 = \frac{1}{24} \frac{l_1 g}{\sigma^0} \frac{5 l_1}{4f} = \frac{5 l_1^2}{96 f \sigma^0}.$$

The correspondence between $l_0 (\mu m)$ and λ^1 for $g^{-1} = 320 \ \Omega cm^2$ is given in Table 5.1. If the mesh were 48 x 48, the corresponding λ^1 values would be half these values; or l_0 twice as large for the same values of λ^1 when the surface / volume correction is not applied.

Our numerical studies of membrane conductance with a 24 x 24 mesh were carried out with λ^1 values selected from those listed in Table 5.1 where l_0 and l_1, respectively, are the characteristic unit cell sizes associated with corresponding assumptions about the surface / volume ratio. It is expected that characteristic sizes between 5 μm and 50 μm will be appropriate for glia while characteristic sizes between 50 μm and 500 μm will be appropriate for neurons or syncytial glial elements of similar length.

The intracellular conductivity is usually assumed to be 10 mS (Shelton, 1985; Gardner-Medwin, 1983; Havstad, 1976), but here some studies were carried out with intracellular conductivities of 4 mS and 2 mS to establish the sensitivity of the results to the intracellular conductivity, because this conductivity is uncertain. Knowledge of the sensitivity of results is useful for comparisons with the qualitative investigations of Chapter V.

Table 5.1. Unit Cell Lengths.

$10^3\lambda^1$	$l_0(\mu m)$	$l_1(\mu m)$
100	153600	328
50	76800	234
20	3072	146
10	1536	103
5	768	72.1
2	308	46.0
1	154	32.5
0.1	15.4	10.3

6.0. PARAMETER STUDIES

6.1. Computation of Coefficients from Canonical Problems

Since the unit cells are unchanged by an interchange of the space coordinates, the canonical problems are the same for each coordinate direction. The computation of the bulk coefficients reduces to the evaluation of integrals of the form

$$(6.1) \qquad \int_W K_1(\vec{w})\{K_2 + \frac{\partial\psi}{\partial w_j}\}dA,$$

where K_j, $j=1,2$ is proportional to $\sigma(w_1, w_2)$ and ψ, a typical canonical solution is independent of the spatial direction. Thus, bulk coefficients reduce to scalars (cf. Section III.2.2). In addition, because of the symmetry discussed in Section

3.2, the off-diagonal elements in the bulk coefficient formulas are zero under averaging. The integral (6.1) over the intracellular region may be evaluated directly since K_1 is constant intracellularly. It is convenient to avoid numerical integration of the derivative when the integral is taken over the extracellular region. For this purpose, the second term of (6.1) is integrated by parts in W_j and the periodic boundary conditions are used to give

$$(6.2) \qquad \int_W K_1 \frac{\partial \psi}{\partial w_j} \, dA = - \int_W \psi \frac{\partial K_1}{\partial w_j} \, dA.$$

As $\partial K_1 / \partial W_1$ (the case of $j=1$) is a set of line sources, this reduces the calculation to a summation over the source locations.

In computing coefficients from the finite difference solutions, it is possible to assume either that the membrane lies halfway between the adjacent mesh points on opposite sides of the membrane, or that the membrane contains the extreme extracellular and extreme intracellular mesh points. The first assumption necessitates an extrapolation to determine solution values at the membrane. This extrapolation cannot improve the asymptotic accuracy (in h) of the coefficient estimates, so nothing is lost if (Figure 3.1 and 3.2) the available values at the extreme mesh points are used instead. Thus, the extracellular space fractions referred to below use the second assumption.

6.2. Bulk Conductivity and Flux Proportional to Electric Field

The coefficients D_1 and D_2 of the average governing equations (III.2.17) contain the averages of the canonical solutions κ_p and χ_p which represent, physically, $O(\epsilon)$ fluxes proportional to the extracellular potential gradient, $\nabla \phi_0$. The fluxes proportional to $\nabla_w \chi_p$, where χ_p is the perturbation in ϕ, and $\nabla_w \kappa_p$, where κ_p is the the perturbation in C, are discussed in this section. Using (III.2.17), the bulk conductivity may be identified with the coefficient D_1 because $D_1 \nabla \phi_0$ is the bulk electrical current which is proportional to $\nabla \phi_0$.† The effective transcellular conductance is defined as the coefficient $D_2 = \sigma_o^0 M_W \{ t_K t_\sigma (1 + \nabla_w \chi_{p1}) + \nabla_w \kappa_{p1} \}$ and in the uncoupled model the transcellular conductance is defined by $\sigma_o^0 M_W \{ t_K t_\sigma (1 + \nabla_w \chi_{p1}) \}$. The effective transcellular conductance is a weighted average of intracellular and extracellular flux which is predominantly intracellular because $t_K^o << t_K^i$ and physically represents the ionic flux proportional to ϕ_0. The coefficient D_2 is compared to the transcellular conductance of the uncoupled model in Appendix IV.B. These quantities have similar numerical values because the intracellular transport number $t_K^i \simeq 1$ and $t_K^o \simeq 0$. The flux associated with $\nabla_w \kappa_p$ occurs in the definition of D_2 but not in the transcellular conductance. This flux may be interpreted physically as the diffusive ionic transport due to local concentration gradients caused by ionic flux through cells. The average of $\nabla_w \kappa_p$ makes a positive contribution to D_2 of 9% at $l_1 = 32.5$ μm and 5% at $l_1 = 146$ μm, compared to the total effective transcellular conductance. Since χ_{p1} in the coupled and uncoupled models are distinct, however, $\nabla_w \kappa_p$ does not determine the relative magnitudes of the conductances in the coupled and

---

† As noted in Chapter III, we do not distinguish between the one- and two-tier models except in Section IV.6.3, so we write here: $D_1 := \sigma_o^0 M_W \{ t_\sigma (1 + \partial \chi / \partial W_1) \}$ where $t_\sigma = \sigma_0 / \sigma_o^0$.

uncoupled models.

Computed bulk conductivity versus cell sizes are shown in Figure 6.1.A, and corresponding effective bulk transcellular conductance estimates in Figure 6.1.B for straight arrays of square cells (72 x 72 point solutions with an extracellular space of 23%). These calculations assumed an extracellular conductivity of 20 mS and an intracellular conductivity of 10 mS, which has been taken as typical. The bulk conductivity estimates range from 2.8 to 3.9 mS in the parameter range of biological interest ($l_1 = $ 32.5 μm to $l_1 = $ 146 μm), and are an increasing function of the cell size (membrane conductance). For comparison, conductance estimates from an uncoupled calculation are presented in the figures. When $l_1 = 32.5$ μm, the coupled and uncoupled models agree to three significant figures, while at $l_1 = 146$ μm, they differ in this coefficient by about 20%. These values are consistent with observed conductivities ($\simeq$ 5 mS) for bulk cortex and cerebellum (Nicholson, 1980). An extensive review of experimental data on electrical properties of biological tissue may be found in Schanne and Ruiz P.-Ceretti, (1978). At low membrane conductances, L = 10.3 μm, bulk conductivity is 2.62 mS and transcellular conductance is approximately 2% of this.

The bulk transcellular conductance ranges from 7% of bulk conductivity at $l_1 = 32.5$ μm, to 30% at $l_1 = 146$ μm. This agrees closely with the uncoupled model at 32.5 μm, but is some 13% less than the uncoupled model at $l_1 = 103$ μm. Gardner-Medwin (1983) found that transcellular current, as measured by K^+ transport over a large (5 mm) region was about 6% of the total current. Hence, the present theory suggests that transcellular current is at least as large as was observed in that experiment, and supports the

Figure 6.1. Bulk conductivity (A) and transcellular conductance (B) versus cell size (l_1) are plotted for coupled and uncoupled models for $\sigma^0 = 20$ mS, and $\sigma^i = 10$ mS. A logarithmic vertical scale is used in B.
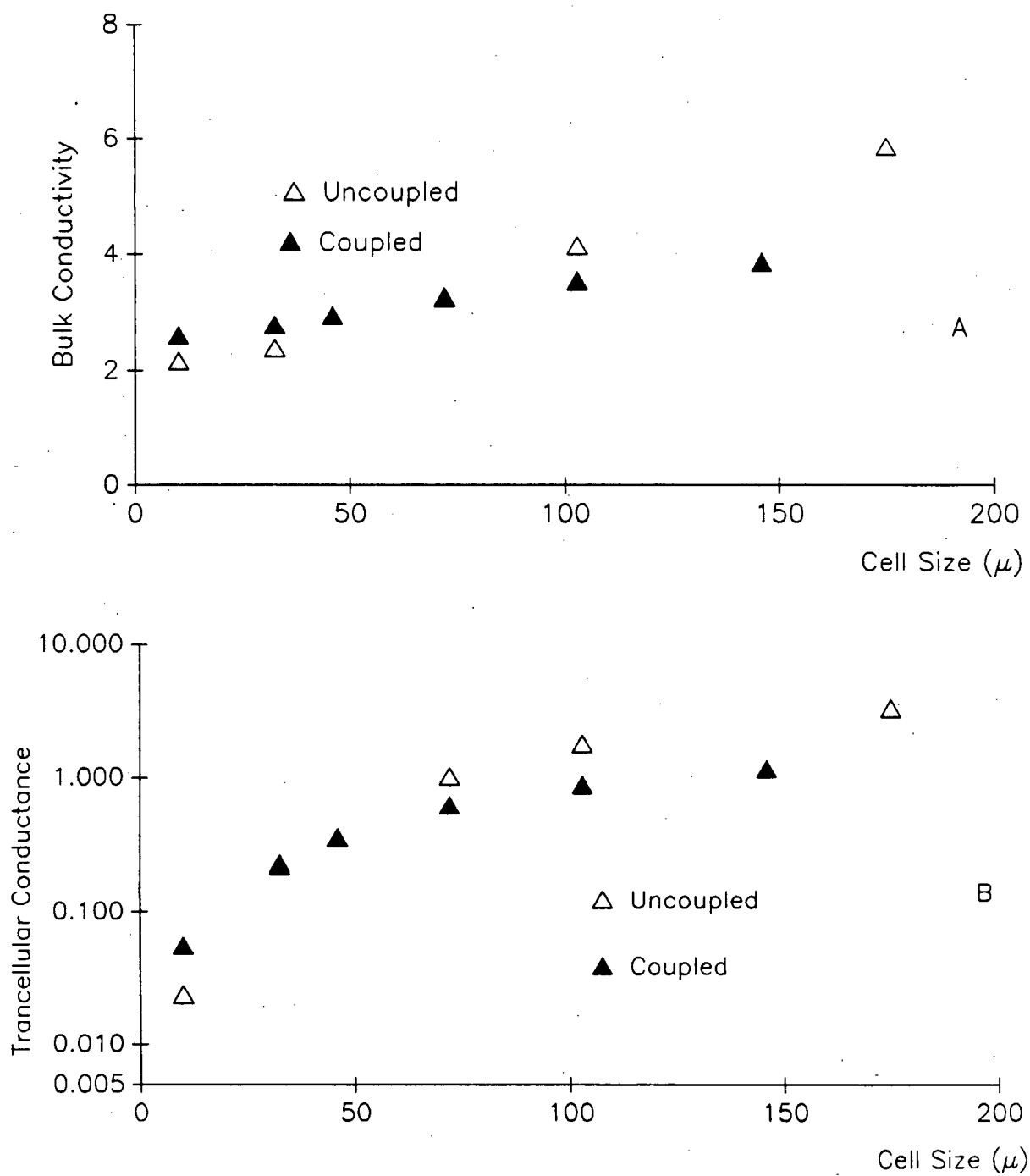
Figure 6.1   Cell Size and Bulk Conductivity

Table 6.1. E_1, D_1, and D_2 by Cell Length.

l_1 (μm)	D_1(10 mS)	D_2(10 mS)	E_1
32.5	.280	.024	.019
46	.296	.040	.032
72.1	.327	.069	.059
103	.355	.096	.084
146	.386	.122	.111

experimental demonstration that such currents are significant.

It is useful to be able to deduce the values of coefficients other than D_1 and D_2 from fluxes proportional to $\nabla \phi$ because these fluxes are easy to measure experimentally (Gardner-Medwin, 1983a). The coefficient, $E_1 = \sigma_0 M_W \{ t_\sigma (t_\beta + \nabla_w \chi_{v1}) \}$, is formally distinct from the effective transcellular conductance, but it will be shown by direct calculation that the effective transcellular conductance D_2 is a useful approximation to E_1 (and E_2). The coefficients E_1 and E_2 play an important role in determining the magnitude of the spatial buffering effect. Examination of Table 6.1, shows that this approximation will be in error by at most 4 to 18%.

Typical values of D_1, D_2, and E_1 are tabulated in Table 6.1. The values of D_1 correspond to Figure 6.1.A, and may be compared to uncoupled values displayed there, while D_2 and E_1 do not have analogues in the uncoupled model.

It is seen that while D_1 does not vary greatly over the biological range of cell size/conductivity, ($\simeq$ 30%) the coefficients D_2 and E_1 vary by a factor of

$\simeq$ 5.

6.3. Effect of Intracellular Conductivity on Bulk Conductivity

Figures 6.2.A and 6.2.B show the bulk conductivity and effective transcellular conductance when intracellular conductivity is 10 mS (Section 6.2), 4 mS, and 2 mS. While the influence of intracellular conductivity σ^i was relatively slight from $l_1 = 32.5$ μm up to $l_1 = 103$ μm, bulk transcellular conductance was sensitive to the membrane conductance. Between $l_1 = 32.5$ μm and $l_1 = 103$ μm, the transcellular conductance changes by a minimum of 220% over each of the three choices of σ^i while the change in transcellular conductance for any λ^1 from 10 mS to 2 mS is at most 27%. At $l_1 = 146$ μm, a five-fold reduction in σ^i reduces transcellular current by 45%.

These results demonstrate directly that for the parameter values discussed in Sections 6.2 - 6.3, the intracellular and extracellular electric potential are described qualitatively by the asymptotic analysis (of Chapter V) for electrical space constants which are long compared to cell length. These asymptotic solutions and hence, the numerical conclusions, do not depend strongly on geometry. In addition, it is biologically significant that these model cells which exhibit bulk transcellular currents from 7 to 30% of total current had electrical space constants which were long compared to the cell dimension, and thus were electrotonically unlike an electrical syncytium.

In the one-tier model, coefficients other than D_1 and D_2 are also insensitive to the intracellular conductivity. The values of E_1, F_1, and F_2 for $\sigma^i = 10$, 4 and 2 mS for various membrane conductances are tabulated in Tables 6.2. The values of E_2 were close to those of E_1. As suggested above, E_2 is

Figure 6.2. Bulk conductivity (A) and transcellular conductance (B) versus cell size (l_1) are plotted for $\sigma^1 = $ 10, 4, and 2 mS. A logarithmic vertical scale is used in B.
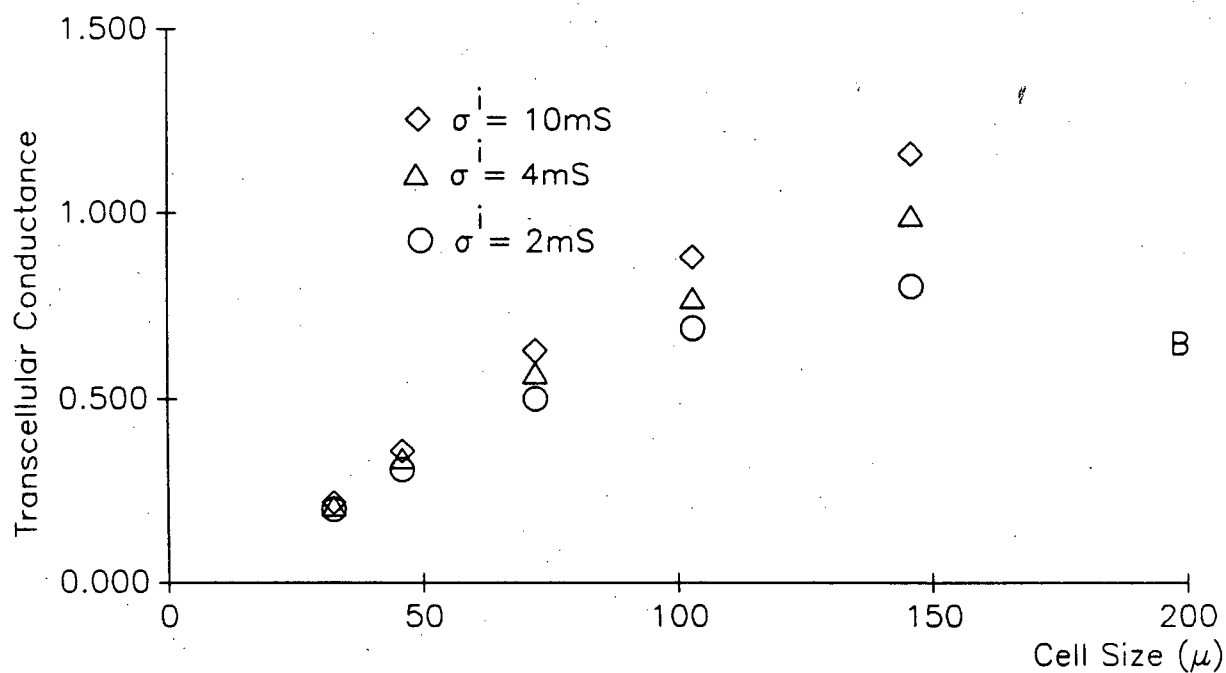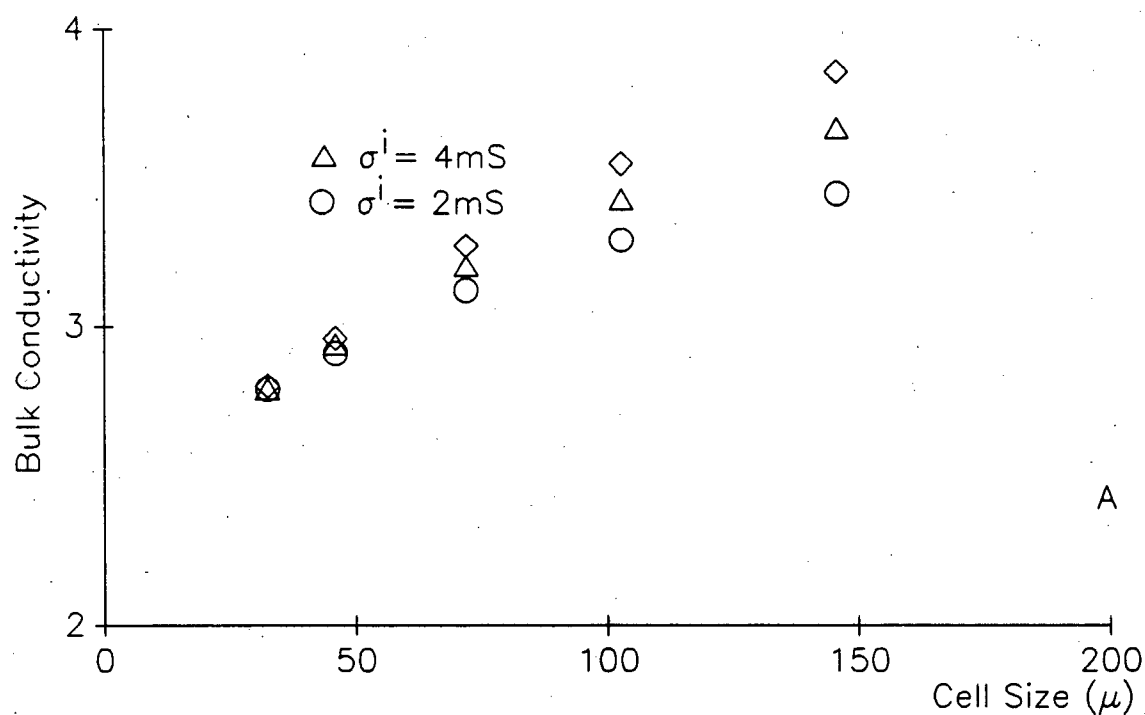
Figure 6.2   Intracellular Conductivity and Bulk Conductivity

closely approximated by the transcellular conductance for these cases and thus depends on the intracellular conductivity in a similar way.

6.4. Tissue Structure

The derivation in Chapter III assumes that the tissue has a two-tier structure as discussed in Section II.2.2. Thus, it is assumed that a periodic array of asymptotically larger cells is imbedded in a periodic array of asymptotically smaller cells. A one-tier model would assume that cells are surrounded by an extracellular medium consisting only of electrolyte with conductivity $\simeq$ 20 mS, while a two-tier model assumes an extracellular medium containing another cell type, surrounded by extracellular electrolyte. The assumptions of such a model are illustrated schematically in Figure 6.3. The cells have been assumed to be two-dimensional and square, as before, and the cells are not shown to scale.

Numerical solutions were obtained under the assumptions of the two-tier model. It is assumed that the areas N, in the unit cell V, and G, in the subcell W, have the same relative ICS fraction, x, and that the total ECS fraction is $a = 0.2$. To obtain this ECS fraction, over the two-tier unit cell, the relative intracellular space fraction, x, of each unit cell; V or the subcell W must satisfy $x + x(1 - x) = 0.8$ since the total ICS in V is the space occupied by N plus the space occupied in its (relative) extracellular space by the areas G. Therefore the intracellular space fraction is x = 56%. For this reason, the solutions were obtained for $a = 0.44$, and assuming that the membrane conductance is zero at $O(\epsilon^{-1})$, as already assumed in Chapter III. The bulk parameters for the extracellular space were then used in a further set of studies

Table 6.2.A. E_1 Coefficient Versus Intracellular Conductivity

l_1 (μm)	10 mS	4 mS	2 mS
32.5	.019	.018	.017
46	.032	.031	.028
72.1	.059	.054	.046
103	.084	.074	.061
146	.111	.090	.075

Table 6.2.B. F_1 Coefficient Versus Intracellular Conductivity

l_1 (μm)	10 mS	4 mS	2 mS
32.5	1.83	1.77	1.68
46	3.11	2.94	2.69
72.1	5.47	4.72	4.06
103	6.76	5.32	4.37
146	6.25	3.97	3.10

Table 6.2.C. F_2 Coefficient Versus Intracellular Conductivity

l_1 (μm)	10 mS	4 mS	2 mS
32.5	4.55	4.49	4.40
46	5.93	5.76	5.51

72.1	8.42	7.79	7.15
103	9.99	8.76	7.82
146	9.93	7.99	7.16

Figure 6.3. A two-dimensional two-tier model is schematically illustrated. The asymptotically larger population (N) is surrounded by an asymptotically smaller population (G). Unit cells are bounded by dashed lines. The spatial coordinate in the larger unit cell is V and in the smaller unit cell, W. The diagram is not to scale, since the ratio of the sizes of smaller to larger unit cells tends to zero in the mathematical model.
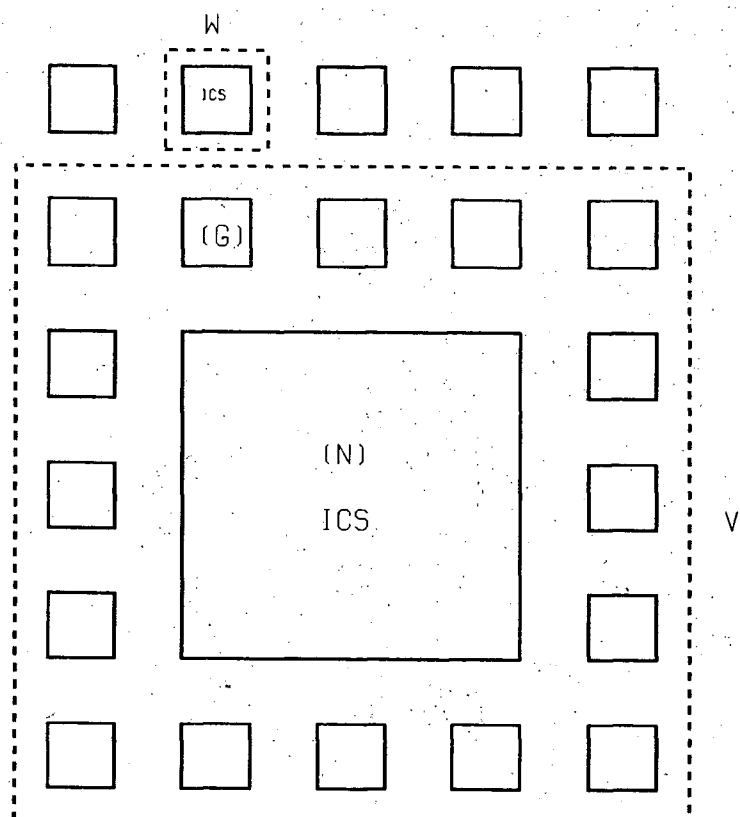
A Two Dimensional Two-tier Model

Figure 6.3

at $a = 0.44$. Thus, we took $\sigma_0^0 = 5.39$ mS, in place of $\sigma_0^0 = 20$ mS. As described above, the total extracellular space remains the same. If bulk parameters depend sensitively on tier structure, these studies could produce very different results from the one-tier studies with $a = 0.2$. The results for the uncoupled model, discussed in Appendix B, indicate that bulk conductivity is altered by a factor of 2 to 3 by differing tier structures (Figure B.3.A), but bulk transcellular conductance is not sensitive to tier structure.

Conductivity estimates obtained for the coupled two-tier model are shown in Figure 6.4. These results indicate a strong coupling effect at all membrane conductance values, since they differ significantly from the uncoupled results. The computed values of bulk and transcellular conductance are also significantly different than those seen in the one-tier coupled model. Computed bulk conductivities are about half the one-tier results, ranging from 1.56 mS to 1.82 mS. In addition, the transcellular conductance was consistently lower than the one-tier result by a factor of 3 to 5. The transcellular conductance as a fraction of bulk conductivity varies from 7.5% at $l_1 = 32.5$ μm to 16% at $l_1 = 146$ μm (vs. 25% in the one-tier study). Thus, while the bulk and transcellular conductances were not sensitive to the intracellular conductivity (Section 6.3), the extracellular conductivity has a significant effect on these quantities in a coupled model. This effect is to decrease bulk and transcellular conductance, and to decrease transcellular conductance as a fraction of bulk conductivity. The reasons for differences between one- and two-tier models are now discussed.

The local, coupled, canonical problem for χ_p has not been simplified by our use of the transport number theory. Thus, it is expected that for some parameter values, interactions between electrical potential and concentration will

Figure 6.4. Bulk conductivities (A) and transcellular conductance (B) versus cell size (l_1) are plotted for one-tier and two-tier models. The one-tier model is indicated by filled squares and the two-tier model by open triangles. A logarithmic vertical scale is used in B.
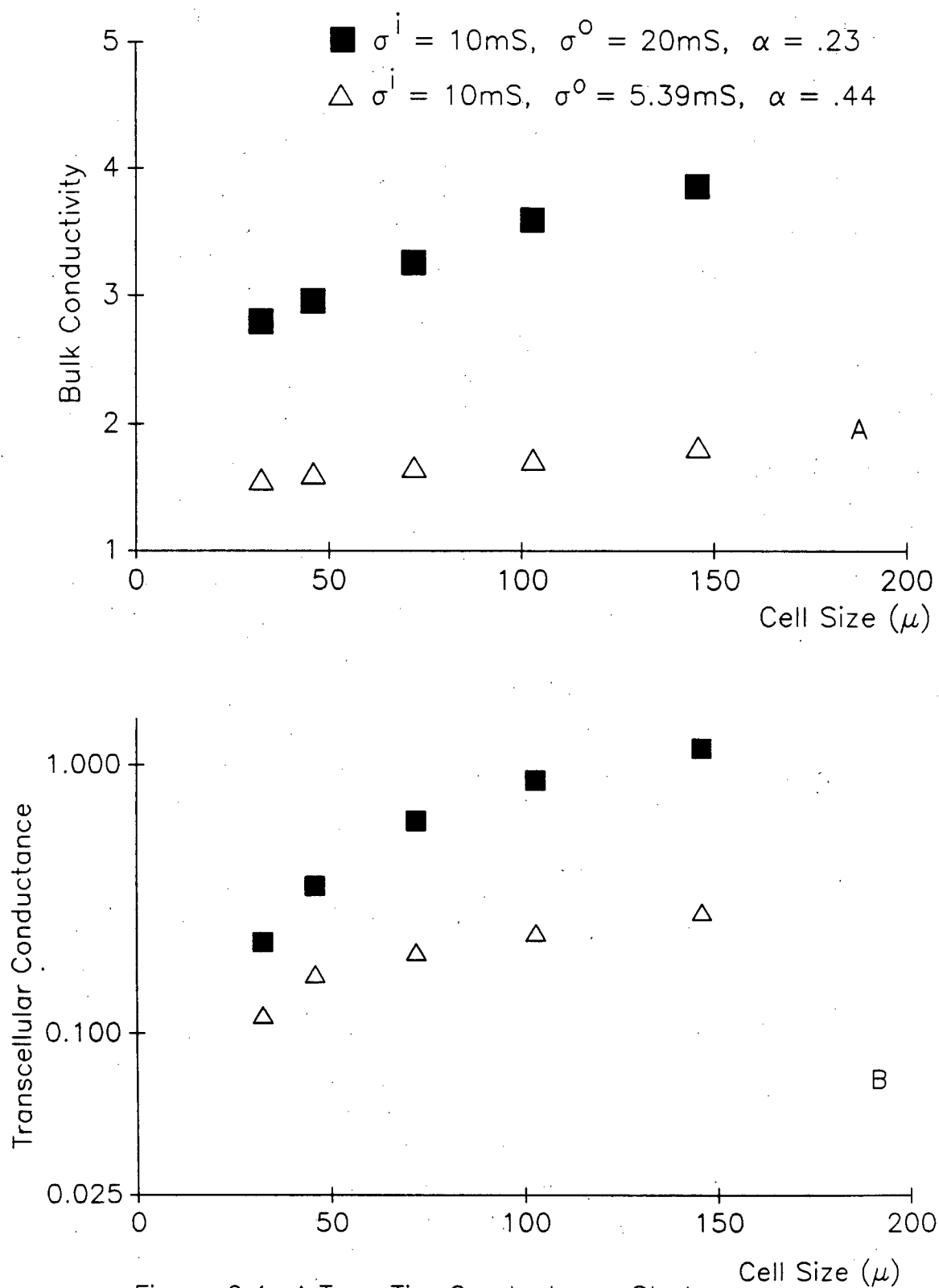
Figure 6.4   A Two–Tier Conductance Study

be significant. The average ionic fluxes associated with χ_p and κ_p are tabulated

in Table 6.3. It is found that there is a large fractional change in ionic flux

associated with the C perturbation (column 3), κ_p, over different membrane

conductance values, and that this flux may become negative at $l_1 = 146$ μm.

Thus, the coupling effect on transcellular conductance seen in the two-tier

results may be interpreted physically as follows. Transcellular conductance in an

uncoupled model increases with the membrane conductance, because more electrical

current proportional to $\nabla_v \phi_0$ takes an intracellular route. In a coupled model,

inward transmembrane current results in a depletion of $[K^+]$ near the outside of

the membrane, and outward transmembrane current results in accumulation of

$[K^+]$ near the outside of the membrane. This causes hyperpolarization of the

membrane near the region of inward current and depolarization near the region

of outward current (refer to Figure I-4.1 of Chapter I). The resulting intracellular

current flows in the direction opposite to $\nabla_v \phi_0$ and tends to cancel it. This

effect is accentuated as the extracellular conductivity becomes smaller relative to

membrane conductance, because increased electrical K^+ transport through the

membrane and decreased electrical K^+ transport in the extracellular medium

causes more depletion (accumulation).

The values of D_1, D_2, and E_1 for the two-tier model are tabulated in

Table 6.4. It is seen that D_2 remains a reasonable approximation to E_1. Other

coefficients are discussed in the next few sections.

Studies with staggered arrays were performed for $\sigma^0 = 20.0$ mS, $\sigma^i =$

10.0 mS, with $a = .2$ for one- and two-tier models. There was little difference

between the results for staggered arrays and straight arrays. The coefficients D_1

and D_2 are tabulated in Table 6.5.A-C, for straight and staggered arrays for

Table 6.3. Fluxes due to ϕ and C Perturbations.

l_1 (μm)	$M_W\{t_K t_\sigma(1+\nabla_w\chi_{p1})\}$	$M_W\{\nabla_w\kappa_{p1}\}$
32.5	.0098	.0019
46.0	.0144	.0023
72.1	.0184	.0019
103.0	.0237	.0002
146.0	.0324	-.0038

Table 6.4. Coefficients in (III.2.17) for Two-Tier Model.

l_1 (μm)	D_1(10 mS)	D_2(10 mS)	E_1
32.5	.156	.0117	.0079
46.0	.161	.0167	.0127
72.1	.166	.0203	.0164
103	.172	.0239	.0212
146	.182	.0286	.0289

the one-tier and two-tier model. The other coefficients followed the same pattern. This is in contrast to the results for the uncoupled model (Appendix IV.B), in which the differences between staggered and straight arrays grew more pronounced as membrane conductance increased. Thus, the coupling between concentration and electrical potential, which is expected to become more significant with higher membrane conductance, apparently reduced the effects of geometry.

Table 6.5.A. D_1 and Array Geometry: One-Tier Model.

l_1 (μm)	Straight (mS)	Staggered (mS)
10.1	2.62	2.50
32.5	2.80	2.69
46.0	2.96	2.84
72.1	3.27	3.15
103.0	3.55	3.44
146.0	3.86	3.75

Table 6.5.B. D_2 and Array Geometry: One-Tier Model.

l_1 (μm)	Straight (mS)	Staggered (mS)
10.1	.056	.055
32.5	.242	.239
46.0	.397	.389
72.1	.693	.691
103.0	.955	.958
146.0	1.222	1.222

Table 6.5.C. D_1 and Array Geometry: Two-Tier Model

l_1 (μm)	Straight (mS)	Staggered (mS)

32.5	1.56	1.43
46.0	1.61	1.48
72.1	1.66	1.53
103.0	1.72	1.60
146.0	1.82	1.70

Table 6.5.D. D_2 and Array Geometry: Two-Tier Model

l_1 (μm)	Straight (mS)	Staggered (mS)
32.5	.117	.121
46.0	.167	.172
72.1	.202	.207
103.0	.239	.242
146.0	.286	.290

The existence of tier-structure is an important theoretical possibility, because coupling between concentration and electrical potential becomes important in the two-tier model. Also, as discussed in Chapter VI, spatial buffering occurs by a different mechanism in this model. However, while the two-tier model seems plausible, there is currently no experimental evidence to support this relatively complicated assumption. Thus, the chief conclusion of this section is that the predictions of the one- and two-tier models are broadly similar and the differences between straight and staggered arrays are not large.

6.5. Ionic Flux Terms Proportional to Concentration Gradient

The coefficients specified by the κ_c and χ_c canonical problem are associated with the potassium concentration gradient. If the membrane conductance were zero, this canonical problem would simply be the governing equation for diffusive flux. Since the membrane is permeable to potassium, however, its concentration at the membrane affects the Nernst potential to all orders. Thus, these coefficients do not depend exclusively on the diffusive properties of the tissue, but also reflect the interaction of the local Nernst potential with 'unstirred layers' (Schultz, 1980) at the membrane. These effects have not been included previously in a model of this kind and the coefficients $F_1 = \sigma_0^0 \nu^{-1} M_W \{t_\sigma \nabla_w \chi_{c1}\}$ and $F_2 = \nu^{-1} \{M_W \{(\theta C_{io} \nabla_w \kappa_{c1} + \theta) + \sigma_0^0 t_K t_\sigma \nabla_w \chi_{c1}\}\}$ do not correspond to any commonly employed physical quantity, such as conductivity or diffusion coefficient. For this reason, we do not discuss uncoupled estimates, or the behavior of the component averages of F_1 and F_2. As discussed in Appendix IV.A, the solutions for χ_c and κ_c converge slowly as mesh size tends to zero at larger values of the membrane conductance and our estimates of F_1, and F_2 are likely less accurate than the estimates of D_1 and D_2.

At small values of the membrane conductance, F_2 is proportional to the bulk diffusion coefficient, reduced by the extracellular space fraction and microscopic geometry of the medium. At $l_1 = 10.3$ μm, which corresponds to a high membrane resistivity, bulk conductivity is 2.6 mS which is 2.6/20= .13 as a fraction of extracellular conductivity. On this basis, it may be calculated (for comparison) that F_2, the coefficient of $\nabla^2 C_0$ in (III.2.17) would be 2.64 with g=0. If g=0, then $F_1 = 0$ in the model.

In the one-tier models the effect of non-zero g is to increase F_2 by

factors between 1.7 and 3.8, above the value expected with pure diffusion. In the one-tier model the coefficient F_2 is positive and comparable to F_1 in magnitude. In the two-tier model, F_1 is nearly zero at $l_1 = 103$ μm and negative at $l_1 = 146$ μm. In both models the ionic flux associated with the C perturbation, κ_c, is more stable to changes in membrane conductance, while the ionic flux associated with the ϕ perturbation, χ_c, is more sensitive to such changes. The κ_c-flux varies from 2.9 to 4.55 in the one-tier model and from 7.22 to 8.81 in the two-tier model, while the χ_c-flux varies from 1.6 to 5.36 in the one-tier model and from -.177 to 10.2 in the two-tier model.

It is interesting that in the two-tier model, the variations in F_1 and F_2 are chiefly due to χ_c, the perturbation in the electrical potential ϕ. In our models, F_1 and F_2 are the coefficients of $\nabla^2 C$ in the bulk equation (III.2.17). In the original physical equations for electrolyte solution, the coefficient of $\nabla^2 C$ is simply a diffusion coefficient.

The values of F_1 and F_2 are shown in Figures 6.5A and 6.5B, respectively, for various values of σ^i, the intracellular conductivity, and a, the extracellular space fraction, in a one-tier model. In the one-tier model, F_1 and F_2 are increasing functions of membrane conductance up to $l_1 = 103$ μm. However, both coefficients are relatively insensitive to the parameters over these ranges (i.e., vary by factors of about 2 to 3 when the independent parameters vary by factors of 5 to 20). A maximum in the values of F_1 and F_2 consistently occurs at $l_1 = 103$ μm, though it is not pronounced. Electrically mediated transcellular ionic flux associated with χ_c is due to local accumulation/depletion of potassium. Thus, the maximum may be due to the accumulation/depletion effect described in the last section.

Figure 6.5. Coefficients of $\nabla^2 C$ (in III.2.17) versus cell size (l_1) are plotted for different intracellular conductivities $(\sigma^1 = 10, 4, 2mS)$ and extracellular space fractions $(a = 0.16, 0.23, 0.37)$. For comparison, the value of F_2 corresponding to pure diffusion is indicated in B by a filled square.
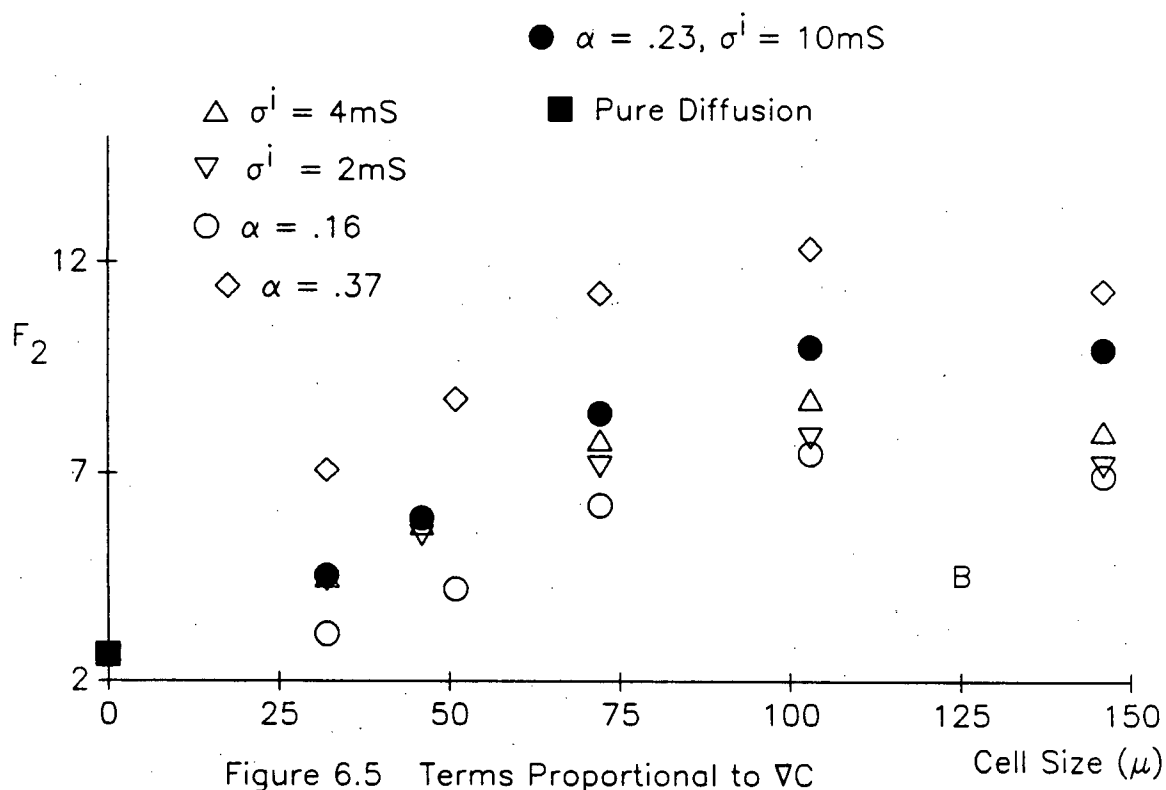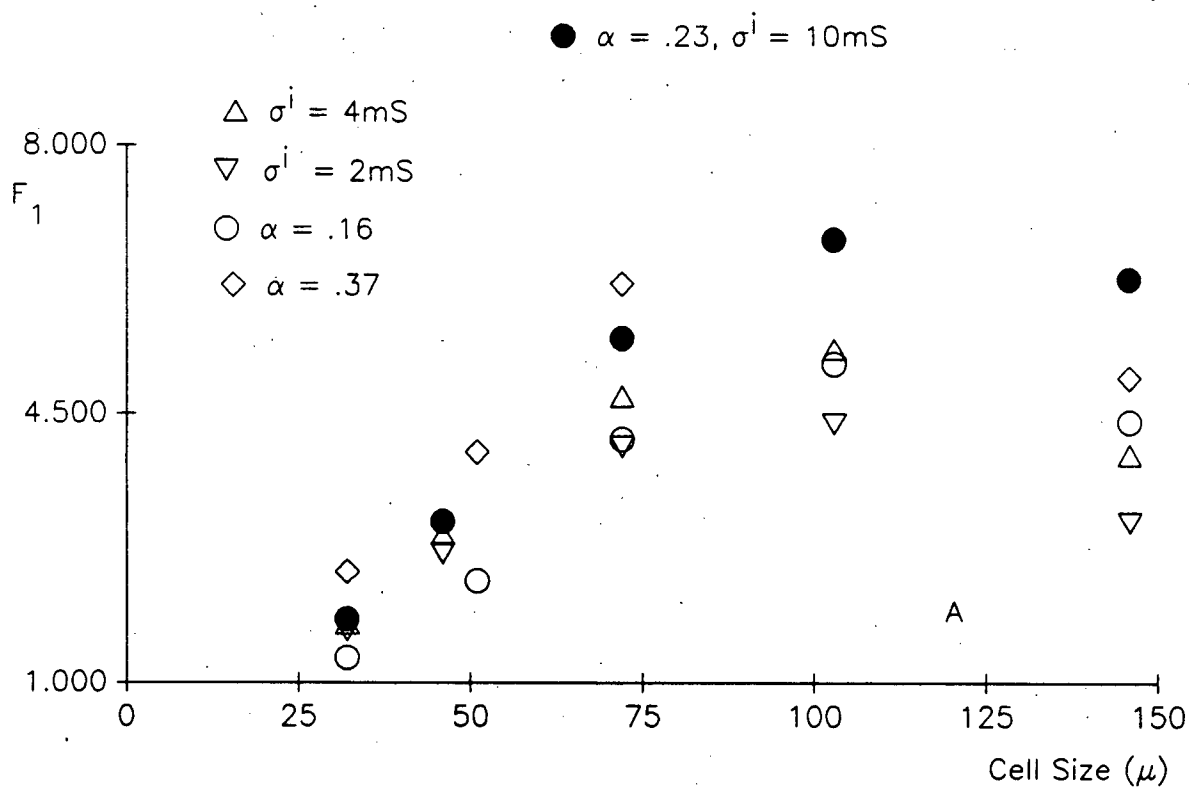
Figure 6.5 Terms Proportional to ∇C

Figure 6.6. Coefficients of $\nabla^2 C$ (in III.2.17) versus cell size (l_1) are plotted for one- and two-tier models. Note that the coefficient F_1 is negative in A at $l_1 = 146$ μm.
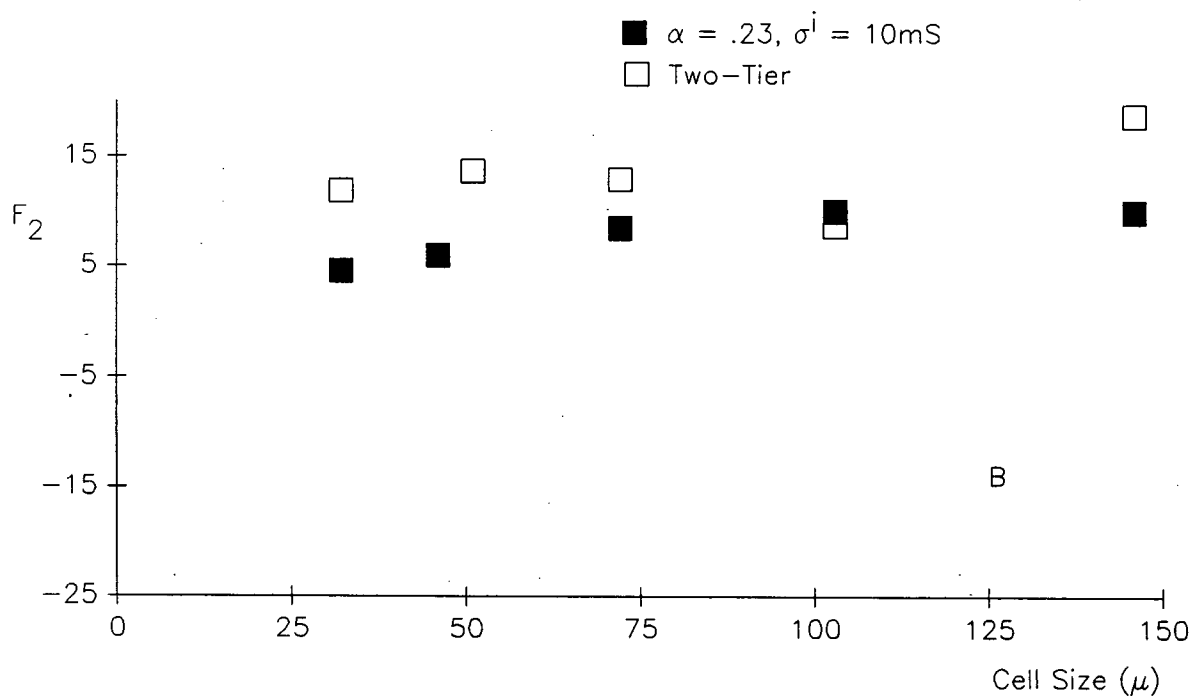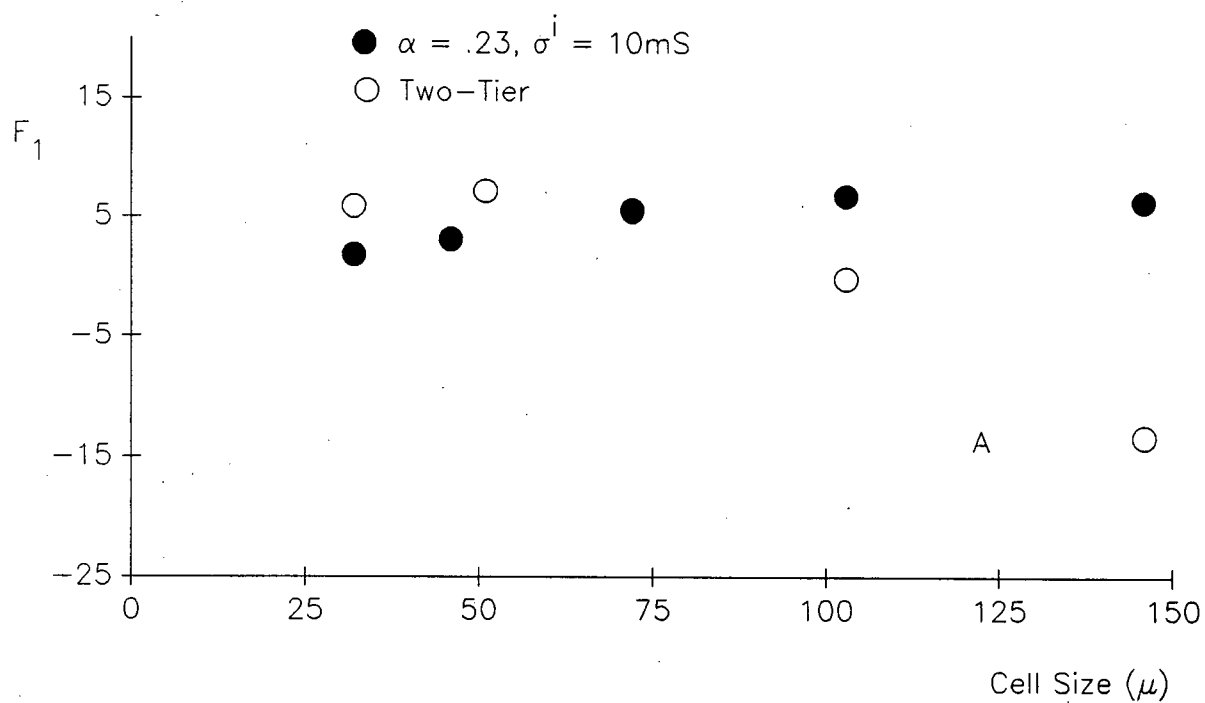
Figure 6.6   Terms Proportional to ∇C and Tier Structure

The coefficients F_1 and F_2 for the two-tier model at various cell sizes are shown in Figure 6.6. It is seen that F_1 and F_2 are not monotone functions of the membrane conductance in the two-tier model, with F_1 is decreasing above $l_1 = 46$ μm, becoming negative near $l_1 = 103$ μm. This reversal of sign does not qualitatively affect the solutions to the bulk equation (III.2.17) since the effect of negative F_1 is balanced by other coefficients (see Chapter VI).

The coefficient F_2 has a minimum near $l_1 = 103$ μm. This cannot be simply explained as an accumulation/depletion effect. Presumably, this minimum occurs because the solution surface for χ_c changes its shape at larger values of the membrane conductance ($l_1 = 146$ μm). In other studies (not presented here), in which t_K^o was lowered to .0074, this minimum did not occur.

6.6. Ionic Flux Terms Proportional to Nernst Potential Gradient

The coefficients specified by the κ_v and χ_v canonical problems are associated with the Nernst potential gradient. These coefficients are averages of ionic and electric fluxes due to the ambient gradient in the Nernst potential determined by $\ln(C_{2o}^o/C_{2o}^i)$. These fluxes are different from the fluxes averaged in F_1 and F_2 because the F coefficients only reflect accumulation and depletion of K^+ near the cell. It is shown in Chapter VI that the fluxes associated with the Nernst potential represent the most important contributions to spatial buffering at most cell sizes in the one-tier model.

The values of E_2 are shown in Figure 6.7A for various values of σ^i, the intracellular conductivity, and a, the extracellular space fraction. Values of E_1 are not shown because they are nearly identical to E_2. The coefficients are relatively insensitive to the parameters over these ranges (i.e., vary by factors of

Figure 6.7. In A, the coefficient of $\nabla^2 V$ (in III.2.17) versus cell size (l_1) is plotted for different intracellular conductivities $(\sigma^1 = 10,\ 4,\ 2\ mS)$ and extracellular space fractions $(a = 0.16,\ 0.23,\ 0.37)$. The same coefficient is plotted against cell size for one- and two-tier models in B. Both figures use logarithmic vertical scales.
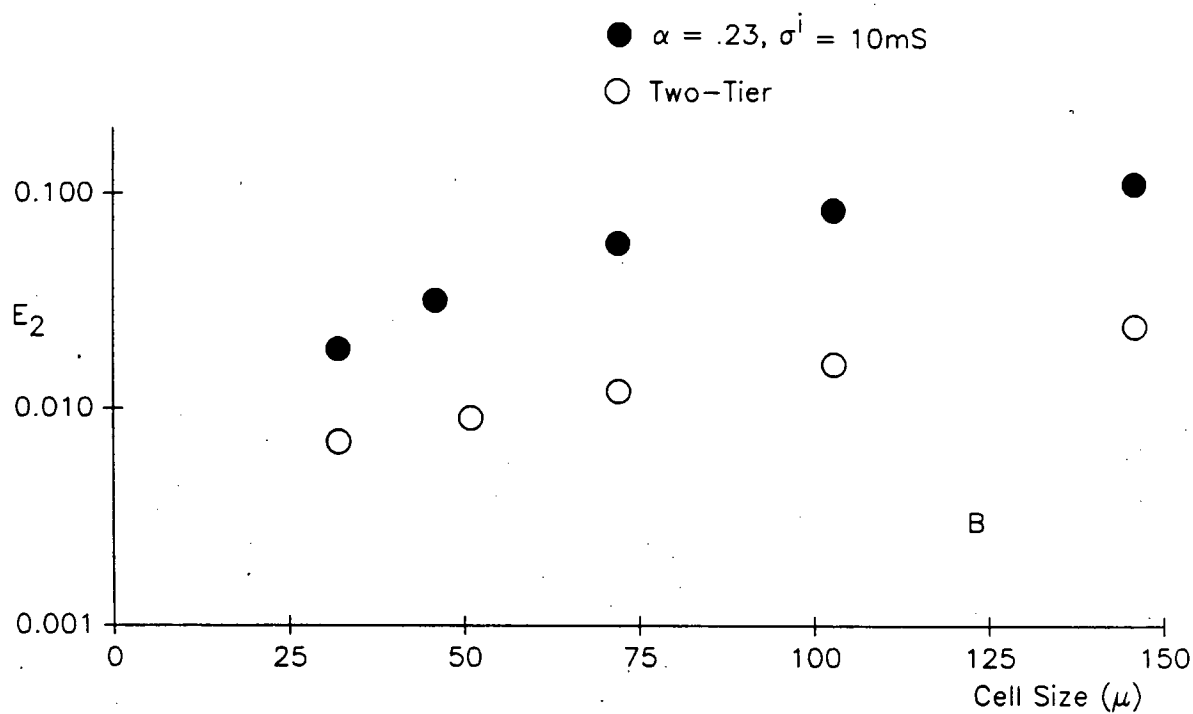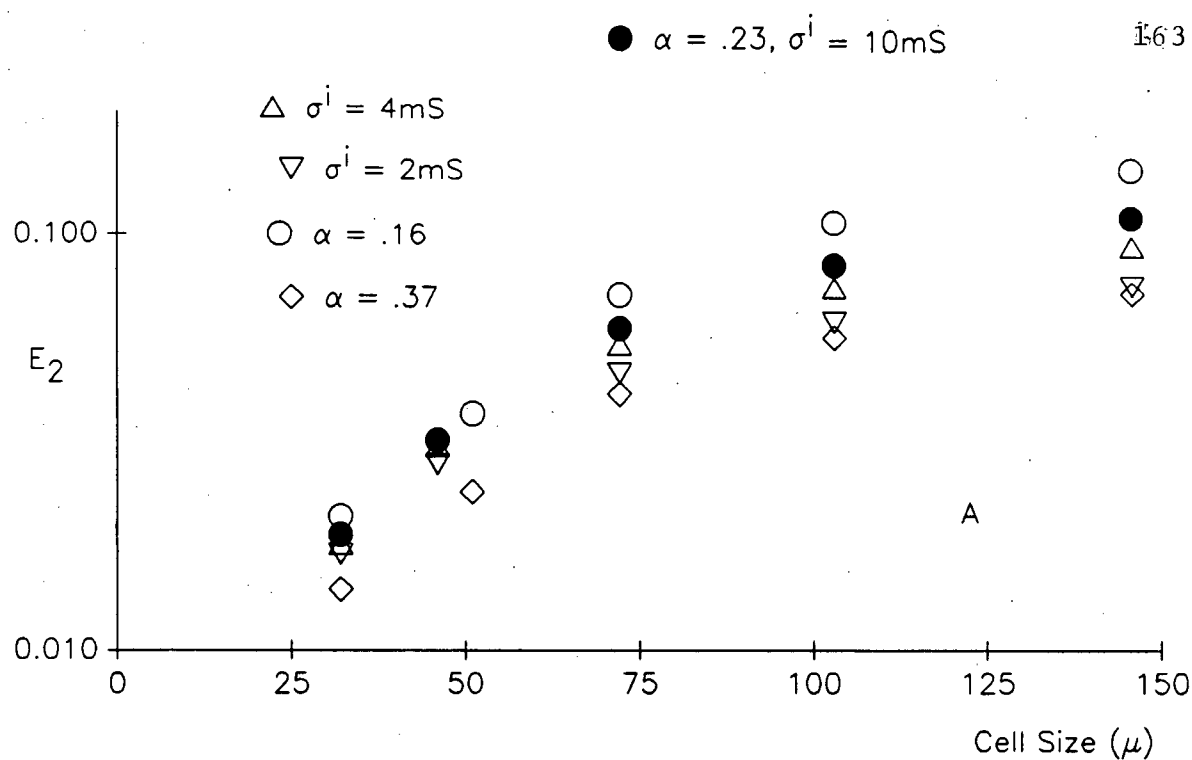
Figure 6.7 E_2 Coefficient and Model Structure

about 5 when the independent parameters vary by factors of 5 to 20) and are an increasing function of cell size.

The coefficient E_2 for the one-tier and two-tier models at various cell sizes is shown in Figure 6.7B. It is seen that this coefficient is considerably reduced in the two-tier model. The lower values of E_2 imply that spatial transport of potassium by means of flux terms proportional to V_0 is significantly reduced in this model. The relationship between transcellular conductance and E_2 was maintained in both models, (with ratio $\simeq$ 1.1). More precisely, the ratio of transcellular conductance to E_2 varies from approximately 1.2 ($l_1 = 32.5$ μm) to 1.0 ($l_1 = 146$ μm), for both (one- and two-tier) cases. This is important because transcellular conductance can be measured more easily than E_2, or E_1. Relationships like the one between D_2, E_1, and E_2 ($D_2 \simeq E_1 \simeq E_2$) are useful because this may reduce the number of measurements which are necessary in practice. The ratio of effective transcellular conductance to bulk conductivity, D_2/D_1, is the observed transport number in a current passing experiment (see Chapter VI). It is useful, to examine the relationships between D_2/D_1 and E_2 since these might provide further reductions in labour (cf. Gardner-Medwin, 1983b). A plot of E_2 versus D_2/D_1 is presented in Figure 6.8, using log axes. It is seen that there is a linear trend in this plot, but that the data from different parameter·studies lie on different lines.

APPENDIX IV.A. CONSISTENCY CHECKS ON THE COUPLED SOLUTION

Variation of mesh size was complicated by the fact that both intracellular and extracellular spaces had to remain in the same proportion at the new mesh size. For example if a solution was obtained on a 24 x 24 mesh with an

Figure 6.8. The coefficient E_2 versus bulk transport number D_2/D_1 is plotted for different cell sizes, values of σ^1, and a, for one- and two-tier models. Logarithmic horizontal and vertical axes are used in A. In B, points from the two-tier model are plotted together with points from a one-tier model using linear axes. It is seen that relationships between E_2 and transport number were approximately linear within the studies identified by the legend symbols. Unless indicated otherwise by the legend, $a=0.23$ and $\sigma^1=10$ mS.
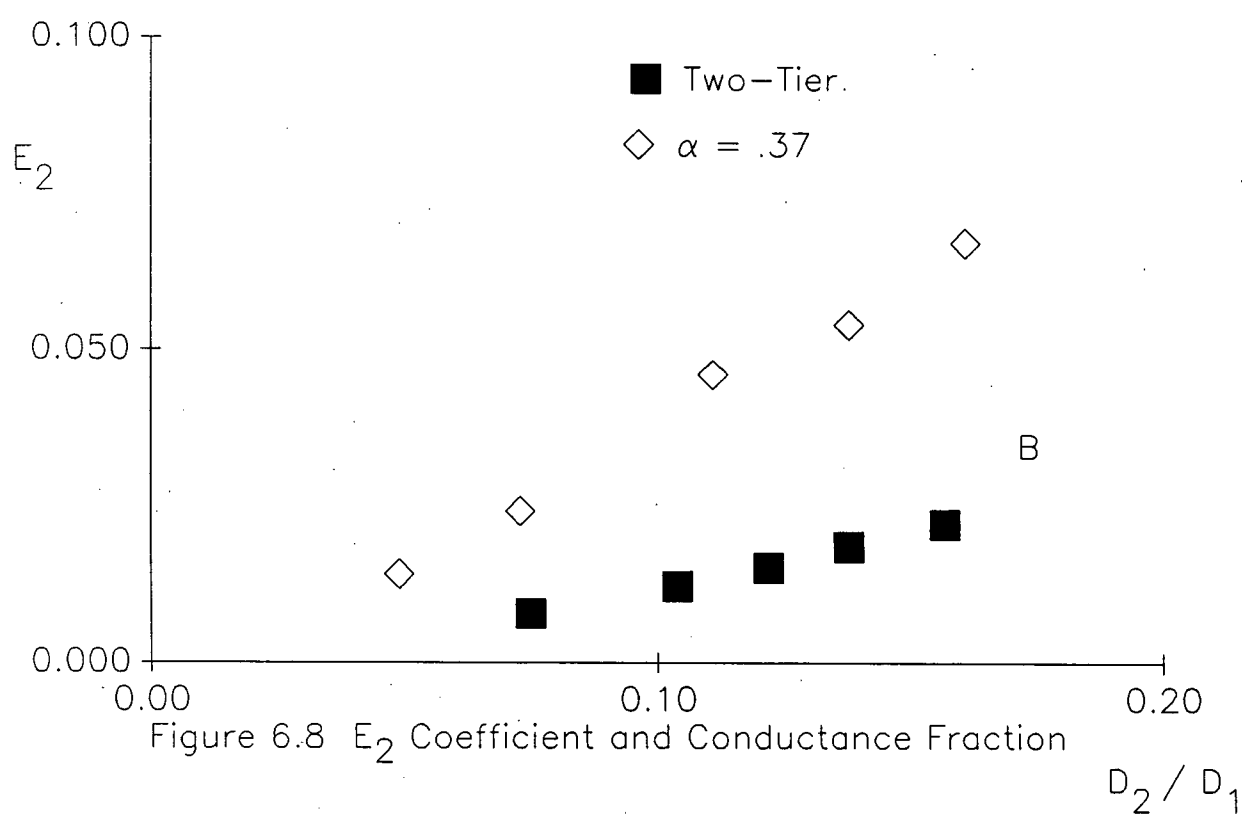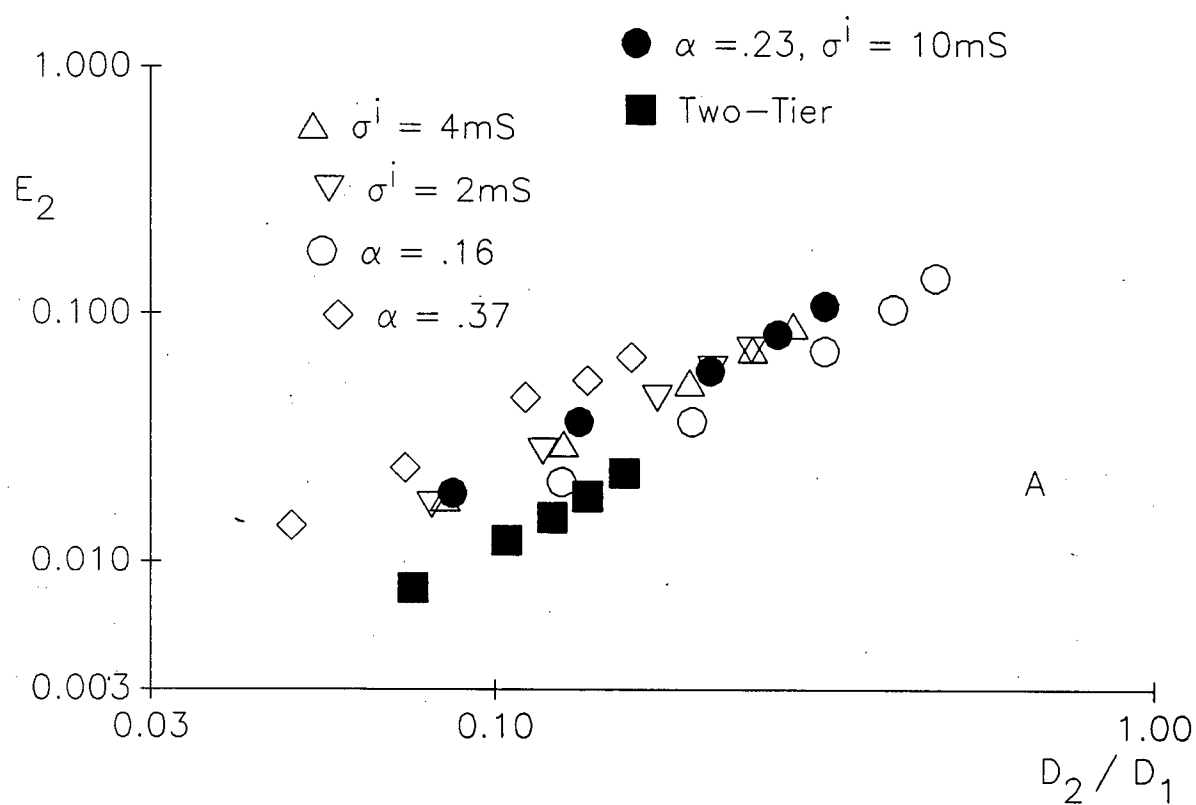
Figure 6.8 E_2 Coefficient and Conductance Fraction

intracellular dimension of $(22-3)h = 19h$ and an extracellular dimension of $3h =$ $(24 - (19 + 2))h$, the new mesh had to preserve intracellular proportions of $19/24$ and extracellular proportions of $3/24$ † so that the resulting numerical solutions would correspond to the same underlying cell shapes.

For this reason, such variation of mesh size was limited to the integer multiples of a smallest mesh size; 24 x 24 , 48 x 48, 72 x 72 and 96 x 96. The results suggested that all coefficient estimates except χ_c and κ_c were already accurate within 5% at the 48 x 48 size. While 72 x 72 results were obtained for most cases, it is clear, in retrospect, that the use of 48 x 48 solution results would have led to the same general conclusions as those drawn from the 72 x 72 results whenever both were available. In addition, 72 x 72 computations were necessary for extracellular space fractions < 0.2 in order to obtain a reasonable number of extracellular mesh points. Such studies did not compare the smaller and larger meshes, and were undertaken because the extracellular space may be reduced under some physiological conditions. The solution properties for the pairs (χ_p, κ_p), (χ_v, κ_v), are shown in Tables A.1 and A.2, for $a = .23$.

In the case of the coefficients χ_c and κ_c, however, it was necessary to use 96 x 96 results for the largest values of the membrane conductance in order to be sure that the finite difference solutions converged as mesh size h $->0$. At the three largest values of membrane conductance the coefficient derived from the 72 x 72 solution appeared accurate within 25, 10, and 5 %, respectively compared to the 96 x 96 results (column 3, Table A.3). More accurate solutions were not obtained because, in the absence of equally accurate

---

† This is an extracellular space of $1 - (21/24)^2 = 23\%$.

experimental data, this did not seem to be useful.

The properties of the solutions referred to in Tables A.1-A.3. are representative of the other cases. Table A.1 displays solution maxima and selected averages of the canonical solutions χ_p and κ_p. These solutions appear in the terms of ϕ_1 and C_{i1} proportional to $\nabla\phi_0$ in (III.2.12). The solution χ_p occurs in the definitions of D_1 and D_2 and κ_p occurs in the definition of D_2 in (III.2.18).

Table A.1.A. Maxima of χ_p and the Average $\sigma_0 M_W\{t_\sigma(1+ \nabla_w\chi_{p1})\}$.

$10^3\lambda^1$	48 x 48		72 x 72	
	Max	Average	Max	Average
20	4.28	.392	4.38	.386
10	4.45	.357	4.54	.355
5	4.61	.327	4.70	.327
2	4.80	.295	4.87	.296
1	4.88	.280	4.96	.280

Table A.1.B. Maxima of χ_p and the Average $\sigma_0 M_W\{t_K t_\sigma(1+ \nabla_w\chi_{p1})\}$.

$10^3\lambda^1$	48 x 48		72 x 72	
	Max	Average	Max	Average
20	4.28	.121	4.38	.116
10	4.45	.090	4.54	.088
5	4.61	.063	4.70	.063
2	4.80	.035	4.87	.036
1	4.88	.022	4.96	.022

Table A.1.C. Maxima of κ_p and the Average $\sigma_0 M_W \{t_K t_\sigma \nabla_w \kappa_{p1}\}$.

$10^3 \lambda^1$	48 x 48		72 x 72	
	Max	Average	Max	Average
20	3.54	.0034	3.62	.0062
10	3.28	.0064	3.32	.0075
5	2.88	.0059	2.92	.0063
2	2.14	.0036	2.18	.0037
1	1.51	.0022	1.55	.0022

Table A.2 displays solution maxima and selected averages of the canonical solutions χ_v and κ_v. These solutions appear in the terms of ϕ_1 and C_{i1} proportional to ∇V_0 in (III.2.12). The solution χ_v occurs in the definitions of E_1 and E_2 and κ_v occurs in the definition of E_2 in (III.2.18).

Table A.2.A. Maxima of χ_v and the Average $\sigma_0 M_W \{t_\sigma (t_\beta + \nabla_w \chi_{v1})\}$.

$10^3 \lambda^1$	48 x 48		72 x 72	
	Max	Average	Max	Average
20	4.36	.116	4.36	.111
10	4.51	.086	4.60	.084
5	4.66	.059	4.74	.059
2	4.81	.032	4.90	.032
1	4.89	.019	5.00	.019

Table A.2.B. Maxima of χ_v and the Average $\sigma_0 M_W\{t_K t_\sigma (t_\beta + \nabla_w \chi_{v1})\}$.

$10^3 \lambda^1$	48 x 48		72 x 72	
	Max	Average	Max	Average
20	4.36	.105	4.36	.100
10	4.51	.077	4.60	.076
5	4.66	.053	4.74	.053
2	4.81	.029	4.90	.029
1	4.89	.017	5.00	.017

Table A.2.C. Maxima of κ_v and the Average $\sigma_0 M_W\{t_K t_\sigma \; t_\beta \nabla_w \kappa_{v1}\}$.

$10^3 \lambda^1$	48 x 48		72 x 72	
	Max	Average	Max	Average
20	3.36	.0032	3.42	.0055
10	3.10	.0057	3.16	.0066
5	2.72	.0052	2.77	.0055
2	2.02	.0032	2.07	.0033
1	1.41	.0019	1.47	.0019

Table A.3 displays selected averages and solution maxima of the canonical solutions χ_c and κ_c. These solutions appear in the terms of ϕ_1 and C_{i1} proportional to ∇C_{i0} in (III.2.12). The solution χ_c occurs in the definitions of F_1 and F_2 and κ_c occurs in the definition of F_2 in (III.2.18). Results from a 96 x 96-grid-solution are included since these solution pairs converged slowly as the

mesh became finer.

Table A.3.A. The Average $\nu^{-1}\sigma_0 M_W\{t_\sigma \nabla_w \chi_{c1}\}$.

$10^3\lambda^1$	48 x 48	72 x 72	96 x 96
20	1.81	4.74	6.25
10	4.84	6.12	6.76
5	4.69	5.21	5.47
2	2.95	3.11	
1	1.77	1.83	

Table A.3.B. The Average $\nu^{-1}\sigma_0\{M_W\{t_K t_\sigma \nabla_w \chi_{c1}\}\}$.

$10^3\lambda^1$	48 x 48	72 x 72	96 x 96
20	1.58	4.15	5.48
10	4.23	5.36	5.94
5	4.11	4.58	4.81
2	2.59	2.73	
1	1.55	1.61	

Table A.3.C. The Average $\nu^{-1}\{M_W\{ (\theta C_{io} \nabla_w \kappa_{c1} + \theta)\}\}$.

$10^3\lambda^1$	48 x 48	72 x 72	96 x 96
20	4.70	4.56	4.45
10	4.35	4.16	4.05
5	3.86	3.70	3.61

2	3.28	3.20
1	2.99	2.94

Table A.3.D. Maxima of χ_c .

$10^3\lambda^1$	48 x 48	72 x 72	96 x 96
20	.219	.556	.721
10	.582	.714	.778
5	.564	.610	.631
2	.359	.367	
1	.217	.218	

Table A.3.E. Maxima of κ_c .

$10^3\lambda^1$	48 x 48	72 x 72	96 x 96
20	.756	1.93	2.52
10	3.40	4.20	4.59
5	5.93	6.45	6.71
2	8.62	8.89	
1	9.93	10.10	

The position of the maxima in the coefficients of Table A.3 at $10^3\lambda^1 = 10$ for the 48 x 48 solution, may be inaccurate since it becomes less pronounced on larger grids, however, the maximum occurs consistently at this value of λ^1 and is physically reasonable, as discussed in Section 6.3.

APPENDIX IV.B. UNCOUPLED BULK CONDUCTIVITY

Results of the uncoupled calculations for straight arrays of square cells (48 x 48 point solutions with an extracellular space of 19.7%) are shown in Figure B.1. The bulk conductivity versus cell sizes and intracellular conductivity are shown in Figure B.1.A, and the corresponding bulk transcellular conductance estimates in Figure B.1.B. The bulk conductivity estimates range from 2 - 7 mS over a large range of the membrane conductance, $l_1 = 10.3$ μ to $l_1 = 234$ μ, and are an increasing function of the cell size (membrane conductance). These values are consistent with conductivities observed for bulk cortex and cerebellum (Nicholson 1980). This agreement of the computed values with data occurs despite the fact that the model geometry is unrealistic. The bulk transcellular conductance was defined as:

(B.1) $$a_\beta := M_W \{ t_\beta (1 + \partial \chi / \partial W_1) \}$$

and corresponds to the proportion of bulk conductivity due to current flow through cells. The factors affecting this quantity are investigated here.

This bulk transcellular conductance ranges from 7% to 36% of bulk conductivity in the parameter range which is likely to correspond to glia (that is, cells with characteristic size from 32.5 μ -103 μ).

It is seen from Figure B.2 that the influence of intracellular conductivity σ^i was relatively slight, from small values of l_1 up to $l_1 = 51\mu$ and that bulk transcellular conductance was determined by the membrane conductance. Between $l_1 = 32.5$ μ and $l_1 = 103$ μ, which corresponds to a ten-fold change in λ, the transcellular conductance changed by a factor of eight, while the effect of a

Figure B.1. Bulk conductivity (A) and transcellular conductance (B) versus cell size are plotted for $\sigma^1 = 10$, 4 mS in the uncoupled model. A logarithmic vertical scale is used in B.
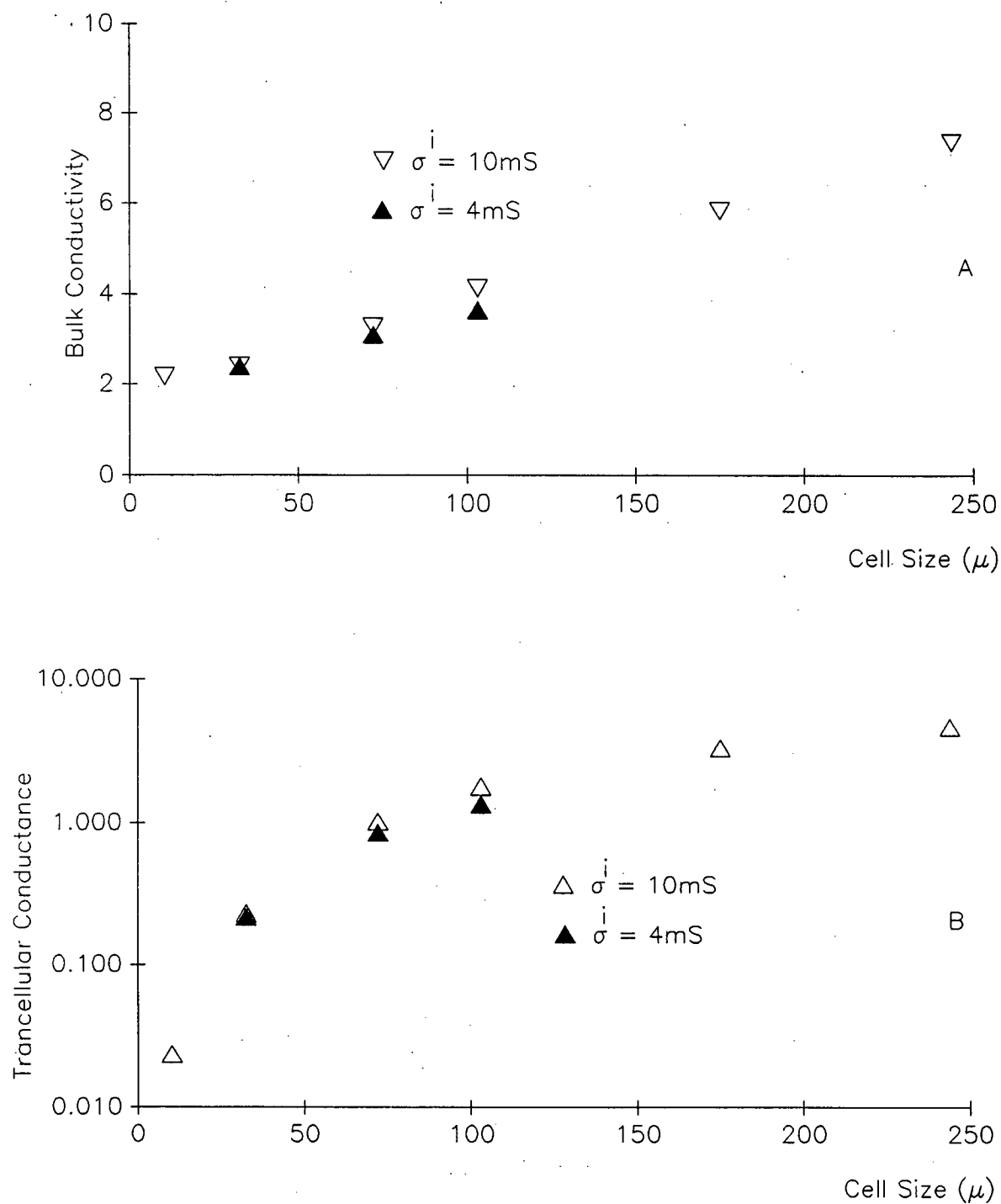
Figure B.1   Cell Size and Bulk Conductivity

Figure B.2. Bulk conductivity (A) and transcellular conductance (B) versus cell size over a large range ($l_1 \simeq 0.1$ μ to $\simeq 100$ μ) are plotted for $\sigma^1 = 10$, 4, 2 mS in the uncoupled model. Logarithmic horizontal axes are used in A and B, and a logarithmic vertical axis is used in B.
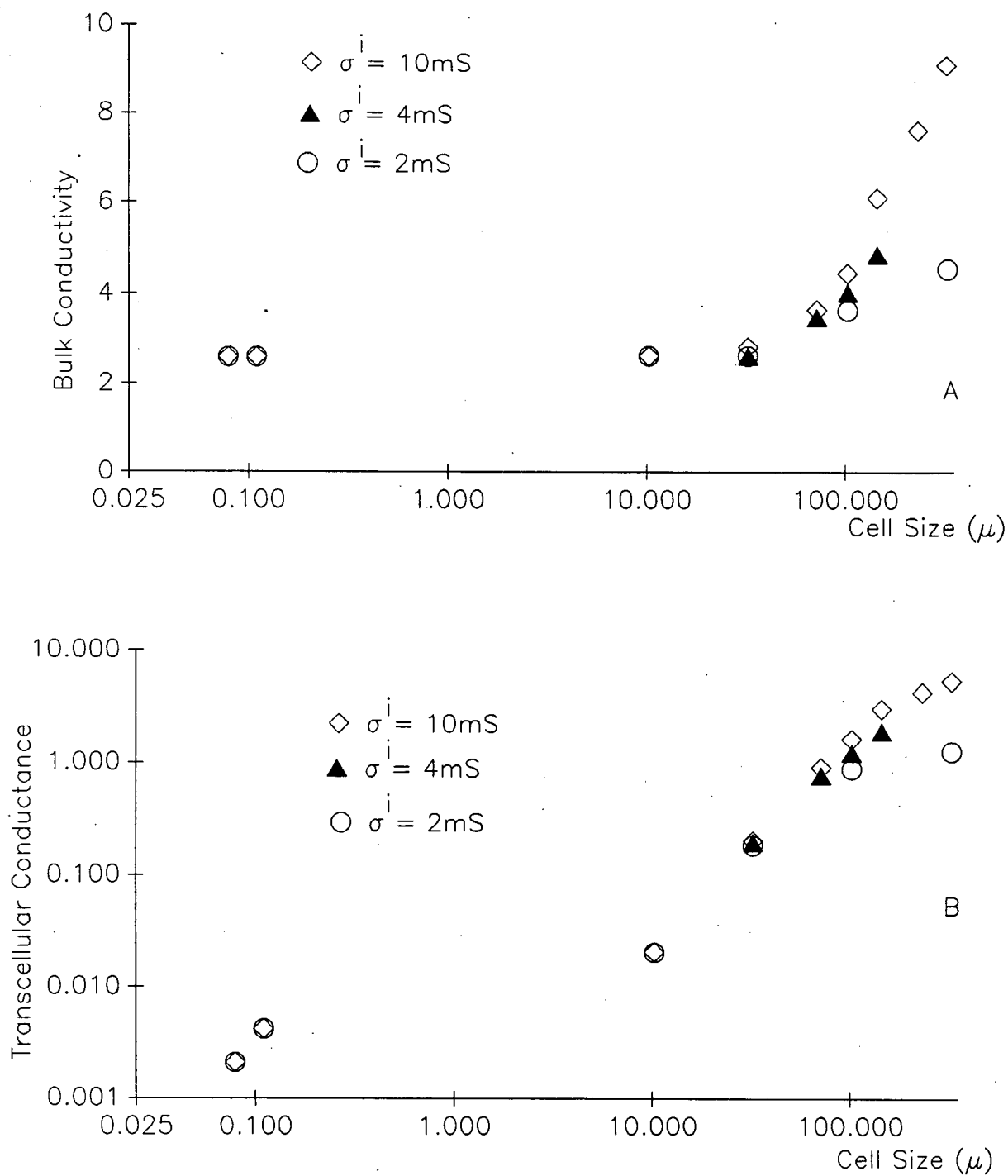
Figure B.2   Intracellular Conductivity and Bulk Conductivity

five-fold reduction in intracellular conductivity at $l_1 = 32.5$ μ is 10% and at $l_1 = 103$ μ; 54%. It is biologically significant that these model cells which exhibited bulk intracellular conductivities from 7 to 36% had electrical space constants which were long compared to the cell dimension, and thus were electrotonically unlike an electrical syncytium.

The derivation in Chapter III assumes that the tissue has a two-tier structure. Thus, it is assumed that a periodic array of asymptotically larger cells is imbedded in a periodic array of asymptotically smaller cells. The assumptions of such a model were illustrated schematically in Figure 6.3 and are described in Section 6.4.

Uncoupled conductivity estimates obtained in this way are shown in Figure B.3. If tier structure has no effect, the results (Δ) in Figure B.3 would be the same as the results for (O) except for the errors made in selecting the ECS fraction due to the discrete nature of the mesh and in selecting the extracellular conductivity. In fact the bulk conductivity estimates for $a = 0.44$ (two-tier model) are about 1.4 times the values obtained at $a = 0.23$ for a simple square cell. This is a significant but not large discrepancy, given the simplicity of the model.

On the other hand, the agreement between the transcellular conductance values is remarkable. It is seen that these values are close to those for the one-tier studies, suggesting that the dependence on tier structure is not critical in the uncoupled case.

In order to determine the effect of extracellular space (ECS) fraction on bulk parameters, numerical solutions were obtained for several values of the extracellular space fraction. First, the values of $a = 0.2$ and $a = 0.23$ were selected in order to establish the sensitivity of the solution to the ECS fraction near the

Figure B.3. Bulk conductivities (A) and transcellular conductance (B) versus cell size (l_1) are plotted for one-tier and two-tier uncoupled models. The one-tier model is indicated by open circles and the two-tier model by open triangles. The filled squares are the results obtained at the finest length scale, which are used to determine σ_0 in the two-tier study.
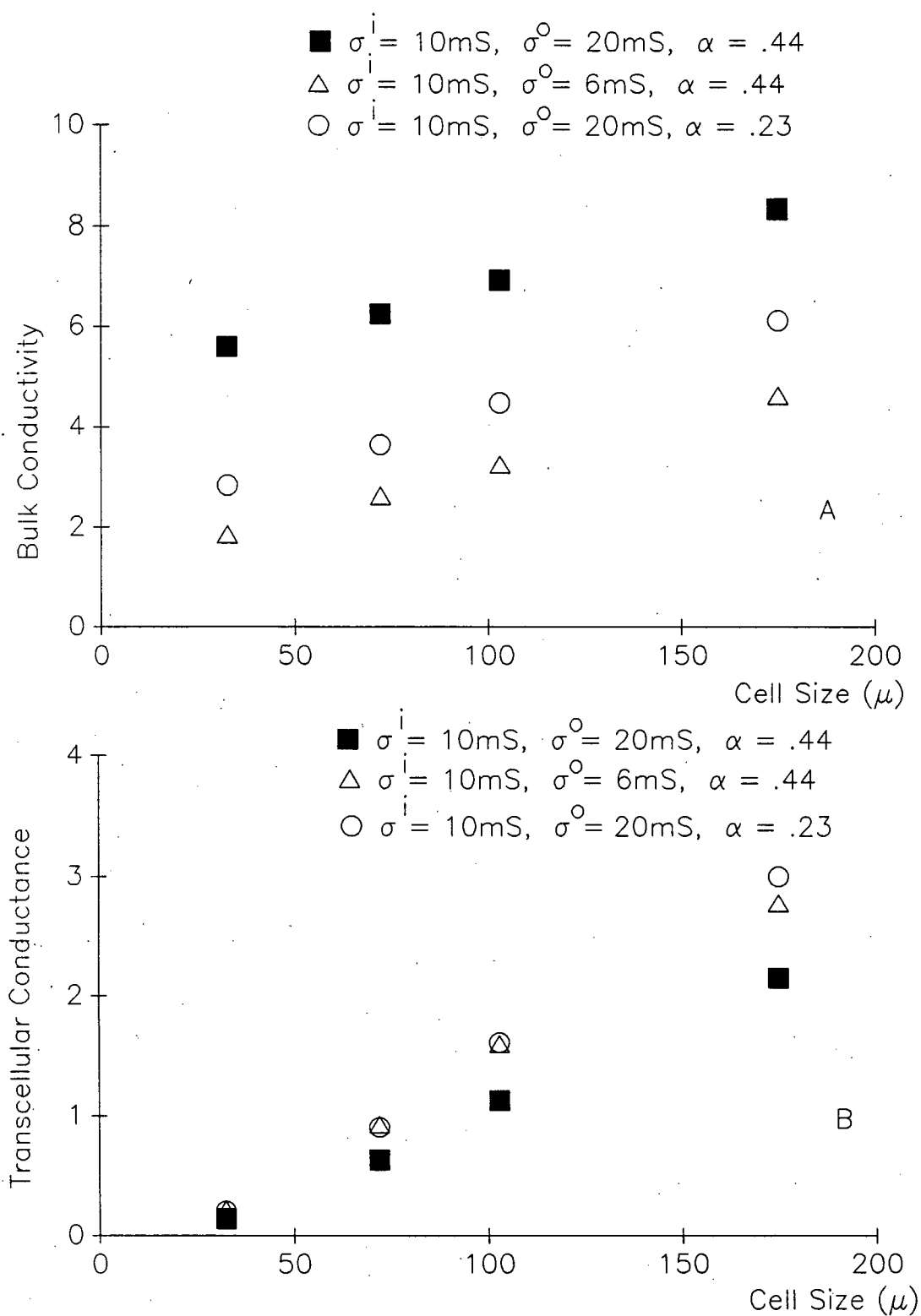
Figure B.3 A Two—Tier Conductance Study

normal physiological value. In addition solutions were obtained at $a=0.44$, and $a=0.12$. The bulk conductivity estimates for these ECS fractions are shown in Figure B.4.

The bulk conductivity is an increasing function of a while the transcellular conductance is a decreasing function of a. It is seen that the bulk conductivities are highly sensitive to the ECS fraction and increases by a factor between 2 and 6 between $a=0.12$ and $a=0.44$ for different characteristic cell lengths. Transcellular conductance increases by about 50% at $l_1=73$ μ, as a changes from $a=0.44$ to $a=0.12$, however the effect of a change in ECS fraction from $a=0.2$ to $a=0.12$ is not large. Thus, for situations in which the ECS fraction a is lowered, it is expected (all else being equal) that bulk conductivity will decrease and slightly more transcellular current will flow. This is biologically significant in situations in which the ECS fraction is decreased.

Because simple geometrical assumptions have been made, it is important to establish the sensitivity of the results to the geometrical arrangement of the cells.

The results of studies undertaken with staggered arrays are shown in Figure B.5 along with corresponding values for straight arrays. It is seen that while staggered arrays exhibit significantly lower bulk conductivity values, transcellular conductance remains stable from one type of array to the other, across a large range of membrane and intracellular conductivity values. In the biological parameter range it depends chiefly on characteristic size/membrane conductance.

Figure B.4. Bulk conductivities (A) and transcellular conductance (B) versus cell size (l_1) are plotted for $a = 0.12$, 0.2, 0.23, and 0.44 in the uncoupled model. A logarithmic vertical scale is used in B.
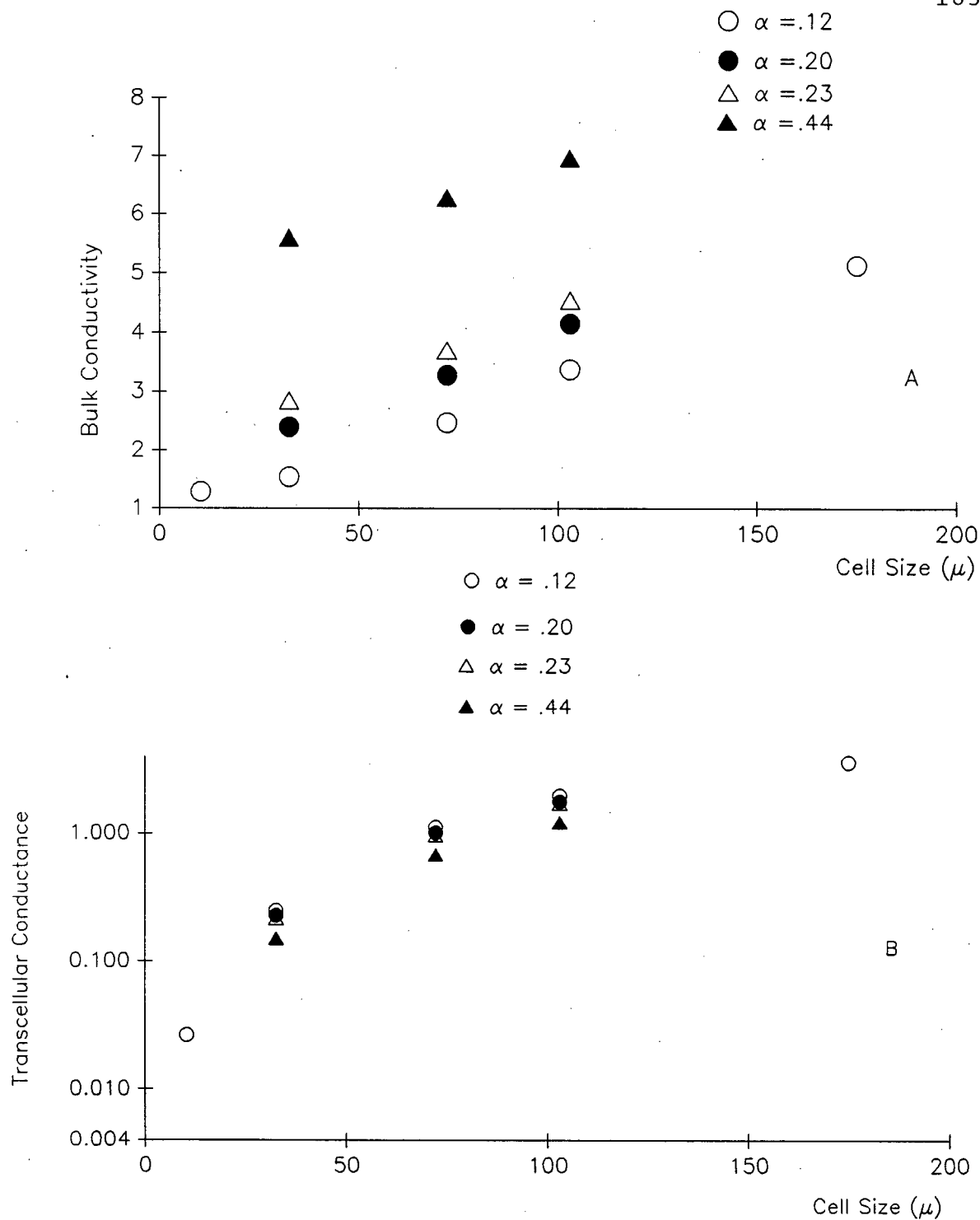
Figure B.4   Extracellular Space Fraction and Bulk Conductivity

Figure B.5. Bulk conductivities (A) and transcellular conductance (B) versus cell size (l_1) are plotted for each combination of a straight array, a staggered array, and $\sigma^1 = 10$ and 2 mS in the uncoupled model. A logarithmic vertical scale is used in B.
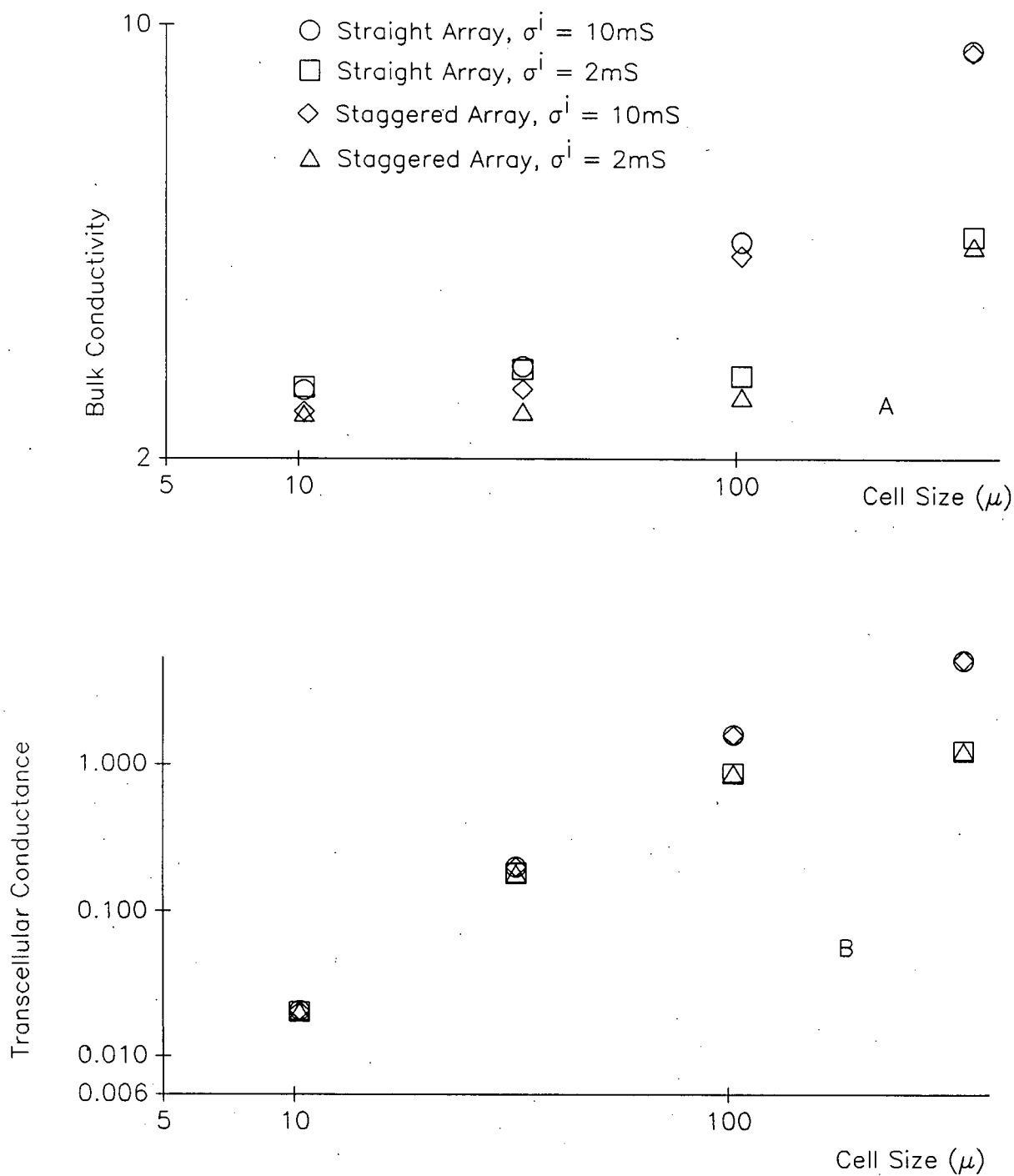
Figure B.5   Array Geometry and Bulk Conductivity

V. THE ROLE OF ELECTROTONIC PARAMETERS IN TISSUE MODELS

1.0. INTERPRETATION OF THE MODEL

1.1. Introduction

The tissue model used here has been chosen to be simple and easy to solve, and involves a number of assumptions which may seem unrealistic, such as a square geometry, and asymptotic assumptions about lengths and membrane properties of cell populations. Further analysis is required to see which aspects of our artificial tissue model would be expected to reflect observations of real tissue.

While numerical results are affected by these assumptions, dimensional analysis (Lin & Segel, 1965) predicts that the bulk physical properties of tissue depend on the dimensionless parameters formed from combinations of the characteristic physical parameters in the tissue, and we may hope to determine the nature of this dependence from the model. In fact the expansion procedure of Chapters II and III exploited the dependence of such properties on ratios of the characteristic cell lengths. However, the dependence of bulk properties on dimensionless parameters associated with conductance properties of the cell has not been discussed. Dimensionless parameters formed by combining the characteristic conductance properties of the cell are called electrotonic parameters. An asymptotic analysis in these parameters gives information about the correspondence between the asymptotic model and real tissue, the dependence of transcellular current on geometry, and provides analytic confirmation of the main features of the numerical solutions.

Comparison of the results of Sections IV.6.2 and IV.6.3 with Appendix

IV.B demonstrate numerically that the averages of the coupled and uncoupled models yield averages which have similar dependence on electrotonic parameters. Thus, it is assumed that an analysis of the uncoupled case is sufficient to obtain the qualitative features of this dependence. The asymptotic analyses to be carried out in Sections 2.2 and 2.3 assume in addition, that the intracellular conductivity is less than the extracellular conductivity and that the membrane conductance is either large or small. The two-tier studies of Section IV.6.4 do not satisfy these assumptions since the extracellular conductivity is less than the intracellular conductivity. The analyses of this chapter do not apply to the two-tier case, however, as seen in Appendix IV.B, the conclusions would remain correct if there were no coupling between electrical potential and ionic concentration at $O(\epsilon)$.

Because this chapter focuses on the physical interpretation of the model, we give a physical interpretation of transcellular flux before proceeding with a perturbation analysis of the relationship between transcellular flux and electrotonic parameters. In the light of this discussion, it is seen that the averaged parameters of Chapters II and III are not uniquely determined unless (as stated in Chapter II) specific assumptions are made concerning the asymptotic properties of electrotonic parameters. In Section 3.0, a conclusion is drawn concerning the relative contribution of cells of different sizes to transcellular current.

1.2. Formal Analogy Between Intracellular Flux and Electrostatic Polarization

As described in Section IV.1.2, the electrical flux component of the potassium flux vector ($i=2$ in equation (IV.1.2)) is discontinuous because of the

differences in extracellular and intracellular transport properties. Potassium disappears from the ECS at one location and reappears at another remote location with little time delay. This complicates the interpretation (though not the derivation) of differential equations for the average electrical flux of potassium. This problem of physical interpretation is not new, however, and occurs in a classical model of dielectric polarization (Landau & Lifshitz, 1960; Garland & Tanner, 1978). This analogy is demonstrated and it is suggested that the reader view bulk electrically mediated transport through inclusions as analogous to the existence of bulk polarization in an (inhomogeneous) dielectric medium.

Let the flux strength of some quantity (such as potassium) at the cell membranes be $f(\vec{w}) = \nabla\psi \cdot \vec{n}$ where ψ is a potential function, $\vec{n}$ denotes the outward unit normal to the membrane and $f(\vec{w})$ is doubly periodic. The quantity $\int_M \vec{w} f(\vec{w}) dS$ will be referred to as the flux dipole moment of f. Although the flux dipole moment of each cell is small, their sum may produce a bulk flux dipole moment which is significant. If the function $f(\vec{w})$ were the density of electrical charge, the integral $\int_M \vec{w} f(\vec{w}) dS$ over a single cell would be the electrical dipole moment of the charge distribution over a single cell.

The bulk flux dipole moment is a vectorial quantity which reflects the intracellular flux through cells. If f represents transmembrane ionic flux, then the bulk flux dipole moment represents the intracellular ionic transport owing to the presence of the cells. Under certain circumstances it is equal to the average of the ionic flux vector intracellularly.

If the intracellular potassium flux is equal to $\nabla\psi$, and $\nabla^2\psi = 0$ then the bulk flux dipole moment associated with the flux distribution $f(\vec{w})$ is numerically equal to the integral of the interior flux through all the cells. This follows by

applying the divergence theorem to the components of the vector $\nabla \cdot (W_i \nabla \psi)$ where W_i denotes the ith component of $\vec{w}$:

$$(1.1) \qquad \int_{ICS} \nabla \psi dA = \int_{ICS} (\nabla \cdot (w_1 \nabla \psi), \nabla \cdot (w_2 \nabla \psi)) dA = \int_M \vec{w} \frac{\partial \psi}{\partial n} dl.$$

The intracellular flux mentioned is a virtual flux, rather than a real flux because $\nabla^2 \psi \neq 0$ at the membrane. However, the flux dipole moment still equals the integrated intracellular flux in our model because the flux dipole moment is additive over regions in space.

This definition is primarily of theoretical interest (experimental measurement of bulk coefficients is discussed in Chapter VI) in providing a physical interpretation of the formal averaged coefficients. If spatial buffer capacity is defined as the average potassium flux associated with a unit voltage gradient in the transmembrane potential, then the bulk flux dipole moment per unit voltage gradient is proportional to the spatial buffer capacity of an array of cells. This may be verified by reference to the averaged equations (III.2.17) in which the coefficient of $\nabla^2 V$ corresponds to a bulk flux dipole moment.

2.0. ASYMPTOTICS IN THE ELECTROTONIC PARAMETERS

2.1. Correspondence with Canonical Problem

In the calculations of Chapters II and III (see Table II.2.4) we defined $\tilde{g}$:= $Lg / \bar{S}$ where $g := g_2$ (S cm^{-1}) is the dimensional (two-dimensional) value of the membrane conductance to K^+, L is an appropriate length scale, and $\bar{S}$ depends on the extracellular conductivity and diffusion coefficients. The quantity

$(g/\overline{S})^{-1}$, which has the dimension of cm, is an electrotonic length scale arising from the electrical parameters only.

In this section we let $\vec{w} = \vec{x}/L_1$ and $\widetilde{g} = L_1 g/\overline{S}$ (these do not correspond to definitions in Chapter III). This is done to make fluxes of the form $g(\phi^i - \phi^0)$ and $\partial \phi/\partial n$ of $O(1)$ rather than $O(\epsilon^{-1})$ in the analyses of this Section and Sections 2.2-2.3. The tilde in $\widetilde{g}$ is dropped in the calculations which follow.

The canonical $O(\epsilon)$ problems (Chapter III) which determine average properties for conductivity, diffusion, and potassium transport consist of solving the potential equation with periodic boundary conditions and constant (intracellular and extracellular) conductivities. We now calculate the qualitative dependence of the solutions and the flux dipole moments on the electrotonic parameters.

In the calculation which follows we consider the two-dimensional problems

$$(2.1) \qquad \nabla \cdot (\sigma \nabla \phi) = 0,$$

where σ is the electrolyte conductivity, ϕ is the electrical potential and (2.1) holds extracellularly and intracellularly. The jump condition at the cell membrane is

$$(2.2) \qquad \sigma \frac{\partial \phi}{\partial n} = g(\phi^i - \phi^0),$$

which actually is two equations, with $\sigma \partial \phi/\partial n$ evaluated intracellularly and extracellularly, $\vec{n}$ is an outward normal vector, g is membrane conductance, and $\phi^i - \phi^0$ is the transmembrane potential. Boundary conditions are given as $\phi = A$ on

one edge of the unit cell (say x_1=constant), ϕ=B on the opposite edge, and $\partial\phi/\partial n$ =0 on the remaining edges of the crystallographic unit cell.

The latter problem is equivalent to a typical canonical problem from (III.2.12) - (III.2.16) because the solution of (2.1) - (2.2) with the conditions described has the form $\phi= Aw_1 + \chi^1$ where w_1 is a spatial coordinate and χ^1 satisfies

$$(2.3) \qquad \nabla\cdot(\sigma\nabla\chi^1) = 0,$$

with periodic boundary conditions and jump conditions at the membrane given by

$$(2.4) \qquad \sigma\{\nabla\chi^1\cdot\vec{n} + n_1\} = g\{\chi^{1i}-\chi^{1o}\}$$

where n_1 is the first component of $\vec{n}$, the outward unit normal vector, and χ^1 and χ^2 in $\vec{\chi}$ are analogous in form because the biological cells are assumed to be square. Note that χ=constant does not satisfy the jump condition (2.4) which is non-homogeneous. By geometric symmetry, ϕ must agree with the previously stated conditions (2.1) - (2.2). Thus, because of the symmetry, the canonical problem for χ may be replaced by a problem with fixed rather than periodic boundary conditions and a fixed ambient voltage gradient.

2.2. Electrotonically Short Case and Transmembrane Transport

We define the new parameters $\gamma:= \sigma^i(\sigma^0 + \sigma^i)^{-1}$ where σ^0 and σ^i are the extracellular and intracellular conductivities, respectively, $\lambda:=\sigma^i g^{-1}$ (cm) where g is the membrane conductance, and $\xi:= L_1/\lambda$ where L_1 is the unit cell

length.

The asymptotic dependence of ϕ on γ and ξ now is calculated for the unit cell. In view of the equivalence described in Section 2.1, this calculation should give qualitative information on the effects of these parameters on bulk properties. Because the potential equation is unaffected by length scaling, and boundary and jump conditions will be satisfied uniformly as the dimensionless conductivity $\gamma \rightarrow 0$ and electrotonic length parameter $\xi \rightarrow 0$ or ∞, it is expected that the expansion in γ and ξ will be regular.

Rewriting the jump conditions (2.2) using the definitions of γ, ξ, and λ and scaling $\vec{w} = \vec{x} / L_1$, as in Chapter II, gives the equations:

$$(2.5) \qquad (i) \quad \frac{\gamma}{1-\gamma} \frac{\partial \phi^i}{\partial n} = \frac{\partial \phi^i}{\partial n}, \qquad (ii) \quad \phi^i - \phi^0 = \xi^{-1} \frac{\partial \phi^i}{\partial n} = \frac{\partial \phi^i}{\partial n},$$

where (2.5i) arises from combining intracellular and extracellular jump conditions. It is assumed that ϕ may be expanded in the form:

$$(2.6) \qquad \phi = \phi_0 + \xi^{\pm 1} \phi_{01} + \gamma \phi_{10} + O(\xi^{\pm 2}) + O(\gamma^{\pm 2}) + \dots$$

where $+$ and $-$ correspond to $\xi \rightarrow 0$ and $\xi \rightarrow \infty$, respectively, and we will write ϕ_0 for ϕ_{00}. Since the boundary conditions on the unit cell have no ξ or γ dependence, $\phi_{ij}^0 = 0$ on the boundary of the unit cell when i or j > 0.

The leading-order behavior of ϕ will be deduced from the dependence of the jump conditions on γ and ξ. In this section we assume $\xi \rightarrow 0$, i.e., the ratio of cell length to the electrical length scale λ is small, and so the '+' sign is used in (2.6).

Using (2.6) in the jump conditions (2.5) yields:

$$(2.7) \qquad \frac{\gamma}{1-\gamma}\left(\frac{\partial \phi^i_0}{\partial n} + \gamma\frac{\partial \phi^i_{10}}{\partial n} + \xi\frac{\partial \phi^i_{01}}{\partial n} + \ldots\right)$$

$$(2.8) \qquad \begin{aligned} \xi(\phi^i_0 + \gamma\phi^i_{10} + \xi\phi^i_{01} + \ldots &- \phi^0_0 - \gamma\phi^0_{10} - \xi\phi^0_{01} - \ldots) \\ = \frac{\partial \phi^i_0}{\partial n} + \gamma\frac{\partial \phi^i_{10}}{\partial n} &+ \xi\frac{\partial \phi^i_{01}}{\partial n} + \ldots, \end{aligned}$$

Thus, to $O(1)$:

$$(2.9) \qquad (i) \quad \frac{\partial \phi^0_0}{\partial n} = 0, \qquad\qquad (ii) \quad \frac{\partial \phi^i_0}{\partial n} = 0.$$

Since (2.1) holds, the leading-order intracellular solution, ϕ^i_0 is constant and the extracellular solution, ϕ^0_0 is determined and non-constant. Because $\nabla^2 \phi^0_0 = 0$ away from the membrane, the boundary conditions $\partial \phi^0_0 / \partial n = 0$ and $\phi^0_0 = $ const $= \phi^i_0$ would imply ϕ^0_0 identically constant by a standard expansion procedure from the theory of partial differential equations (Carrier & Pearson, 1978). Since ϕ^0_0 is not identically constant, $\phi^i_0 - \phi^0_0$ is not identically constant on the membrane.

To $O(\gamma)$:

$$(2.10) \qquad (i) \quad \frac{\partial \phi^i_0}{\partial n} = \frac{\partial \phi^0_{10}}{\partial n}, \qquad\qquad (ii) \quad \frac{\partial \phi^i_{10}}{\partial n} = 0.$$

The left side of (2.10i) vanishes by (2.9ii). Thus, by (2.10ii) ϕ^i_{10} is constant

while $\phi_{10}^0 = 0$ because the boundary conditions have no γ dependence on the unit cell.

To $O(\xi)$:

(2.11)   (i) $\dfrac{\partial \phi_{01}^0}{\partial n} = 0$,   (ii) $\phi_0^i - \phi_0^0 = \dfrac{\partial \phi_{01}^i}{\partial n}$

As in the case of ϕ_{10}, $\phi_{01}^0 = 0$ because the boundary conditions on the unit cell have no ξ dependence.

Since the transmembrane potential is $O(1)$, the transmembrane current to leading-order is $i_m = g(\phi_0^i - \phi_0^0)$. In order to obtain a steady state solution at $O(\xi)$, the constant ϕ_0^i must be chosen so that the average transmembrane current is zero.

The flux dipole moment in this case may be estimated by assuming that ϕ_0^0, the extracellular potential (which satisfies $\partial \phi_0^0 / \partial n = 0$ at the membrane), is a linear function of the space variable. References to the discussion of (2.3) - (2.4) and the numerical solutions show that ϕ_0^0 will have a voltage variation over the membrane which is greater than that which occurs if ϕ_0^0 were linear. Since χ is bounded, however, the voltage variation over the membrane locus will have the same asymptotic order as for the case of linear extracellular potential. The assumption of linearity has been used in models for conductivity of brain tissue and produced good agreement with data (e.g., Ranck, 1963).

It has been assumed that the cell is square. The discussion of equations (2.5) - (2.11), with the assumption of linear extracellular potential implies that to leading order, the transmembrane current is a linear function of x_1'. The transmembrane current per unit extracellular voltage drop over the unit cell is

given by $i_m = g \, x_1/L_1$ (Amp/Vcm) where we use the dimensional value of g $(S \, cm^{-1})$. Thus, the first component of flux dipole moment vector (1.1) per unit voltage gradient is:

$$\int_M x_1 \, i_m \, dl = 2 \int_{-fL_1/2}^{fL_1/2} x_1 g \frac{x_1}{L_1} \, dx_1 + 2 \int_{-fL_1/2}^{fL_1/2} \frac{fL_1}{2} \frac{gf}{2} dx_2$$

$$(2.12) \qquad = \frac{2}{3} gf^3 L_1^2 \, , \qquad (cm\Omega^{-1})$$

where f is the cell length as a proportion of the unit cell length, dl is the differential line element on the membrane in two dimensions, and the second term comes from integrating over the ends of the cell. The second component of flux dipole moment is zero because the integrand is odd. Thus, the quantity (2.12) is proportional to the membrane conductance and the square of the cell length. This result could not be obtained from dimensional analysis alone since (as will be shown in Section 2.3) the flux dipole moment can have other forms. The dependence of the numerical solutions on g shows that this asymptotic case corresponds more nearly to the biological situation. By the previously demonstrated equivalence between flux dipole moment and virtual intracellular flux (as explained in Section 1.2), it is seen that (2.12) is the (approximate) total transcellular current flow per unit voltage gradient per unit cell. It may be interpreted as a transcellular conductance. As the units of a voltage gradient are $V \, cm^{-1}$, the product of the quantity (2.12) with a voltage gradient has units of amperes.

2.3. Electrotonically Long Case and Transmembrane Transport

In the electrotonically long case, $\xi^{-1} \to 0$ and the '−' sign is selected in the expansion form (2.6). The boundary conditions (2.5) become, on substitution of the expansion (2.6):

$$(2.13) \qquad \frac{\gamma}{1-\gamma}\left(\frac{\partial \phi_0^i}{\partial n} + \gamma \frac{\partial \phi_{10}^i}{\partial n} + \xi^{-1}\frac{\partial \phi_{01}^i}{\partial n} + ...\right)$$

$$\phi_0^i + \gamma \phi_{10}^i + \xi^{-1}\phi_{01}^i + ... - \phi_0^o - \gamma \phi_{10}^o - \xi^{-1}\phi_{01}^o - ...$$

$$(2.14) \qquad = \xi^{-1}\left(\frac{\partial \phi_0^i}{\partial n} + \gamma \frac{\partial \phi_{10}^i}{\partial n} + \xi^{-1}\frac{\partial \phi_{01}^i}{\partial n} + ...\right).$$

Thus to $O(1)$:

$$(2.15) \qquad \text{(i)} \quad \frac{\partial \phi_0^o}{\partial n} = 0, \qquad\qquad \text{(ii)} \quad \phi_0^i - \phi_0^o = 0.$$

The extracellular solution is the same as in the short case, and the intracellular solution is determined from it via (2.15ii). Hence $\partial \phi_0^i / \partial n \neq 0$, because $\phi_0^i = \phi_0^o$ and ϕ_0^o is non-constant at the membrane by the same argument as that in Section 2.2 following equation (2.9).

To $O(\gamma)$:

$$(2.16) \qquad \text{(i)} \quad \frac{\partial \phi_0^i}{\partial n} = \frac{\partial \phi_{10}^o}{\partial n}, \qquad\qquad \text{(ii)} \quad \phi_{10}^i - \phi_{10}^o = 0,$$

while to $O(\xi^{-1})$:

(2.17)   (i) $\dfrac{\partial \phi_{01}^{0}}{\partial n} = 0,$ (ii) $\phi_{01}^{i} - \phi_{01}^{0} = \dfrac{\partial \phi_{0}^{i}}{\partial n}.$

Since $\phi_{0}^{0} = \phi_{0}^{i}$, $\phi_{10}^{0} = \phi_{10}^{i}$, and $\partial \phi_{0}^{i}/\partial n \neq 0$, the leading-order transmembrane potential is given by (2.17ii).

The previous discussion (2.13) - (2.17) has established the leading-order form of the transmembrane current. The flux dipole moment vector is approximated using the same assumptions as before: ϕ_{0}^{0} is assumed linear and the cell is square. The transmembrane current per unit voltage gradient (Amp / V cm) is $i_{m} = g\xi^{-1}(\phi_{01}^{i} - \phi_{01}^{0}) = \sigma^{i}L_{1}^{-1}\,\partial\phi_{0}^{i}/\partial n = \sigma^{i}/L_{1}$ on the membrane locus where $x_{1} =$ constant and is zero on the membrane locus where $x_{2} =$ constant, assuming that ϕ_{0}^{0} is linear in the x_{1} direction and $\phi_{0}^{0} = \phi_{0}^{i}$ at the membrane. Hence, the first component of the flux dipole moment vector per unit voltage gradient may be computed as:

(2.18) $\displaystyle\int_{M} x_{1}\, i_{m}\, dl = 2 \int_{-fL_{1}/2}^{fL_{1}/2} \frac{fL_{1}}{2}\, \frac{\sigma^{i}}{L_{1}}\, dx_{2} = \sigma^{i}f^{2}L_{1} \,,$

$(cm\Omega^{-1}).$

The second component of the flux dipole moment is zero by symmetry.

These calculations give an approximation to the total intracellular current per unit voltage gradient per unit cell when ξ is large, i.e., physical cell length is large compared to the electrotonic length scale. This would be true for a syncytium, or network of electrically connected cells.

The asymptotic calculations were undertaken in order to determine which

properties of the numerical solutions are likely to characterise real tissue. The bulk properties of tissue are expected to depend on both electrotonic parameters and shape-dependent geometric parameters which are $O(1)$.

The asymptotic analyses give the dependence of the flux dipole moment on the electrotonic parameters, ξ and γ, for extreme values of these parameters. These analyses do not indicate quantitatively how large or small such parameters must be in order for this description to be accurate. Also, because of the assumption that ϕ^0 is linear, this description does not take into account the effect of the square cell geometry on ϕ^0. However, in the electrotonically short case, (which is biologically relevant) the intracellular solution is constant and hence independent of geometry.† Thus, in this case, the difference between the two-dimensional and three-dimensional results is a geometrical factor, independent of the solution for ϕ. Because of the assumption of linearity of ϕ^0, dependence of the flux dipole moment estimate on the geometry is due only to the fact that the membrane locus appears in the integral. Since the numerical solution indicates that the analysis of the short case is accurate for this geometry, the numerical results in two dimensions should be applicable to three dimensions in the manner described.

In view of the complexity of the three-dimensional geometry of neural tissue, the selection of a square two-dimensional geometry is a drastic simplification. For example, neural tissue contains much fine structure and relatively complex shapes. Yet, in many respects, reasonable agreement with experiments was obtained. This likely occurs for the following reasons. First, geometry may be unimportant in the electrotonically short case, as suggested

---

† A similar remark holds in the electrotonically long case.

above. Second, the qualitative features of the two-tier calculation of Chapter III show that there is no significant transcellular current when cell dimensions are sufficiently fine, if physical membrane properties of fine structures are the same as those of coarse structures.

Other successful models have assumed (Ranck, 1963; Havstad, 1976) that because the tissue contains elements with random orientations, the electrical properties of neural tissue may be modelled by superposition of the properties of arrays of cylinders which are, perpendicular and parallel respectively, to the ambient gradients. This assumption will not be discussed in detail here, but we have followed these authors in using a geometrically simple model of the tissue. The length scales suggested for cells here (32 μm - 72 μm) are characteristic of the longitudinal dimensions of cell processes. Cylinders oriented perpendicular to ambient gradients would have small effective size and would not contribute much to bulk transcellular current.

These calculations show that the parameter ξ, which depends on the cell length, determines the nature of the solution for the potential. Because the cell length formally depends on ϵ, the asymptotic order of this ratio ξ must be chosen in order to complete the formal asymptotic model.

2.4. Choice of Scaling

In the canonical problems of Chapter III, the dimensionless parameter g appears at different orders of ϵ in the jump conditions. The reasoning used in selecting appropriate asymptotic assumptions for g is now discussed.

A fundamental assumption of dimensional analysis asserts that any bulk coefficient P of an inhomogeneous medium will be some function of the

dimensionless parameters which characterize the medium multiplied by a dimensional constant K,

(2.19) $P = K \; \tilde{P}(\epsilon, \; a, \; \beta, \; ... \;)$

where $\tilde{P}$ is to be determined from a canonical boundary-value-problem, and the selection of dimensionless parameters is not unique. An approximation for $\tilde{P}$ is to be found by taking a limit as $\epsilon \longrightarrow 0$.

In some possible selections of dimensionless parameters ϵ, a', β', ... , the parameters a', β', ... may depend on ϵ. For example, g may depend on ϵ. Surprisingly, the dependence of g on ϵ does not follow from the definition and must be chosen in the asymptotic model.† The definition $\tilde{g} = L_0 g / \overline{S}$ is not an explicit function of $\epsilon = L_1 / L_0$ and it is not possible, in general, to pose the canonical boundary-value-problem for $\tilde{P}$ in a form which does not involve g (dropping the tilde).

The dependence of g on ϵ may be chosen as follows. In the physical tissue, the parameters ϵ and ξ take definite values and an approximation to P evaluated at these parameters is desired. While the asymptotic approximation is formed from the limit $\epsilon \longrightarrow 0$, so that ϵ is not fixed, it is reasonable to suppose that the best approximation to P is obtained by keeping the parameter(s) ξ, fixed at the values which characterise the tissue. This is equivalent to fixing $L_i g$ where L_i is the (dimensionless) cell length. Using this principle, the order of g may be determined from the physical properties of the cells.

---

† It has been previously observed that the homogenization procedure (letting $\epsilon \longrightarrow 0$) may not produce a unique answer, without choices of the general type described here (cf. Babuska, 1976).

For example, we compare the case of small cells and moderate measurement length, for which $L_1 = O(\epsilon)$ and $L_0 = O(1)$, and the case of cells of moderate length and a large expanse of tissue, for which $L_1 = O(1)$ and $L_0 = O(\epsilon^{-1})$. Both situations result in $L_1 / L_0 = O(\epsilon)$. Suppose that the shapes and relative placement of the biological cells in crystallographic unit cells are geometrically similar. In order to keep ξ fixed, g must be $O(\epsilon^{-1})$ in the first case and $O(1)$ in the second. These assumptions correspond to different dimensional values of g, i.e., different physical membrane properties. Such assumptions would lead to canonical boundary-value-problems which are identical, and thus lead to the same bulk coefficients. In contrast, keeping the dimensional g value fixed across the two cases, would lead to g appearing at $O(\epsilon)$ and $O(1)$ respectively, and produce different bulk coefficients for each case. Both sets of assumptions are mathematically consistent, but correspond to the different physical models described.

When two electrotonic and two asymptotic length scales exist as described in Chapter II, this rule can still be used, though it will not be possible to fix all dimensionless parameters other than ϵ. If there are two cell lengths, L_g and L_n, and two sets of membrane conductances, g_g and g_n, then the dimensionless membrane conductances are $\tilde{g}_g = L_g g_g / \overline{S}$ and $\tilde{g}_n = L_n g_n / \overline{S}$. If it is assumed that L_g, L_n, g_g, and g_n are such that $L_g = O(\epsilon)$, $L_n = O(1)$ $g_g = O(\epsilon^{-1})$, and $g_n = O(1)$, then the electrotonic parameters ξ of each population are fixed but the quantity $L_g g_n = O(\epsilon)$ is not fixed as $\epsilon \longrightarrow 0$.

3.0. Neurons, Glia and Electrical Scale

Neurons comprise some 50% of the tissue volume in the brain, yet several recent models of the electrical properties of neural tissue have neglected current flow through neurons because of their high membrane resistance (Nicholson, 1973; Gardner-Medwin, 1983).† While the extent of connections between glia in vertebrate neural tissue is not yet established (Gardner-Medwin,1983), glia have been thought to contribute more significantly to electrical bulk tissue properties because of their low membrane resistance and the (possible) electrical connections between them. However, the analyses of this Chapter lead to the physiological conclusion that transcellular current through neurons should not be neglected.

Havstad (1976) suggested values of 3000 Ωcm^2 for the resistivity of neuronal membrane and 320 Ωcm^2 for glial membrane, and 14 μm for the characteristic diameter of a neuronal segment and 1.8 μm for a glial cell process. It is also expected that the cell lengths of the two populations will be roughly in the same ratio, with glial processes extending some 20 μm - 50 μm and neuronal processes some 100 μm - 500 μm, though with much variation. Such values are approximate, but consistent, in general, with values cited by others (Schanne & Ruiz-Ceretti, 1978; Shelton, 1985; Gardner-Medwin, 1983; Nicholson, 1973; Lajtha, 1978). Thus, membrane resistivities and characteristic cell dimensions of neurons and glia differ by an order of magnitude, but maintain roughly the same ratio. As discussed below, the characteristic diameters of cell segments determine (in part) the electrotonic length scales in three

---

† These were not neglected by Ranck, (1963, 1964) and Havstad (1976) in their studies of brain impedance, but their studies dealt with alternating current (AC) for which capacitive rather than resistive properties of membrane are more significant.

dimensions.

The characteristic dimensions of the cells stated above suggest that neurons and glia are 'electrical scale models' of one another. The idea of an electrical scale model may be understood by reference to cable theory (Jack et al., 1975). As stated in Chapter I, it is commonly assumed that electrotonic transmission in cylindrical cells is described by the cable equation. The electrical space constant Λ (cm) is defined as

$$(2.20) \qquad \Lambda^2 = R_m d / (R_0 + R_i),$$

where d is the diameter of the cell, R_m is membrane resistivity and R_0 and R_i are extracellular and intracellular resistivities.

If the space coordinate $\bar{x} := x/L$ is normalized so that the length of the cell is unity, then the dimensionless ratio $\xi := L/\Lambda$, called the electrotonic length, appears in the exponential steady state solutions to the cable equation, thus determining the electrical properties of the cell. One cell is an 'electrical scale model' of another cell if it has the same electrotonic length and geometrical shape as the other cell. This is because the solutions for the transmembrane potential differ only by a change of spatial scale. If two cells are geometrically similar, their ratios of diameter to width are the same, and equation (2.20) and the definition of ξ show that the membrane resistances of electrical-scale-model cells must be proportional to their length. This result in three dimensions is the same as the two-dimensional result described in Section 2.4.

The discussion of Section 2.4 implies that two tissues composed of cells which are electrical scale models of one another in two dimensions have the

same bulk electrical properties. According to the above discussion and the parameter values cited, if neuronal and glia geometry were the same (and if glia are not syncytial), neurons and glia would be three-dimensional electrical scale models of one another. Thus, it is expected that the leading-order bulk properties of a tissue composed entirely of neurons would be similar to the bulk properties of a tissue composed entirely of glia. Hence, the argument that neurons do not influence bulk DC tissue properties because of their high membrane resistance is incorrect.

It is possible that factors other than membrane resistance, e.g., geometry, make the contribution of neurons to bulk tissue properties neglible. However, it seems unlikely that geometry alone could reduce the contribution of 50% of the tissue volume to a neglible amount. If glia are syncytial, then their contribution to tissue properties might be substantially larger than that of neurons; however, the analyses of this Chapter suggest that it is unlikely that this could reduce the contribution of neurons to a neglible amount since the effects of connections between glia (increasing average electrotonic length) are bounded.

VI. SUMMARY AND BIOLOGICAL CONCLUSIONS

1.0. THE ASYMPTOTIC APPROACH

Governing equations for averaged ion transport properties of a model of brain tissue (III.2.17) have been derived using an asymptotic method that reduces the calculation of the averages to the solution of periodic boundary-value problems. A simple tissue model has been chosen for analysis and it has been argued that the properties of this model correspond to those in real tissue. Simple equations for the extracellular potential and potassium concentration are obtained for describing current passing and field potential experiments. While other approaches are possible (e.g., McPhedran & McKenzie, 1978; McKenzie et al., 1978; Havstad, 1976; Lehner, 1979), the asymptotic approach has the following advantages:

(i) It correctly specifies, in general, the canonical microscopic problem for a large number of disconnected (physically separated) cells. Other approaches, such as assuming a uniform potential gradient (Havstad, 1976) or a priori symmetry in the cells (McKenzie et al., 1978), do not. Examination of bulk conductivity versus extracellular space fraction (Figure IV-B.4) show that bulk conductivity increases by a factor between 11 and 2 as a changes from $a = 0.12$ to $a = 0.44$, for various cell sizes. Since the extracellular space fraction has changed by the same factor ($0.44 / 0.12 = 3.66$) for each cell size and the geometry has not changed, it is seen that the effect of the adjacent cells on bulk flux, precisely specified by our model, is significant.

(ii) Bulk parameters are computed using only the microscopic parameters which appear in the model, and these need not be estimated from the bulk parameter data.

(iii) The governing equation predicts all average bulk properties rather than simply a single one. This, with the above features (i-ii) means that bulk conductivity, current passing, and spatial buffering are all specified functions of the microscopic parameters. If all the experimental observations were consistent with these functions, the model would satisfy an exceptionally demanding criterion.

(iv) The joint asymptotic analysis of dimensionless electrotonic and cell length parameters arises naturally in our approach and has not been appreciated in other approaches. This analysis (Chapter V) gives information about the sensitivity of the results to changes in membrane and intracellular conductivities.

(v) Finally, a new and surprising result of this approach is that the systematically averaged equation for potassium concentration does not contain a true diffusion term. The coefficients of the terms in (III.2.17) proportional to $\nabla^2 C$ are different from those which would be obtained with a non-permeating ion and are a factor of 2 or 3 times larger than (it would be) if only diffusion occurred. This is due to an 'unstirred layer' at the membrane which causes local variations in the transmembrane electrical potential. The term 'unstirred layer' refers to the concentration gradient which develops near a membrane due to electric current flow or other flux through the membrane. This fact could lead to experimentally observable results if the tissue has a two- or multi-tiered structure.

Limitations of the present approach are discussed in Section 5.0.

2.0. BIOLOGICAL CONCLUSIONS

2.1. Introduction

In the model of spreading depression developed by Tuckwell and Miura (1978), the advancement of the SD wave depends upon the electrical response of neural membrane to changes in $[K^+]_0$. Also, it has been speculated that $[K^+]_0$ might (Prince, 1978), or might not (Somjen, 1984) play a significant role in epilepsy and other forms of bulk neuronal response (Leibovitz, 1977). Finally, variations in the concentration $[K^+]_0$ may have a wide variety of physiological consequences under normal conditions (Krnjevic & Morris, 1981). The role of $[K^+]_0$ in these phenomena is not established, in part because of variations in physiological parameters between different preparations and variation during the phenomena themselves. For example, the extracellular space and extracellular electrolyte composition are known to change during SD (Nicholson & Kraig, 1981) and epilepsy (Prince, 1978). When many changes occur simultaneously, it can be difficult to decide which factors are mediating and which are epiphenomenal. Therefore, it is desirable to determine the existence and magnitude of potassium spatial transport mechanisms e.g., transcellular current and spatial buffering, to describe the dependence of such transport on tissue parameters, as well as to estimate these parameters from experiments.

In the following sections the implications of our model for these problems are discussed. Our most important conclusion is that electrically mediated spatial transport does not require specialized cells and is relatively robust, i.e., this transport occurs in significant amounts with physiologically relevant parameter values. Thus, this form of K^+ transport must occur and must play a significant

role in a wide variety of physiological situations. Such a conclusion is difficult to obtain from experimental studies. Some difficulties in incorporating ion transport theory into the bulk conductivity theory is described in Section 4. It is suggested that these difficulties can be resolved by experiment.

2.2. Properties of the Averaged Steady Equations

In many respects the properties of the averaged equations obtained here are similar to those of the steady diffusion equation, i.e., Laplace's equation and the 'spatial buffering' equations based on the cable model (SBCM) used by Gardner-Medwin (1983b). This is not surprising because these equations both describe conservative fluxes of electrical current and K^+. The averaged equations of this thesis have a form similar to the SBCM equations in the asymptotic limit of the electrical space constant for the cells going to zero. However, we emphasize that our equations cannot be 'derived' by the latter procedure. The SBCM equations contain bulk and transcellular conductances as empirical, rather than derived, constants. In addition, the limiting forms of the SBCM would contain a diffusion term, unlike the present model.

The values of the bulk coefficients in the present model are independent results of the model, unlike the coefficients of the SBCM. In this section we discuss properties of the averaged model equations in one dimension.

To compare the results from our model with experiments which have involved passing current across the cortical surface over relatively long periods, it is important to establish the steady state properties of the solutions. Non-constant steady solutions to the model are obtained by prescribing $C^0 = C_d$ at some fixed depth and $C^0 = C_s$ at the surface of the cortex. Such boundary conditions

are chosen arbitrarily, however. The most realistic steady solutions are those with finite non-zero $[K^+]_0$ at infinity since $C^0 = [K^+]_0$ presumably tends to a constant deep within the tissue. If C were governed by Laplace's equation, it is obvious that the only such solution is C=constant. The same is true for our averaged equations (III.2.17) as shown below.

The nature of the steady solutions for C may be deduced as follows. In one dimension, the governing equations (III.2.17) become, if there are no sources:

$$D_1\phi_{uu} + E_1V_{uu} + F_1C_{uu} = 0,$$

(2.1)

$$D_2\phi_{uu} + E_2V_{uu} + F_2C_{uu} = \tau C_t,$$

where D_j, E_j, and F_j, $j=1,2$ $V := \nu^{-1}\ln(C^0/C^i)$ are as defined in Sections IV.6.2 and IV.6.6 and the subscript u denotes a partial derivative with respect to the space variable u. In the steady state $\tau C_t = 0$, and the equations can be integrated directly. Integrating once, however, yields the first-order differential equations:

(2.2) $$D_j\phi_u + E_jV_u + F_jC_u = K_j.$$

Using the definition of V, eliminating $\partial\phi/\partial u$ from (2.2), and solving for C_u yields

(2.3)
$$C_u = \frac{\nu(K_1 D_2 - K_2 D_1)C}{\nu(D_2 F_1 - D_1 F_2)C + E_2 - E_1} \quad .$$

For steady solutions in which C is constant and non-zero, (2.3) requires $D_2 K_1 - D_1 K_2 = 0$ and C identically constant, as was stated above. The importance of this result is that the spatial derivatives of concentration and membrane potential $C_u = V_u = 0$ and hence the coefficients E_j and F_j do not appear in (2.2) and therefore, cannot be estimated from a steady state current passing experiment. However, as noted in Chapter IV, the coefficients, E_1 and E_2, may be estimated within 10% to 15% (in any of the models employed here) from the value of D_2, where D_2 is interpreted physically as the transcellular conductance. The significance of E_2 is described in the next Section 2.3.

In the steady state with C=constant, the electrical flux is given by $D_1 \phi_u = K_1$ and the ionic flux by $D_2 \phi_u = K_2$. Since both fluxes are proportional to the electric field, the ionic flux as a fraction of electric current in such an experiment is $K_2 / K_1 = D_2 / D_1$. Thus, D_2 / D_1 is the observed transport number in a current passing experiment. As shown in Chapter IV (Figure 6.8), the values of E_2 and D_2 / D_1 are not related. The value of the bulk conductivity D_1, however, with the observed transport number, will suffice to reliably determine E_1 and E_2.

Since the present model predicts a reliable relationship between D_1, D_2 and E_1 and E_2, the governing equations could be tested by independent measurements of these quantities. While D_1 and D_2 could be obtained from steady state experiments, it would be necessary to measure membrane potentials

and K^+ transport during a time-dependent experiment to obtain E_1 and E_2. If E_1 and E_2 are not as predicted, the model would have to be modified.

2.3. Magnitude of Spatial Buffering

The relationship between the bulk coefficients and the magnitude of spatial buffering may be deduced by eliminating ϕ_{uu} from (2.1) to obtain:

$$(2.4) \qquad \hat{E} V_{uu} + \hat{F} C_{uu} = \tau C_t,$$

where $\hat{E} = E_2 - (D_2/D_1)E_1$ and $\hat{F} = F_2 - (D_2/D_1)F_1$. The values of D_1, D_2, E_1, F_1, and F_2 are given in Tables IV.6.1 - IV.6.5, and E_2, shown in Figure IV.6.7, is the same as E_1 to two significant figures. Mathematically, we say that spatial buffering occurs when τC_t is more negative (or positive) than it would be if diffusion alone were occurring for $C_{uu} \leq 0$ (or ≥ 0). The coefficient $\hat{E}$ of V_{uu} and $\hat{F}$ of C_{uu} in (2.4) are tabulated for (Case A) $\sigma_o = 20$ mS, $\sigma_i = 10$ mS, $a = 0.2$, in Tables 2.1.A and for the two-tier study (Case B) in Table 2.1.B., where the values of $\hat{E}$ and $\hat{F}$ in Table 2.1.A and 2.1.B differ by some 10% to 30% from the values of E_2 and F_2. The minimum in $\hat{F}$ in Tables 2.1.B and 2.2 corresponds to the minimum in F_2 discussed in Section IV.6.5.

In order to compare spatial buffering to diffusion it is useful to compare the rates of decay of an initial concentration distribution, $C = c(1 + a\sin(bu))$ where $0 \leq a \leq 1$, under (2.4) and under diffusion, respectively. To do this we first obtain a bound for $\nu V_{uu} = C_{uu}/C - (C_u/C)^2$ in terms of C_{uu}. For u such that $C_{uu} \leq 0$, we obtain:

Table 2.1.A. One-Tier Coefficients in Equation (VI.2.4).

$l_1(\mu\text{m})$	$\hat{E}$	$\hat{F}$
32.1	.0174	4.39
46.0	.0280	5.51
72.1	.0460	7.26
103.	.0600	8.17
146.	.0704	7.95

Table 2.1.B. Two-Tier Coefficients in Equation (VI.2.4).

$l_1(\mu\text{m})$	$\hat{E}$	$\hat{F}$
32.1	.0072	11.39
46.0	.0109	12.88
72.1	.0131	12.18
103.	.0154	8.66
146.	.0184	20.80

$$\nu V_{uu} = \frac{-ab^2\sin(bu)}{1 + a\,\sin(bu)} - \left(\frac{ab\,\cos(bu)}{1 + a\,\sin(bu)}\right)^2$$

$$(2.5) \qquad \leq \frac{-ab^2\sin(bu)}{1 + a} = \frac{1}{1 + a}\,C_{uu}.$$

Hence, concentration distributions with small amplitudes (a << 1) lead to a $V_{uu} \leq \nu^{-1}C_{uu}$. Hence, an approximate lower bound for the coefficient of C_{uu}

in (2.4) is ($\hat{F}$ + $\nu^{-1}\hat{E}$). This quantity is tabulated in Table 2.2.

It can be seen that the coefficient of C_{uu} is not very sensitive to the model employed, and does not depend on l in a simple way. Since this coefficient would have been 2.64 with pure diffusion, there is a consistent spatial buffer effect which is between 2 and 8 times the effect of diffusion. To obtain a spatial buffer effect which is 5 times that of diffusion, as deduced by Gardner-Medwin (1983b), requires a coefficient of C_{uu} of approximately 13, which is generally consistent with Table 2.2.

The $\hat{E} V_{uu}$ and $\hat{F} C_{uu}$ terms both contribute significantly to spatial buffering in the one-tier case (Case A), but $\hat{E} V_{uu}$ contributes little in the two-tier case (Case B). This means that in Case A, the spatial buffering effect may be estimated accurately from E_i, while in Case B it is necessary to know all the bulk coefficients, including F_i. The implications of this are discussed in Section 3.3.

3.0. IMPLICATIONS FOR A MODEL OF TISSUE STRUCTURE

3.1. Transfer Cells Are Unnecessary

In the SBCM it is postulated that a sparse network of electrically continuous 'transfer cells' is the substrate of the cable equations employed in that model. In this section, it is argued that the assumption of a glial syncytium is a complex assumption, and that it is unecessary. Gardner-Medwin (1983b) states "the assumption of a syncytium is not strictly necessary " and that an array of cells would behave in essentially the same way. In this thesis this statement has been tested by direct computation and found to be correct in many respects. Differences between the present model and the SBCM are also

Table 2.2. Lower Bound for C_{uu} Coefficient.

l_1 (μm)	Case A	Case B
32.1	11.93	11.78
46.0	11.41	13.46
72.1	9.75	12.89
103.	7.03	9.49
146.	5.31	21.8

noted.

The assumption is complex because the present results and the SBCM indicate that given reasonable assumptions about glial membrane, the bulk transport numbers would be much larger than those observed if all glia were electrically continuous. In addition, Hounsgaard and Nicholson (1983) have examined potassium transport experimentally using ionophoretically applied K^+ and concluded that glia were not electrically continuous in vertebrate cerebellum. Therefore, if the SBCM is used, it is necessary to postulate a sparse network of syncytial transport cells which, because they are sparse, have sufficiently high internal resistance to account for observed bulk transport numbers.

Bulk potassium current within the tissue of between 7% and 30% of bulk electric current is consistent with the present knowledge of parameters for a tissue consisting of disconnected cells (neurons or glia). Therefore, the assumption of syncytial transfer cells is unnecessary, since the observed bulk transport numbers can be accounted for by current flows through non-syncytial elements of the general cell population (neurons and glial cells). The magnitude of the current

depends mainly on the product of membrane conductance and cell length, and to some extent on intracellular resistance, extracellular space, and relative position of the cells with respect to each other. On the other hand, our analysis does not rule out the possibility that specialized transfer cells exist.

It may be possible to test for presence of transfer cells by performing current passage experiments in the presence of pharmacological agents which disrupt the putative coupling between glia (Tang et al., 1985).

The computed transport number range includes values close to experimental observations (0.06 over a 5 mm diameter region) as well as values considerably higher than those observed. If our model is correct, it is predicted that larger transport numbers will be observed with other preparations. In addition, higher transport numbers might be observed at finer length scales, since it is expected that the governing equations will be different on such scales. Differences between preparations also can occur because of tissue (tier) structure or differing surface / volume ratios of cells.

3.2. Disconnected Cells Cannot Be Neglected

Many of the cells in neural tissue are not electrically continuous or syncytial and the present work was undertaken, in part, to assess the importance of such tissue components. The mathematical technique (homogenization) employed here derives for the first time the governing equation for electric current and ionic flux through closely apposed but disconnected cells.

Although our model cells were electrically disconnected, they still exhibited transcellular currents comparable to those obtained from the SBCM. Therefore, even if a sparse syncytial network existed, the disconnected cells in the tissue

could not be neglected. Our model cells were different electrotonically from a
syncytium because transcellular current was independent of the intracellular
conductivity in the biological parameter range (Figure IV.6.2). Instead, this
current depends almost exclusively on the membrane conductance. As shown in
Chapter V, a syncytium may be characterized electrotonically by the fact that
transcellular current depends primarily on its intracellular conductivity.

For high membrane conductance, the transcellular conductance of a coupled
two-tier model, is considerably less than that of an uncoupled model. Most
previous interpretations of such data have been based on uncoupled models,
however. Somjen and Trachtenberg (1979) suggested that the relatively high K^+
conductance of glial membrane implies a bulk tissue conductivity much larger
than the observed value. This suggestion seems to be based on the idea that if
membrane conductance were high, then current would flow through the
intracellular space, so that the bulk conductivity ought to be close to the
intracellular conductivity. Our results show that this conclusion need not be
correct in a coupled two-tier model.

3.3. Tier-structure May Be Important

Because cells of different sizes coexist in neural tissue, we investigated the
effect of cell populations with different asymptotic sizes. The results indicate that
different governing equations will hold for passive transport at different length
scales. Since transcellular flux depends almost entirely on cell size (or membrane
conductance), different populations of cells of known size will characterize the
tissue depending on the given length scale. Such effects have been modelled here
with two cell populations, and it is supposed that the population composed of

smaller cells has the same membrane properties as the larger population. These simple assumptions have been used because little data exists to support more complicated assumptions and the results obtained.

The results of Section 2.3 provide an experimental test of whether a given tissue has a two- or multi-tier structure. In a tissue accurately described by a one-tier model, the magnitude of spatial buffering observed can be predicted from D_1, D_2, E_1, and E_2; which may be deduced from a current passing experiment. If the tissue is accurately described by the two-tier model, however, the prediction of spatial buffering derived using this method will be smaller than the spatial buffering observed.

Another kind of tier structure which may exist, is a network of transfer cells surrounded by disconnected glia. If a sparse network of specialized transfer cells existed, it is likely that surrounding glia would render it ineffective as a means of K^+ transport by raising the effective extracellular transport number for K^+. In Gardner-Medwin's SBCM (1983b) the parameter β may be interpreted as the ratio of the magnitude of spatial buffer flux to diffusive flux and has the form $\beta = (t_K^0)^{-1} R_0 (R_0 + R_i)^{-1}$ where R_i is the bulk transcellular resistance and R_0 is the bulk extracellular resistance. Hence, the given expression indicates that relatively small changes in extracellular transport number t_K^0 can dramatically alter the importance of spatial buffering in a tissue corresponding to the SBCM model. For example, the conservative assumption that 7% of current is transcellular in the surrounding glia, reduces β by a factor of $0.07 / 0.012 = 5.8$.

The model which was used implicitly in the last paragraph was not investigated in this thesis. Therefore, further experimental and theoretical work are necessary to completely assess the possibility that small cells might reduce

the effectiveness of a transport network composed of larger or connected cells.

4.0. COMPARISON WITH EMPIRICAL PROPERTIES OF BULK TISSUE

4.1. Introduction

Nicholson and Phillips (1981) have investigated the properties of diffusive transport of non-permeating ions in brain tissue, and were able to describe such diffusion with a simple isotropic model. The physiologically significant potassium ion, however, is not described by this model. In this section it is shown that it is necessary to use bulk governing equations and to consider diffusion, conductivity, and transport number data in order to obtain a complete model for potassium ion transport.

4.2. Significance of Transcellular Current

If no bulk transcellular current flowed, bulk tissue would have few interesting electrical or ion transport properties. For this reason it is important to demonstrate that significant bulk transcellular current exists. A direct measurement of the bulk transcellular current is provided by the measurement of potassium transport through tissue in the presence of an electrical current (Gardner-Medwin, 1983a). The fact that very few assumptions were made here in deriving a significant bulk transcellular current makes our theoretical study an independent piece of evidence for the existence of significant transcellular flux. The results reported here, however, show that the factors affecting transcellular flux in a coupled model are complicated. Thus, the work presented here is not complete, because the results have not been compared to experiment.

4.3. Scale Effects

The scale effects described in Sections V.2.4 and V.3 are likely to be useful for many different situations because they are particularly simple. The predictions of the present model are similar to those of the SBCM, as they should be in order to explain known observations. However, the present model also contains the possibility of increased, decreased, or anisotropic spatial buffer capacities at shorter or longer length scales. These possibilities have not been systematically investigated, though the existence of such phenomena is suggested by an isolated finding of Gardner-Medwin (1983a). He found that the strength of field potentials due to superfusion of cortex with K^+ over an area of diameter 1 mm produces a smaller (30%) field potential than that over a 5 mm diameter area.

According to the SBCM (Gardner-Medwin, 1983b), spatial buffer fluxes require potassium gradients to be extended for a longer distance than the electrical space constant of the 'transfer cells'. Thus, (it is argued) at very short length scales spatial buffering is not significant compared to diffusion. This argument is correct for the SBCM model. However, we have shown that simple diffusion may not occur in bulk for the potassium ions since disconnected cells contribute to transcellular flux even if a transfer cell network also exists. Therefore this conclusion requires further investigation.

The data on conductivity anisotropy appear to be inconsistent with the finding (Gardner-Medwin, 1983a) that only 6% of DC current passes through cells. If diffusion in the cortex is isotropic and the steady diffusion equation is the same as the equation for steady electric current, it follows that anisotropy must be due to transcellular flux. However, based on our results (or the SBCM),

it seems unlikely that transcellular flux could account for anisotropy of 3:1 to 5:1. Thus, it seems likely that such discrepancies must arise from scale effects.

These effects can be investigated by simultaneous measurement of anisotropic conductivity, diffusion, and spatial buffering at the same length scale. It might be convenient to perform such an experiment in a slice preparation. If the present model is correct, the conductivity, diffusion, and spatial buffering results will be consistent when simultaneous measurements are performed at the same scale, but will vary (together) as the scale of measurement is varied.

5.0. LIMITATIONS

5.1. Transport Number Simplification

The derivation of an averaged governing equation (III.2.17) for electrical current and ionic flux begins with a non-linear equation and results in a linear equation with constant coefficients. Most of the approximations employed can be justified asymptotically or in other, well defined senses (Bensoussan, Lions, & Papanicolaou, 1978). In addition, the convergence properties of similar multiple scale expansions have been investigated numerically to some extent (Bourgat, 1977).

The final simplification of Chapter IV is not an asymptotic approximation of this type, however, and (until proven otherwise) is mathematically ad hoc . It is important to emphasize that existence of a transport number (with constant t_K^o and t_K^i) is assumed throughout the experimental (Barry & Hope, 1969) and thermodynamic literature (Katchalsky & Curran, 1965). In Chapter IV it is shown that no complications are introduced in extending this theory to bulk tissue. Experimental evidence (Gardner-Medwin, 1983a; Gardner-Medwin &

Nicholson, 1983; Havstad, 1976; Nicholson, 1975) suggest that the non-linear effects neglected are not qualitatively significant under many conditions of physiological interest.

5.2. Tortuosity and Geometry Assumptions

It was not practical here to solve a canonical microscopic problem which exhibits the high tortuosity that is characteristic of real neural tissue. This shortcoming of the present work, together with the fact that the coefficients were calculated in two dimensions, complicates the interpretation of our results.

The limited investigation here of the effect of geometry was undertaken in order to assess qualitatively the magnitude and direction of such effects. In this respect our study is similar to the study by McPhedran and McKenzie (1978) of the average conductivity of inhomogeneous media with spherical inclusions arranged in lattices of different types. McPhedran and McKenzie's results are not directly applicable here because they studied spherical inclusions without membranes.

In general our results indicate that when membrane conductance is low in coupled or uncoupled models, there is little difference between the bulk conductivity of straight and staggered arrays of cells. At higher membrane conductances, the uncoupled model shows a reduction of global conductivity in the staggered arrays because interaction between cells is more important at higher membrane conductances. For coupled models, however, the results for straight and staggered arrays were nearly identical in all of our studies because the effects of coupling between transmembrane potential and concentration dominate at higher membrane conductances. Thus, effects of geometry in the coupled model are

insignificant. Staggered arrays and straight arrays conduct similar proportions of transcellular current in both coupled and uncoupled models.

Thus, our results suggest that the unrealistic geometries used here will not seriously affect conclusions about transcellular flux.

6.0. SUMMARY

Historically, previous tissue models have been formulated in order to model a single bulk property such as impedance (Havstad, 1976), spatial buffer capacity (Gardner-Medwin, 1983a b), or diffusion properties (Nicholson & Phillips, 1981). No previous model has attempted to synthesize the modelling of all three properties. An important reason to do this is that reliable observations from the experimental literature (isotropy of diffusion, anisotropy of conductivity, small bulk tissue transport number of K^+) cannot be easily reconciled with previous models of cortical tissue structure.

Electrical models of tissue has been explored extensively; for example, Ranck (1963,1964), Eisenberg et al., (1979), and Nicholson (1973) have given assumptions which have been useful experimentally. Unlike the studies of K^+ transport, these impedance studies contained no direct measurements of transcellular flux. Previous models of cortical conductivity or impedance either have assumed that transcellular flux is the same as it would be in a uniform voltage gradient (Havstad 1976) (an assumption which is qualitatively reasonable), or assumed that transcellular flux is negligible (Nicholson, 1973), or not modelled transcellular flux at all (Nicholson & Freeman,1975). These previous studies also did not model unstirred layers at the membrane, which we have shown to be important under some conditions.

APPENDIX VI.A. RECENT LITERATURE

As noted in the introduction, theoretical work on bulk tissue properties is difficult and has appeared infrequently. Recent work (1985-1989) on conductivity and spatial buffering has chiefly consisted of experimental work on microscopic preparations in vitro and is therefore not directly relevant to the present work on bulk properties. Aspects of these studies are discussed below. The exceptions are Gardner-Medwin's (1986) theoretical exposition of the concept of 'spatial buffer capacity', and Dietzel and Heinemann's (1989) simultaneous experimental study of bulk current sources, spatial buffering, field potentials, and changes in extracellular space. Gardner-Medwin's work is a simple and brief extension of the (1983b) theory. Dietzel and Heinemann found current sources and changes in extracellular space consistent with our model (and the SBCM); but also deduced that other, active, uptake processes played a significant role in the removal of potassium from the extracellular space.

Experimental studies of microscopic systems were of several types. Studies of isolated retinal glial cells included studies of the distribution of potassium conductance, (Brew & Attwell, 1985; Newman, 1986; Reichenbach & Eberhardt, 1988) or cell shape (Eberhardt & Reichenbach, 1987), and metabolic effects of K^+ (Coles, 1989). Other studies examined spatial buffering in intact retina (Karwoski et al., 1989a, b). These studies of retinal cells are of independent interest, but give limited information about the fundamental role of spatial buffering in mammalian cortex and cerebellum. In addition, potassium channels of different kinds have been studied in retinal glial cells (Newman, 1989) and cultured astrocytes (Gray & Ritchie, 1986; Sonnhof & Schachner, 1986; Sonnhof, 1987). These preparations are well suited to obtaining information about the

membrane properties of glial cells and this work will likely lead to further refinement of the microscopic properties used in bulk tissue models. Such findings must be regarded as preliminary, however. In particular, data must be obtained regarding the generality of observed glial membrane properties across cell types and species before such properties are incorporated in general models.

REFERENCES

Aidley, D.J., The Physiology of Excitable Cells, 2nd ed., Cambridge University Press, Cambridge, 1978.

Adam, G.(1973), The effect of potassium diffusion through the Schwann cell on potassium conductance of the squid axon. J. Membr. Biol., 13, 353-386.

Aldrich, R.W., Corey, D.P., Stevens, C.F.(1983), A reinterpretation of mammalian sodium channel gating based on single channel recording. Nature, 306, 436-441.

Ampere, A.M. & Babinet, J., Expose des Nouveles Decouvertes Sur L' Electricite et de Magnetisme, Mequignon-Marvis, Paris, 1822.

Ames, W.F., Non-linear Partial Differential Equations in Engineering, Academic Press, London, 1965.

Aris, R., Mathematical Modelling Techniques, Pitman, London, 1978.

Arrhenius, S., Untersuchungen uber die Galvanishe Leit Fahigkeit der Elektrolyte, Engelmann, Leipzig, 1883.

Babuska, I.(1976), Homogenization approach in engineering, In M. Beckmann & H.P. Kunzi(eds.), Lecture Notes in Economics and Mathematical Systems, 134, 137-153.

Barcilon, V., Eisenberg, R.S. & Mathias, R.T., Microscopic and macroscopic description of the electrical properties of syncytial tissues and invaginated cells, (preprint).

Barry, P.H., & Hope, A.B.(1969a), Electroosmosis in membranes: Effects of unstirred layers and transport numbers, I. Theory. Biophys. J., 9, 700-728.

Barry, P.H., & Hope, A.B.(1969b), Electroosmosis in membranes: Effects of unstirred layers and transport numbers, II. Experimental. Biophys. J., 9, 729-757.

Barrett, J.N. & Crill, W.E.(1974), Specific membrane properties of cat motoneurones. J. Physiol., 239, 301-324.

Batchelor, G.K.(1974), Transport properties of two-phase materials with random structure. Ann. Rev. Fluid Mech., 6, 227-255.

Bensoussan, A., J.-L. Lions & G. Papanicolaou, Asymptotic Analysis for Periodic Structures, North Holland, Amsterdam, 1978.

Bernstein, J.,Elektrobiologie,Friedrich Vieweg & Son, Braunschweig, 1912.

Biedermann, W., Elektrophysiologie, Gustav Fischer, Jena, 1895.

Bourgat, J.F.(1977), Numerical experiments of the homogenization method for operators with periodic coefficients, In Proc. 3rd Int. Coll. Comp. Meth.

Appl. Sci. Eng., Springer, Berlin.

Brazier, M.A.B., A History of the Electrical Activity of the Brain, Pitman, London, 1961.

Brew, H. & Attwell, D.(1985), Is the potassium channel distribution in glial cells optimal for spatial buffering of potassium?.Biophys. J., 48, 843-7.

Bures, J., Buresova, O. & Krivanek, J., The Mechanism and Application of Leão's Spreading Depression of Electroencephalographic Activity, Academic Press, N.Y., 1974.

Cajal, S.R.(1892), A new concept of the histology of the central nervous system, In D.A. Rottenberg & F.H. Hochberg(eds.), Neurological Classics in Modern Translation, Hafner, 1977, N.Y.,7-29.

Carnie, S.L. & Torrie, G.M.(1984), The statistical mechanics of the electrical double layer, In I. Prigogine & S.A. Rice(eds.), Adv. Chem. Phys., LVI, 141-254.

Carpenter, D.O., Hovey, M.M. & Bak, A.F.(1971), Intracellular conductance of Aplysia neurons and squid axon as determined by a new technique. Int. J. Neurosci., 2, 35-48.

Carpenter, D.O., Hovey, M.M. & Bak, A.F.(1973), Measurement of intracellular conductance of Aplysia neurons: evidence for the organization of water and ions. Ann. N. Y. Acad. Sci., 204, 502-533.

Carrier, G.F. & Pearson,C.E., Partial Differential Equations: Theory and Technique, Academic Press, N.Y., 1976.

Caton, R. (1875), The electric currents of the brain. Brit. Med. J., 2, 278.

Chapman, D.L.(1913), A contribution to the theory of electrocapillarity. Phil. Mag., 25, 475-481.

Clark, J.W., & Plonsey, R.(1966), A mathematical evaluation of the core conductor model. Biophys. J., 6, 95-111.

Clark, J.W., & Plonsey, R.(1970a), A mathematical study of nerve fiber interaction. Biophys. J., 10, 937-957.

Clark, J.W., & Plonsey, R.(1970b), Fiber interaction in a nerve trunk. Biophys. J., 11, 281-294.

Cremer, M.(1906), Uber die Ursache der elektromotorischen Eigenschaften der Gewebe, Zugleich ein Beitrag zur Lehre von den polyphasischen Elektrolytketten. Z. Biol (Munich), 47, 562-608.

Cremer, M.(1909), Die allgemeine Physiologie der Nerve, In Nagel, W.A.(ed.), Nagel's Handbuch der Physiologie des Menschen, IV, 793-992.

Crill, W.E., & Schwindt, P.C.(1983), Active currents in mammalian central neurons. Trends in Neurosci., 6, 236-240.

Crill, W.E. & Schwindt, P.C.(1986), Role of persistent inward and outward currents in epileptiform bursting in mammalian neurons, In A.V. Delgado-Escueta, A.A. Ward Jr., D. M. Woodbury & R.J. Porter(eds.), Adv. Neurol., 44, 225-233.

Csillik, B.(1982), Neurons. In A. Lajtha (ed.), Handbook of Neurochemistry, 2nd ed., Vol. I: Chemical and Cellular Architecture, 299-315.

Davson, H.(1976), The blood brain barrier. J. Physiol., 255, 1-28.

Descartes, R., Les Passions de l'Âme, I. Le Gras, Paris, 1664.

Dietzel, I., Heinemann, U., Hofmier, G. & Lux, H.D.(1980), Transient changes in the size of the extracellular space in the sensorimotor cortex of cats in relation to stimulus-induced changes in potassium concentration. Exp. Brain Res., 40, 432-439.

Dietzel, I., Heinemann, U., & Lux, H.D.(1989), Relations between slow extracellular potential changes, glial potassium buffering, and electrolyte and cellular volume changes during neuronal hyperactivity in cat brain.Glia, 2, 25-44.

Donnan, F.G.(1911), Theorie de Membrangleichgewichte un Membranpotentiale bei Vorhandensein von nicht dialysierenden Elektrolyten Ein Beitrag zur physikalish-chemische Physiologie. Z. Elektrochem., 17, 572-581.

du Bois-Reymond, E., Untersuchungen ueber Thierische Elektricitat, Vol. I, Reiner, Berlin, 1848.

du Bois-Reymond, E., <u>Untersuchungen ueber Thierische Elektricitat,</u> Vol. II, Reiner, Berlin, 1849.

Eberhardt, W. & Reichenbach, A.(1987), Spatial buffering of potassium by retinal Muller (glial) cells of various morphologies calculated by a model.Neurosci., <u>22</u>, 687-96.

Eisenberg, R.S., Barcilon, V. & Mathias, R.T.(1979), Electrical properties of spherical syncytia. <u>Biophys. J.</u>, <u>25</u>, 151-180.

Fisher, R.S., Pedley, T.A., Moody, W.J. Jr., Prince, D.A.(1976), The role of extracellular potassium in hippocampal epilepsy. <u>Arch. Neurol.</u>, <u>33</u>, 76-83.

Fuoss, R.M. & Accasina, F., <u>Electrolytic Conductance,</u> Interscience, N.Y., 1959.

Fritsch, G. & Hitzig, E.(1870), Ueber die elektrische Erregbarkeit des Grosshirne. <u>Arch. fur Anat. Physiol. und Wissenshaftl.</u>, <u>1870</u>, 300-332.

Futamachi, K.J., Mutani, R. & Prince, D.A.(1979), Potassium activity in rabbit cortex. <u>Brain Res.</u>, <u>75</u>, 5-25.

Galvani, L., <u>Commentary on the Effect of Electricity on Muscular Motion,</u> translated by <u>R.M. Green,</u> Waverly Press, Baltimore, 1953.

Gardner-Medwin, A.R.(1980),In Nicholson, C., Dynamics of the brain cell microenvironment. <u>Neurosci. Res. Prog. Bull.</u>, <u>18</u>, 177-322.

Gardner-Medwin, A.R.(1982), Possible roles of vertebrate neuroglia in potassium dynamics, spreading depression and migraine. J. Exp. Biol., 95, 111-128.

Gardner-Medwin, A.R.(1983a), A study of the mechanisms by which potassium moves through brain tissue in the rat. J. Physiol. (Lond.), 335, 353-324.

Gardner-Medwin, A.R.(1983b), Analysis of potassium dynamics in mammalian brain tissue. J. Physiol. (Lond.), 335, 393-426.

Gardner-Medwin A.R. & Nicholson, C.(1983), Changes of extracellular potassium activity induced by electric current through brain tissues in the rat. J. Physiol. (Lond.), 335, 375-392.

Gardner-Medwin, A.R.(1986), A new framework for assessment of potassium-buffering mechanisms.Ann. N.Y. Acad. Sci., 481, 287-302.

Garland, J.C. & Tanner, D.B. (eds.), Electrical Transport and Optical Properties of Inhomogeneous Media: American Institute of Physics Conference Proceeding no. 40, American Institute of Physics, N.Y., 1978.

Geselowitz, D.B.(1967), On bioelectric potentials in an inhomogeneous volume conductor. Biophys. J., 7, 1.

Glynn, I.M. & Karlish, S.J.D.(1975), The sodium pump. Ann. Rev. Physiol., 37, 13-55.

Golgi, C.(1906), The neuron doctrine - theory and facts, In Nobel Lectures in Physiology or Medicine, 1901-1921, Elsevier, 1967.

Gouey, G.(1910), . J. de Physique(Paris), 9, 457.

Goldman, D.E.(1943),Potential, impedance, and rectification in membranes. J. Physiol.(Lond.), 108, 37-77.

Grafstein, B.(1956), Mechanism of spreading cortical depression. J. Neurophys., 19, 154.

Gray, W.O. & Lee, P.C.Y.(1977), On the theorems for local volume averaging of multiphase systems. Int. J. Multiphase Flow, 3, 333-340.

Gray, P.T. & Ritchie, J.M.(1986), A voltage-gated chloride conductance in rat cultured astrocytes.Proc. Roy. Soc. (Lond.)B, 228, 267-88.

Havstad, J.W.(1976), Electrical Impedance of Cerebral Cortex: An Experimental and Theoretical Investigation, PhD. Dissertation, Stanford University .

Hebb, D.O.(1955), Drives and the CNS (conceptual nervous system). Psych. Rev., 62, 243-254.

Hebb, D.O.(1958), Alice in wonderland or psychology among the behavioral sciences, In H.F. Harlow & C.N. Woolsey (eds.), In Biological and Biochemical Bases of Behavior, University of Wisconsin Press, Madison .

Helmholtz, H.(1850a), Vorlaufige Bericht uber die Fortpflanzungsgeschwindigkeit der Nervenreizung. Arch. Anat. Physiol., 1850, 71-3.

Helmholtz, H.(1850b), Messungen uber den zeitltchein Verlauf der Zuckung animalischen Muskeln und die Fortpflanzungsgeschwindigkeit der Reizung in den Nerven. Arch. Anat. Physiol., 1850, 276-364.

Hermann, L.(1879), L. Hermann (ed.), In Handbuch der Physiologie Vol.II, Vogel, Leipzig.

Hertz, L.(1982), Astrocytes. In A. Lajtha(ed.), Handbook of Neurochemistry 2nd Edn. Vol. I:Chemical and Cellular Architecture, 319-348.

Hillman, D.G.(1977), Neuronal shape parameters and substructures as a basis of neuronal form, In F.O. Schmitt & F.G. Worden(eds.), The Neurosciences 4th Study Program, 477.

Hodgkin, A.L. & Huxley, A.F.(1952a), Currents carried by sodium and potassium ions through the membrane of the giant axon of Loligo . J. Physiol. (Lond.), 116, 449-472.

Hodgkin, A.L. & Huxley, A.F.(1952b), The components of the membrane conductance in the giant axon of Loligo . J. Physiol. (Lond.), 116, 473-496.

Hodgkin, A.L. & Huxley, A.F.(1952c), The dual effect of membrane potential on sodium conductance in the giant axon of Loligo. J. Physiol. (Lond.), 116, 497-506.

Hodgkin, A.L. & Huxley, A.F.(1952d), A quantitative description of membrane current and its application to conduction and excitation in nerve. J. Physiol. (Lond.), 117, 500-544.

Hodgkin, A.L. & Katz, B.(1949), The effect of sodium ions on electrical activity of the giant axon of the squid. J. Physiol. (Lond.), 108, 37-77.

Hodgkin, A.L. & Keynes, R.D.(1957), Movement of labelled calcium in squid giant axons. J. Physiol. (Lond.), 138, 253-281.

Hodgkin, A.L. & Rushton, W.A.H.(1946), The electrical constants of a crustacean nerve fibre. Proc. Roy. Soc. B., 133, 444.

Horstmann, E. & Meves, H.(1959), Die Feinstruktur des molecularer Rindengraues und ihre physiologishe Bedeutung. Z. Zellforsch. Mikrosk. Anat., 49, 569-604.

Horvath, A.L., Handbook of Aqueous Electrolyte Solutions, Camelot Press, Southampton, U.K., 1985.

Hounsgaard, J. & Nicholson, C.(1983), Potassium accumulation near individual Purkinje cells in cerebellar slices from the guinea pig. J. Physiol. (Lond.), 340, 359-388.

Jack, J.J.B., Noble, D. & Tsien, R.W., Electric Current Flow in Excitable Cells, Clarendon Press, Oxford, 1975.

Johnston, D.(1980), Passive cable properties of Hippocampal CA3 pyramidal neurons. Cellular and Molecular Neurobiology, 1, 41-55.

Kandel, E.R. & Schwartz, J.H., Principles of Neural Science, Elsevier, North Holland, 1983.

Karwoski, C.J., Coles, J.A. & Lu, H.K.(1989a), Current-evoked transcellular K$^+$ flux in frog retina.J. Neurophys., 61, 939-52.

Karwoski, C.J., Lu, H.K. & Newman, E.A.(1989b), Spatial buffering of light-evoked potassium increases by retinal Muller (glial) cells.Science, 244, 578-80.

Katz, B., The Release of Neural Transmitter Substances, Thomas, Springfield, Ill., 1969.

Katchalsky, A. & Curran, P.F., Non-equilibrium Thermodynamics in Biophysics, Harvard University Press, Cambridge, Mass., 1965.

Keller, J.B.(1977), Effective behavior of heterogeneous media, In U. Landman(ed.), Statistical Mechanics and Statistical Methods in Theory and Application, 631-644.

Kettenmann, H., Orkand, R.K. & Lux, H.D.(1984a), Some properties of single potassium channels in cultured oligodendrocytes. Pflugers Arch., 400, 215-221.

Kettenmann, H., Sonnhof, U., Camerer, H., Kuhlmann, S., Orkand, R.K. & Schachner, M.(1984b), Electrical properties of oligodendrocytes in culture. Pflugers Arch., 401, 324-332.

Kimelberg, H.K. & Bourke, R.S.(1982), Anion transport in the nervous system, In A. Lajtha(ed.), Handbook of Neurochemistry, 2nd Edn., Vol. I: Chemical and Cellular Architecture, 31-64.

Kraig, R.P. & Nicholson, C.(1978), Extracellular ionic variations during spreading depression. Neurosciences, 3, 1045-1059.

Krnjevíc, K.(1974), Chemical nature of synaptic transmission in vertebrates. Physiol. Rev., 54, 418.

Krnjevíc, K. & Morris, M.E.(1981), Electrical and functional correlates of changes in transmembrane ionic gradients produced by neural activity in the central nervous system, In T. Zeuthen(ed.), The Application of Ion-Selective Microelectrodes :Research Monographs in Cell and Tissue Physiology, 4, 195-215.

Kuffler, S.W.(1967), Neuroglial cells: physiological properties and a potassium mediated effect of neuronal activity on the glial membrane potential. Proc. Roy. Soc., B., 168, 1-21.

Lajtha, A., Handbook of Neurochemistry, 2nd Edn., Vol. I: Chemical and Cellular Architecture, Plenum, N.Y., 1982.

Landau, L.D., & Lifshitz, E.M., Electrodynamics of Continuous Media, Pergamon Press, N.Y., 1960.

Lashley, K.S.(1950), In search of the engram, In Symposia Soc. Exp. Biol. IV: Physiological Mechanisms in Animal Behavior, Cambridge University Press, Cambridge.

Leão, A.A.P.(1944), Spreading depression of activity in the cerebral cortex. J. Neurophys., 7, 359.

Lebovitz, R.M.(1970), A theoretical examination of ionic interaction between neural and non-neural membranes. Biophys. J., 10, 423-444.

Lehner, F.K.(1979), On the validity of Fick's law for transient diffusion through a porous medium. Chem. Eng. Sci., 34, 821-825.

Lin, C.C. & Segel, L.A., Mathematics Applied to Deterministic Problems in the Natural Sciences,MacMillan, New York, 1965.

Llinas, R. & Sugimori, M.(1980), Electrophysiological properties of in vitro Purkinje cell dendrites in mammalian cerebellar slices. J. Physiol. (Lond.), 305, 197-213.

Lorente de Nó, R.(1947), Analysis of the distribution of the action currents of nerve in volume conductors, In A Study of Nerve Physiology, part 2, Vol. 132, Rockefeller Institute, N.Y. .

MacGillivray, A.D. & Hare, D.(1969), Applicability of Goldmann's constant field assumptions to biological systems. J. Theor. Biol., 25, 113-126.

Mathias, R.T., Rae, J.L. & Eisenberg, R.S.(1979), Electrical properties of structural components of the crystalline lens. Biophys. J., 25, 181-201.

Maxwell, J.C., A Treatise on Electricity and Magnetism, 2nd ed. Vol. I., Clarendon Press, Oxford, 1878.

McKenzie, D.R., McPhedran, R.C. & Derrick, G.H.(1978), The conductivity of lattices of spheres II:the body centred and face centred cubic lattices. Proc. Roy. Soc., Series A, 362, 211-232.

McPhedran, R.C. & McKenzie, D.R.(1978), The conductivity of lattices of spheres I: the simple cubic lattice. Proc. Roy. Soc., Series A, 359, 45-63.

Mitchell, A.R., Computational Methods in Partial Differential Equations, John Wiley, N.Y., 1969.

Miura, R.M.(1981), Non-linear waves in neuronal cortical structures, In R.H. Enns, B.L. Jones, R.M. Miura & S.S. Rangnekar(eds.), Non-linear Phenomena in Physics and Biology, 369-400.

Moody, W.J., Futamachi, K.J. & Prince, D.A.(1974), Extracellular potassium activity during epileptogenesis. Exp. Neurol., 42, 248-262.

Nernst, W.(1889), Die elektromotorische Wirksamkeit der Jonen. Z. Phys. Chem., 4, 129-181.

Newman, E.A.(1986), Regional specialization of the membrane of retinal glial cells and its importance to K$^+$ spatial buffering.Ann. N.Y. Acad. Sci., 481, 273-86.

Nicholson, C.(1973), Theoretical analysis of field potential in anisotropic ensembles of neuronal elements. IEEE Trans. Biomed. Eng., BME-20, 278-288.

Nicholson, C.(1980), Dynamics of the brain cell microenvironment. Neurosci. Res. Prog. Bull., 18, 177-322.

Nicholson, C. & Freeman, J.A.(1975), Theory of current-source-density analysis and determination of conductivity tensor for anuran cerebellum. J. Neurophys., 38, 356-368.

Nicholson, C. & Kraig, R.P.(1981), The behavior of extracellular ions during spreading depression, In T. Zeuthen(ed.), The Application of Ion-Selective Microelectrodes Research Monographs in Cell and Tissue Physiology, 4, 195-215.

Orkand, R.K.(1980), Functional consequences of ionic changes resulting from electrical activity: introductory remarks. Fed. Proc., 39, 1514-1518.

Orkand, R.K., Nicholls, J.G. & Kuffler, S.W.(1966), Effect of nerve impulses on the membrane potential of glial cells in the central nervous system of Amphibia. J. Neurophys., 29, 788-806.

Ostwald, W.(1890), Elektrische Eigenshaften halbdurchlassiger Scheidewande. Z. Phys. Chem., 6, 71-82.

Pape, L.G., & Katzman, R.(1972),Response of glia in cat sensorimotor cortex to increased extracellular potassium. Brain Res., 38, 71-92.

Pellionisz, A. & Llinas, R.(1977), A computer model of cerebellar Purkinje cells. Neuroscience, 2, 37-48.

Peskoff, A.(1979), Electrical potential in three-dimensional electrically syncytial tissues. Bull. Math. Biol., 41, 163.

Peters, A., Palay, S.L., & Webster, H. DeF., The Fine Structure of the Nervous System: The Neurons and Supporting Cells, W.B. Saunders, Toronto, 1976.

Pevzner, L.(1982), Oligodendrocytes, In A. Lajtha(ed.), Neurochemistry, 2nd Edn., Vol. I: Chemical and Cellular Architecture, 357-388.

Phillips, J.M. & Nicholson, C.(1981), Ion diffusion modified by tortuosity and volume fraction in the extracellular microenvironment of the rat cerebellum. J. Physiol. (Lond.), 321, 225-257.

Plonsey, R., Bioelectric Phenomena, McGraw-Hill, N.Y., 1969.

Prince, D.A.(1978), Neurophysiology of epilepsy. Ann. Rev. Neurosci., 1, 395-415.

Puil, E.(1981), S-Glutamate: Its interactions with spinal neurons.Brain Res. Rev., 3, 229-322.

Puil, E., Gimbarzevsky, B. & Miura, R.M.(1986), Quantification of membrane properties of trigeminal root ganglion neurons in guinea pigs. J. Neurophys., 55, 995-1015.

Rall, W.(1959), Branching dendritic trees and motoneuron membrane resistivity. Exp. Neurol., 1, 491-527.

Rall, W.(1969), Time constants and electrotonic length of membrane cylinders and neurons. Biophys. J., 9, 1483-1508.

Ranck, J.B. Jr.(1963), Analysis of specific impedance of rabbit cerebral cortex. Exp. Neurol., 7, 144-152.

Ranck, J.B. Jr.(1964), Specific impedance of cerebral cortex during spreading depression and an analysis of neuronal neuroglial and interstitial contributions. Exp. Neurol., 9, 1-16.

Ranck, J.B. Jr.(1975), Which elements are excited in electrical stimulation of mammalian central nervous system: A review. Brain Res., 98, 417-440.

Ranck, J.B. jr, & Bement, S.L.(1965), The specific impedance of the dorsal columns of cat: an anisotropic medium. Exp. Neurol., 11, 451-463.

Reichenbach, A. & Eberhardt, W.(1988), Cytotopographical specialization of enzymatically isolated rabbit retinal Muller (glial) cells: K^+ conductivity of the cell membrane. Glia, 1, 191-7.

Reichenbach, A., Neumann, M. & Bruckner, G.(1987), Cell length to diameter relation of rat fetal radial glia - does impaired K^+ transport capacity of long thin cells cause their perinatal transformation into multipolar astrocytes?.Neurosci. Let. 73, 95-100, .

Robinson, R.A. & Stokes, R.H., Electrolyte Solutions, Butterworths, London, 1955.

Royden, H.L., Real Analysis, 2end ed., MacMillan, N.Y., 1968.

Sanchez-Palencia, E.(1980), Non-homogeneous media and vibration theory, In Lecture Notes in Physics, 127, Springer, N.Y..

Schanne, O.F. & Ruiz P.-Ceretti, E., Impedance Measurements in Biological Cells, Wiley, N.Y., 1978.

Schoffeniels, E., Franck, G., Hertz, L. & Tower, D.B., Eds., Dynamic Properties of Glia Cells,Pergamon, Oxford, 1978.

Schultz, S.G., Basic Principles of Membrane Transport, Cambridge University Press, Cambridge, 1980.

Schwartzkroin, P.A. & Slawsky, M.(1977), Probable calcium spikes in hippocampal neurons. Brain Res., 135, 157-161.

Segel, L.A.(1966), The importance of asymptotic analysis in applied mathematics. Am. Math. Monthly, 73, 7-14.

Shelton, D.P.(1985), Membrane resistivity estimates in the Purkinje neuron by means of a passive computer model. Neuroscience, 14, 111-131.

Somjen, G.G.(1975), Electrophysiology of neuroglia. Ann. Rev. Physiol., 37, 163-190.

Somjen, G.G.(1979), Extracellular potassium in the mammalian central nervous system. Ann. Rev. Physiol., 41, 159-177.

Somjen, G.G.(1981), The why and how of measuring the activity of ions in extracellular fluid of spinal cord and cerebral cortex, In T. Zeuthen(ed.), The Application of Ion-Selective Microelectrodes: Research Monographs in Cell and Tissue Physiology, 4, 175-193.

Somjen, G.G.(1984), Functions of glial cells in the cerebral cortex, In The Cerebral Cortex, 2, Plenum, N.Y. .

Somjen, G.G. & Aitken, P.G.(1984), The ionic and metabolic responses associated with neuronal depression of Leão's type in cerebral cortex and in hippocampal formation. An. Acad. Brasil Cienc., 56, 495-504.

Sonnhof, U.(1987), Single voltage-dependent K^+ and Cl^- channels in cultured rat astrocytes. Can. J. Physl. Pharm., 65, 1043-50.

Sonnhof, U., & Schachner, M.(1986), Single voltage-dependent K$^+$-channels in cultured astrocytes. Neurosci. Let , 64, 241-6.

Somjen, G.G. & Trachtenberg, M.(1979), Neuroglia as generators of extracellular current, In E.J. Speckman & H. Caspars(eds.), Origin of Cerebral Field Potentials, 21-32.

Spencer, W.A. & Kandel, E.R.(1961a), Electrophysiology of hippocampal neurons. III. Firing level and time constant. J. Neurophys., 24, 260-271.

Spencer, W.A. & Kandel, E.R.(1961b), Electrophysiology of hippocampal neurons. IV. Fast pre-potentials. J. Neurophys., 24, 272-285.

Stafstrom, C.E., Schwindt, P.C. & Crill, W.E.(1984), Cable properties of layer V neurons from cat sensorimotor cortex in vitro. J. Neurophys., 52, 278-289.

Stohr, P. Jr.(1957), Mikcroskopische Anatomie des Vegetativen Nervensystems, In Mullendorff's Handbuch der Mikroskopischen Anatomie des Menschen, Vol.IV, part 5, Springer, Berlin.

Sugaya, E., Takato, M. & Noda, Y.(1975), Neuronal and glial activity during spreading depression in cerebral cortex of cat. J. Neurophys., 38, 822.

Sypert, G.W. & Ward, A.A. Jr.(1974), Changes in extracellular potassium activity during neocortical propagated seizures. Exp. Neurol., 45, 19-41.

Tang, C.H., Orkand, P.M. & Orkand, R.K.(1985), Coupling and uncoupling of amphibian neuroglia. Neurosc. Let., 54, 237-42.

Traub, R.D., Dudek, F.E., Taylor, C.P. & Knowles, W.D.(1985a), Simulation of hippocampal discharges synchronized by electrical interactions. Neuroscience, 14, 1033-1038.

Traub, R.D., Dudek, F.E., Snow, R.W. & Knowles, W.D.(1985b), Computer simulations indicate that electrical field effects contribute to the shape of the epileptiform field potential. Neuroscience, 15, 947-958.

Tuckwell, H.C. & Miura, R.M.(1978), A mathematical model for spreading cortical depression. Biophys. J., 23, 257-276.

Turner, D.A. & Schwartzkroin, P.A.(1984), Passive electrotonic structure and dendritic properties of hippocampal neurons, In R. Dingledine(ed.), Brain Slices, 25-50.

Van Harreveld, A.(1959), Compounds in brain extracts causing spreading depression of cerebral cortical activity and contraction of crustacean muscle. J. Neurochem., 3, 300.

Van Harreveld, A.(1978), Two mechanisms for spreading depression in the chick retina. J. Neurobiol., 9, 419-431.

Van Harreveld, A. & Khattab, F.I.(1967), Changes in cortical extracellular space during spreading depression investigated with the electron microscope. J. Neurophys., 30, 911-929.

Van Harreveld, A. & Ochs, S.(1957), Electrical and vascular concomitants of spreading depression. Am. J. Physiol., 189, 159-166.

Varon, S.S. & Somjen, G.G.(1979), Neuron-glia interactions. Neurosci. Res. Prog. Bull., 17, 1-239.

Walz, W. & Hertz, L.(1983),Functional interactions between neurons and astrocytes II:Potassium homeostasis at the cellular level.Prog. Neurobiol., 20, 133-183.

Zeuthen, T.(ed.), The Application of Ion-Selective Microelectrodes: Research Monographs in Cell and Tissue Physiology, 4, Elsevier/North Holland Biomedical Press, N.Y., 1981.